Geobiology of bituminous carbonates from the Ediacaran Shibantan Member (Dengying Formation, South China)

Dissertation
zur Erlangung des mathematisch-naturwissenschaftlichen Doktorgrades
"Doctor rerum naturalium"
der Georg-August-Universität Göttingen

im Promotionsprogramm Geowissenschaften
der Georg-August University School of Science (GAUSS)

vorgelegt von
Jan-Peter Duda

aus Bremen

Göttingen 2014

Betreuungsausschuss

Prof. Dr. Joachim Reitner, Abteilung Geobiologie, Geowissenschaftliches Zentrum, Georg-August-Universität Göttingen

Prof. Dr. Volker Thiel, Abteilung Geobiologie, Geowissenschaftliches Zentrum, Georg-August-Universität Göttingen

Mitglieder der Prüfungskommission

Referent:

Prof. Dr. Joachim Reitner, Abteilung Geobiologie, Geowissenschaftliches Zentrum, Georg-August-Universität Göttingen

Korreferenten:

Prof. Dr. Volker Thiel, Abteilung Geobiologie, Geowissenschaftliches Zentrum, Georg-August-Universität Göttingen

Prof. Dr. Jörn Peckmann, Department für Geodynamik und Sedimentologie, Erdwissenschaftliches Zentrum, Universität Wien

Weitere Mitglieder der Prüfungskommission:

Prof. Dr. Andreas Pack, Abteilung Isotopengeologie, Geowissenschaftliches Zentrum, Georg-August-Universität Göttingen

PD Dr. Mike Reich, Museum, Sammlungen & Geopark, Geowissenschaftliches Zentrum, Georg-August-Universität Göttingen

Dr. Martin Blumenberg, Bundesanstalt für Geowissenschaften und Rohstoffe (BGR), Hannover

Dr. Jens Dyckmans, Kompetenzzentrum Stabile Isotope, Georg-August-Universität Göttingen

Dr. Klaus Simon, Abteilung Geochemie, Geowissenschaftliches Zentrum, Georg-August-Universität Göttingen

Tag der mündlichen Prüfung:

20.08.2014

'If you have an apple and I have an apple and we exchange these apples then you and I will still each have one apple. But if you have an idea and I have an idea and we exchange these ideas, then each of us will have two ideas'.

Georg Bernard Shaw (1856 – 1950)

Acknowledgements

This thesis is the product of a continuous cultural and scientific exchange and the project greatly benefited from the scientific spirit and enthusiastic support of many persons in or outside academia. Unfortunately, however, not all of those who would deserve being acknowledged can be mentioned in the following and I sincerely apologise for this unfortunate circumstance.

First of all I sincerely thank Joachim Reitner, Maoyan Zhu and Martin Blumenberg for the collaborative initiation and realisation of this bilateral Sino-German research project as well as for their constant scientific support. Maoyan Zhu is furthermore thanked for providing me the possibility to stay in China several times and for his generous hospitality. Volker Thiel and Klaus Simon are acknowledged for their constant scientific support throughout the project. Furthermore I would like to thank my advisors Joachim Reitner, Volker Thiel and Martin Blumenberg, as well as Jörn Peckmann, Jens Dyckmans, Andreas Pack, Mike Reich and Klaus Simon for being on my thesis committee.

Axel Hackmann and Cornelia Conradt are thanked for their constant technical and analytical support. Marie-France Hesse and Gabriele Schmidt are acknowledged for their help with administrative issues. I sincerely thank my friends Tianchen He, Lixia Li, Miao Lu, Cui Luo and Lanyun Miao for their help with various issues in China and in Germany; without their cooperativeness and open-mindedness the project would not have been working. Likewise I am indebted to Filiz Afşar, Martin Blumenberg, Cui Luo, Sebastián Oriolo, Volker Thiel and Frank Wiese for critical and inspiring discussions, constructive criticism and proofreading parts of the thesis. Tara Djokic is sincerely thanked for polishing the language and Christine Berndmeyer for her support in the final stages of the thesis.

I would like to thank Filiz Afşar, Elco Luijendijk, Cui Luo, Silke Meier and Sebastián Oriolo for their companionship and all the great times together, always full of laughter and fun. Klaus Wolkenstein is thanked for being a considerate and patient office mate particularly during stressful times. My love Filiz Afşar, my parents Achim Peter Duda and Marein Köhlenbeck-Duda, my sisters Catharina and Franziska Duda, as well as Aslan and Martina Afşar are thanked for their faith and emotional support through good and hard times.

The study was financially and logistically supported by the Deutsche Forschungsgemeinschaft (DFG; Project BL 971/1-3), the Courant Research Centre Geobiology University of Göttingen (DFG, German Excellence Program), Göttingen International, the Nanjing Institute for Geology and Palaeontology (NIGPAS) of the Chinese Academy of Sciences (CAS), the National Basic Research Program of China (2013CB835006), and the National Natural Science Foundation of China, the Nanjing University (Chinese 'Oversea Famous Scholar Programme'). I am particularly indebted to the German Academic Exchange Service (DAAD) for providing a scholarship which allowed me to stay in China for six months. The intensive presentation of own results on international meetings would not have been possible without financial support provided by Göttingen International, the Unibund Göttingen, the China University of Geosciences in Wuhan, and the International Association of Sedimentologists (IAS).

Preface

The following manuscripts are part of this doctoral thesis (**corresponding author*):

Duda, J.-P.*, Zhu, M., Reitner, J. (submitted): Depositional dynamics of a bituminous carbonate facies in a tectonically induced intra-platform basin: The Shibantan Member (Dengying Formation, Ediacaran Period). *Carbonates and Evaporites* (Chapter 2 of this thesis)

Duda, J.-P.*, Blumenberg, M., Thiel, V., Simon, K., Zhu, M., Reitner, J. (in revision): Geobiology of an Ediacara palaeoecosystem: The Shibantan Member (Dengying Formation, South China). *Precambrian Research* (Chapter 3 of this thesis)

Duda, J.-P.*, Thiel, V., Reitner, J., Blumenberg, M. (accepted): Assessing possibilities and limitations for biomarker analyses on outcrop samples: A case study on carbonates of the Shibantan Member (Ediacaran Period, Dengying Formation, South China). *Acta Geologica Sinica, English Version* (Chapter 4 of this thesis)

Table of contents

- Chapter 1 -

Introduction

1.1 Outline of the study

The first convincing fossil and biogeochemical indications for microbial life on Earth range back to the Palaeoarchaean (ca. 3.5 Ga; Van Kranendonk, 2006, 2007; and references therein). It was not until the Cambrian (ca. 541-485 Ma; Peng et al., 2012; Walker et al., 2013) that most modern metazoan lineages diversified and shaped the modern Phanerozoic world (i.e. the '*Cambrian Explosion*'). This sudden turnover after at least 3 Ga of microbial dominance requires crucial evolutionary developments immediately before the Cambrian. The Ediacaran directly precedes the Cambrian and is indeed already characterised by unique evolutionary inventions (e.g. Knoll et al., 2004, 2006a; Fig. 1.1), but little is known about the geobiological processes which were crucial for these developments. Geobiological studies of Ediacaran successions are therefore crucial in understanding the coevolution of life and Earth across the Precambrian-Cambrian boundary.

Ediacaran palaeoecosystems with architecturally complex soft-bodied organisms (i.e. Ediacara-type fossils) are particularly interesting in this regard since some of these fossils possibly represent stem-group metazoans (e.g. Fedonkin and Waggoner, 1997; Gehling et al., 2005; Narbonne, 2005; Xiao and Laflamme, 2009; Sperling and Vinther, 2010; Narbonne et al., 2012; and references therein; see 1.3.2 The Ediacaran biosphere for details). However, the geobiology of these palaeoecosystems is still poorly understood. The reason is these environments were usually linked to volcaniclastic and siliciclastic settings (e.g. Narbonne, 2005; Callow and Brasier, 2009) so that biogeochemical signatures are commonly not well preserved. For instance, organic biomarkers are typically lacking, although one exception from the White Sea locality has been reported (Kelly, 2009). Contemporaneous carbonates may conserve more information about the palaeoenvironments and biology, thus promising to fill this major preservational gap.

As yet there are only two carbonate systems with Ediacara-type fossils; the Khatyspyt Formation in

Siberia (e.g. Fedonkin, 1990; Khomentovsky, 1990; Knoll et al., 1995) and the Shibantan Member of the Dengying Formation in south China (e.g. Sun, 1986; Steiner et al., 1993; Zhu et al., 2007). These systems could be a key to the geobiology of palaeoecosystems with Ediacara-type fossils, but little is known about the sedimentology and biogeochemistry of these palaeoenvironments. The aim of this study was therefore a comprehensive geobiological characterisation of the Shibantan Member, intergrating both sedimentological and biogeochemical aspects.

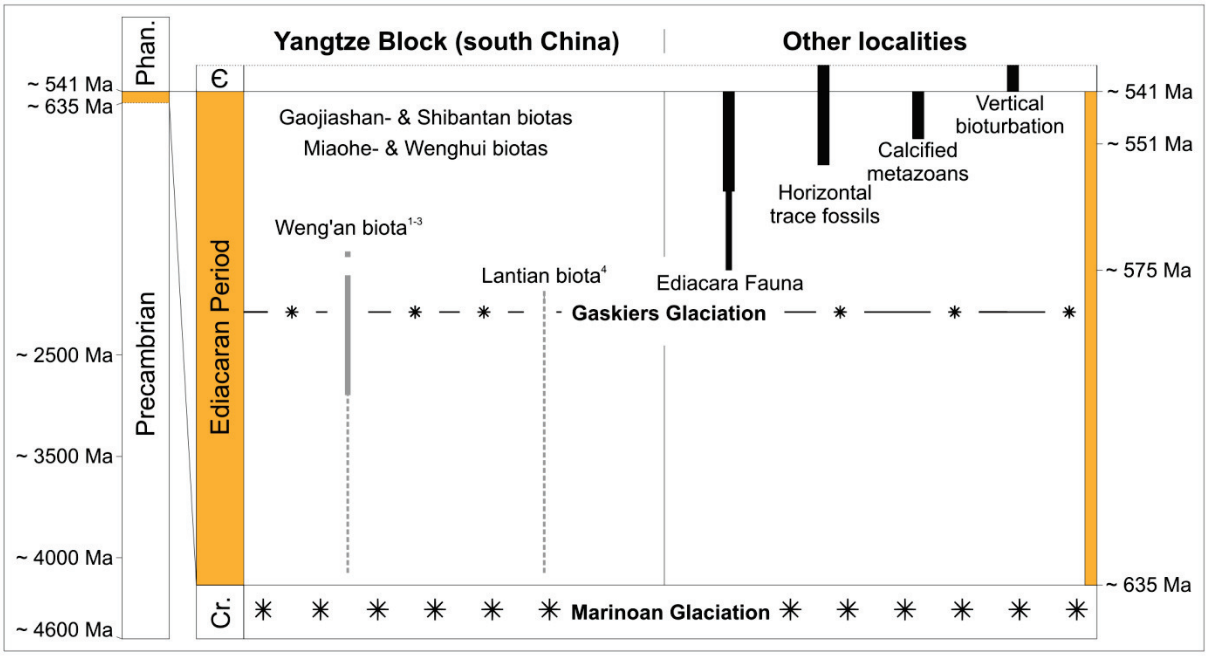

Fig. 1.1 Major events of the Ediacaran Period (modified after Erwin and Valentine, 2013). Cr: Cryogenian; Є: Cambrian. Grey squares denote radiometric ages; grey dashed lines denote litho- and/or biostratigraphic age constraints. Dates for the Yangtze Block from (1-3) Barfod et al. (2002), Chen D. et al. (2004), Chen Y. et al. (2009) and (4) Yuan et al. (2011).

1.2 Study area

The study area is located in the Hubei Province of south China close to Yichang (i.e. the Yangtze Gorges area; Fig. 1.2a). In this region, Ediacaran successions are well exposed around the Huangling Dome (commonly referred to as Huangling Anticline; Fig. 1.2b) where they form massive cliffs commonly dissected by river gorges (Fig. 1.3a). This situation is expressed in the name of the Shibantan Member (shíbăntān = 石板滩; Chinese for '*river bank with platy rocks*'). This study is mainly based on one new section in the eastern rim (Xinshipai-Section; Fig. 1.2b, 1.3b; see Chapter 2 for details) and several outcrops in the southern part of the Huangling Dome (e.g. the Zhoujia'ao-Quarry; Fig. 1.2b, 1.3c, d; see Chapter 3 and Chapter 4 for details).

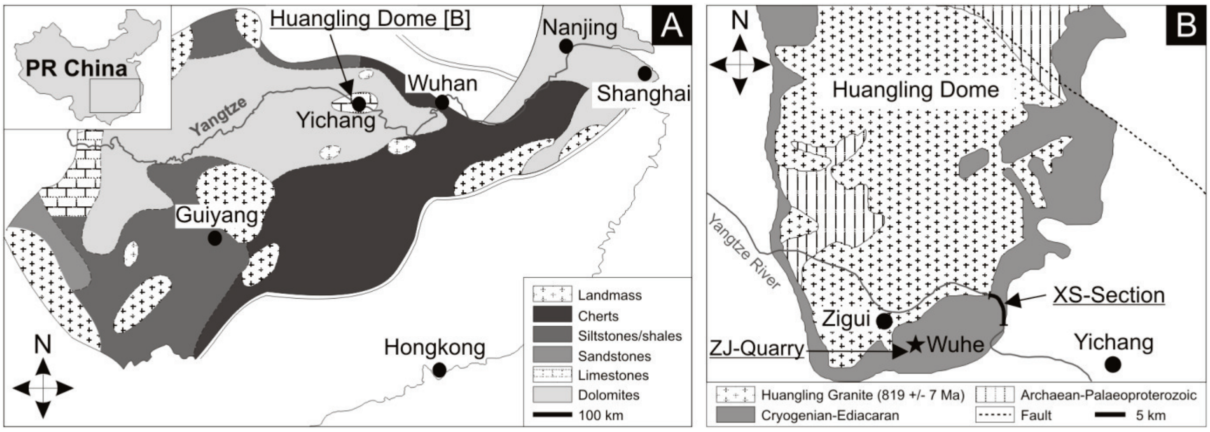

Fig. 1.2 Geological context of the Shibantan Member. (A) Facies distribution on the Dengying Platform at time of deposition. The working area is located in the direct vicinity of Yichang (see arrow). (B) Detail from (A), showing the location of the Xinshipai- (XS-) Section and the Zhoujia'ao- (ZJ-) Quarry at the southern part of the Huangling Dome. (A) Modified after Zhu et al. (2007), (B) modified after Chen Z. et al. (2013). Age of the Huangling Granite from Ma et al. (1984).

Fig. 1.3 Important exposures in the Yangtze Gorges area. (A) Cliffs of the Dengying Formation along the Yangtze River (opposite to the Xinshipai-Section). The estimated vertical distance between the water level and the base of the radio mast (see arrow) is ca. 110-150 m. (B-D) Rocks of the Shibantan Member along the Xinshipai-Section (B) and in the Zhoujia'ao-Quarry (C, D). Photos (A) and (B) courtesy of Marta Rodriguez-Martinez, photo (C) courtesy of Cui Luo.

1.3 Geobiology of the Ediacaran Period

1.3.1 Pre-Ediacaran evolution of complex life

Prior to the Ediacaran, fossils of complex multicellular life forms are generally rare and the respective biological affinities remain ambiguous. For instance, cm-sized structures in 2.1 Ga black shales in Gabon (Africa) are interpreted as highly organised and spatially discrete populations of colonial organisms but are of uncertain biological affinity (Albani et al., 2010). Younger but more widespread fossils such as *Grypania* (ca. 1.85-1.45 Ga), a mm-sized carbonaceous and commonly coiled fossil (Fig. 1.4a), as well as *Horodyskia* (1.48-0.42 Ga), a mm-sized fossil characterised by a pearl-necklace-like structure, are also disputed but commonly interpreted as eukaryotic (e.g. Knoll et al., 2006b; Javaux, 2011; Retallack et al., 2013; and references therein). Also Acritarchs (i.e. an artificial group including organic walled microfossils without any reference to their biological affinity) in the 1.5 Ga Roper Group (Australia) are interpreted as eukaryotes (Javaux et al., 2001). The potential red-alga *Bangiomorpha* (ca. 1.2 Ga) finally exhibit cellular differentiation and specialisation (Butterfield et al., 1990; Butterfield, 2000; Fig. 1.4b). Enigmatic macroscopic discoidal fossils which roughly resemble Ediacara-type fossils (see 1.3.2 The Ediacaran biosphere) occur already in Cryogenian strata, but respective reports are scarce (e.g. Hofmann et al., 1990; Zhang X. et al., 2006; Nagovitsin et al., 2008).

The first fossil evidence for metazoan life on Earth are possible organic biomarker signatures of demosponges in Cryogenian rocks (i.e. exceptionally high 24-isopropylcholestane / 24-*n*-propylcholestane-ratios of ≥ 0.5; McCaffrey et al., 1994; Love et al., 2009). However, symbiotic bacteria of recent sponges contain genes coding for the biosynthesis of 24-isopropyl steroids (Siegl et al., 2011) which has been used as an argument against biomarker evidence for early metazoan life (Antcliffe, 2013; Antcliffe et al., 2014). Suspected Cryogenian sponge-grade fossils (e.g. Maloof et al., 2010; Brain et al., 2012) and spicules (e.g. Brasier et al., 1997; Reitner and Wörheide, 2002) are even more disputed (cf. Antcliffe et al., 2014). The same is true for rock textures that potentially show the presence of sponges (Neuweiler et al., 2009a, b; Planavsky, 2009). However, since molecular clock data suggest that the earliest development and diversification of metazoans started in the Cryogenian

Period (e.g. Peterson and Butterfield, 2005; Peterson et al., 2008; Erwin et al., 2011), organic biomarkers may record early and cryptic stages of metazoan evolution.

Fig. 1.4 Examples of Precambrian complex life forms. (A) *Grypania*, a possible fossil eukaryote; (B) *Bangiomorpha*, a potential red-alga (Butterfield, 2000); (C) Acanthomorphic acritarch (Willman and Moczydłowska, 2008); (D, E) Morphologically complex macrofossils of the Lantian biota; (F) Potential metazoan embryo of the Weng'an biota (Xiao et al., 1998); (G, H) The possible metazoans *Dickinsonia* (G; Narbonne et al., 2012) and *Kimberella* (H; Fedonkin and Waggoner; 1997); (I, J) Morphologically complex macrofossils from the Miaohe biota (specimens published in Xiao et al., 2002). (K) The Ediacara-type fossil *Eoandromeda* from the Miaohe biota (see arrows); (L) Cloudina including borings (see arrows; Hua et al., 2003). (A, K): Collection of Prof. Maoyan Zhu (NIGPAS, CAS, PR China); (D, E): Collection of Prof. Joachim Reitner (GZG, University of Göttingen).

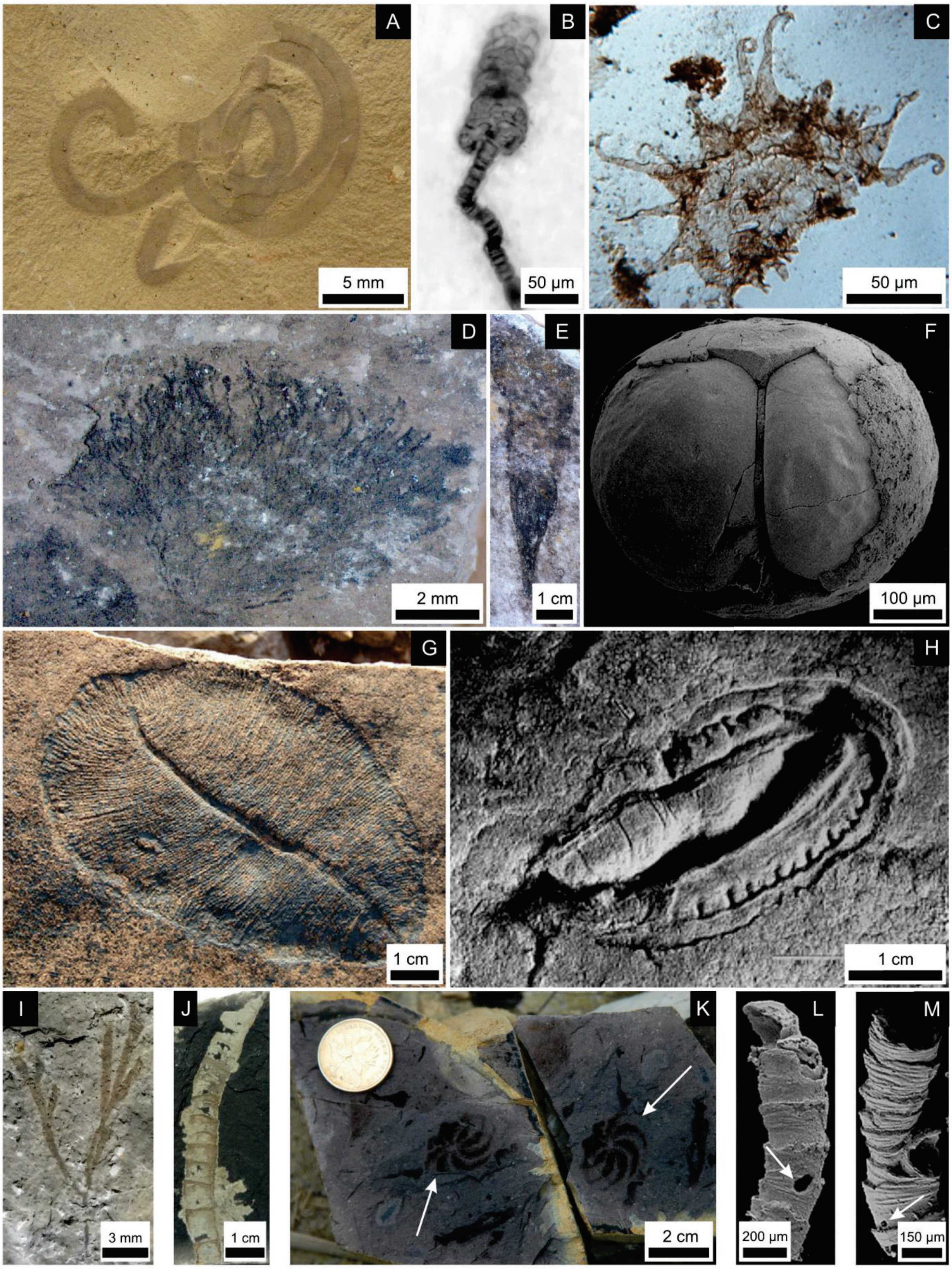
A
5 mm
B
50 µm
C
50 µm
D
2 mm
E
1 cm
F
100 µm
G
1 cm
H
1 cm
I
3 mm
J
1 cm
K
2 cm
L
200 µm
M
150 µm

1.3.2 The Ediacaran biosphere

Rocks deposited at the beginning of the Ediacaran Period record unique evolutionary developments that resulted in the diversification of metazoans on Earth (Fig. 1.1). The lower part of the Ediacaran Period is characterised by diverse associations of relatively large (typically 400-600µm) acanthomorphic (i.e. spiny) acritarchs (Knoll and Walter, 1992; Knoll, 2000; Narbonne et al., 2012; and references therein; Fig. 1.4c). These acritarchs are also prominent in early diagenetic chert nodules and phosphorites of the Doushantuo Formation (e.g. McFadden et al., 2009; Yin C. et al., 2011; Liu et al., 2013, 2014; Xiao et al., 2014). In addition to microfossils, there is ample evidence for the proceeding evolution and diversification of complex multicellular life forms during that time (Fig. 1.1). For instance, a diverse assemblage of morphologically complex carbonaceous macrofossils of partly algal affinity is preserved in the >579 Ma Lantian Formation (therefore referred to as the '*Lantian biota*'; Fig. 1.1, 1.4d, e), which is the basinal equivalent of the Doushantuo Formation (Yuan et al., 1999, 2011). At the same time, phosphorite beds of the middle Doushantuo Formation in Guizhou (ca. 599-576 Ma; Barfod et al., 2002; Chen D. et al., 2004; Chen Y. et al., 2009) contain various fossils including possible multi-cellular algae and potential metazoan embryos (i.e. the '*Weng'an biota*'; e.g. Xiao et al., 1998, 2004; Xiao and Knoll, 1999, 2000; Yin L. et al., 2007; Yin Z. et al., 2013; Fig. 1.1, 1.4f). Furthermore, putative larval and adult stages of various metazoans such as sponges, cnidarians and bilaterians have been described from these units (e.g. Li C. et al., 1998; Xiao et al., 2000; Chen J. et al., 2000, 2002, 2004), but the interpretation of these structures is still contentious (e.g. Zhang Y. et al., 1998; Bailey et al., 2007; Huldtgren et al., 2011; Bengtson et al., 2012).

The upper part of the Ediacaran is characterised by the establishment and diversification of the classic Ediacara-type organisms (Knoll et al., 2004, 2006a; Narbonne, 2005; Xiao and Laflamme, 2009; Narbonne et al., 2012; and references therein; Fig. 1.1). Although the biological affinities of the Ediacara biota are still debated, forms such as *Dickinsonia* (amongst others interpreted as placozoan; Fig. 1.4g) and *Kimberella* (amongst others interpreted as mollusc; Fig. 1.4h) are commonly regarded as representing stem-group metazoans (e.g. Fedonkin and Waggoner, 1997; Gehling et al., 2005; Narbonne, 2005; Xiao and Laflamme, 2009; Sperling and Vinther, 2010; Narbonne et al., 2012). The presence of metazoans is further evidenced by the appearance of horizontal trace fossils in the same settings (e.g. Martin et al., 2000; Jensen et al., 2006; Knoll et al., 2006a; Narbonne, 2005; Xiao and Laflamme, 2009; Narbonne et al., 2012; and references therein). Another feature of these settings is the widespread and abundant occurrence of *Vendotaenia*-like fossils (essentially carbonaceous tubes with a simple morphology; commonly interpreted as algae, sulphur-oxidising bacteria or treated as problematica; e.g. Vidal, 1989; Gnilovskaya, 1990; Hofmann, 1992; Cohen et al., 2009). A typical feature of these environments was that Ediacara-type organisms and the producers of the horizontal traces were intimately associated with benthic microbial mats (e.g. Seilacher, 1999). Ediacara-type organisms became extinct at end of the Ediacaran (e.g. Narbonne, 2005; Xiao and Laflamme, 2009; Narbonne et al., 2012; Fig. 1.1).

Assemblages with Ediacara-type fossils occur worldwide and can temporally and ecologically be grouped in the Avalon-, the White Sea- and the Nama assemblages (Waggoner, 2003; Narbonne, 2005; Xiao and Laflamme 2009; Narbonne et al., 2012; Tab. 1.1). However, it is not clear if the distribution of these assemblages was mainly influenced or even exclusively controlled by evolution, biogeography, palaeoecology, and/or taphonomy (e.g. Waggoner, 2003; Grazhdankin 2004; Narbonne 2005; Xiao and Laflamme, 2009; Narbonne et al., 2012). This makes conclusions concerning the early evolution of metazoans difficult, but could be overcome by investigating further fossil Lagerstätten with Ediacara-type fossils. The Ediacaran Khatyspyt Formation in Siberia as well as coeval black shales and carbonates from south China (see below) are particularly interesting in this regard since they represent the only known settings in which carbonaceous compression fossils (i.e. preserved as a thin film of carbon) and Ediacara-type fossils co-occur (Grazhdankin et al., 2008; Zhu et al., 2008).

Assemblage	**Age (Ma)**	**Important sites**	**Biota**	**Environments**
Avalon	579-559	Newfoundland NW Canada England	Mainly rangeomorphs; rare trace fossil	Deep-water
White Sea	560–550	E Europe Australia	Most diverse assemblage including *Kimberella* and *Eoandromeda*; abundant trace fossils	Shallow-water
Nama	549-541	Namibia	Several rangeomorphs and erniettomorphs; *Cloudina* and *Namacalathus*	Shallow-water

Tab. 1.1 Simplified overview about characteristics of fossil assemblages with Ediacara-type fossils (see Waggoner, 2003; Narbonne, 2005; Xiao and Laflamme, 2009; Narbonne et al., 2012; and references therein).

For example, in the uppermost shale of the Doushantuo Formation various types of carbonaceous compression fossils including colonial prokaryotes and multicellular algae are preserved (e.g. the '*Miaohe biota*' in the Yangtze Gorges area and the '*Wenghui biota*' in Guizhou Province; Steiner, 1994; Ding L. et al., 1996; Xiao et al., 2002; Zhu et al., 2008; Zhao Y. et al., 2004; Fig. 1.1, 1.4i-k). Furthermore, the Miaohe biota includes the eight-armed Ediacara-type fossil *Eoandromeda*, a possible radial symmetric metazoan, which is also preserved as a carbonaceous compression (Zhu et al., 2008). This is special since Ediacara-type fossils are usually preserved as impressions in siliciclastic or volcaniclastic rocks and do not co-occur with carbonaceous compression fossils (e.g. Narbonne, 2005; Narbonne et al., 2012). *Eoandromeda*, however, is e.g. also known from the White Sea assemblage of Australia (Tab. 1.1) where it is preserved as impressions on the bases of sandstone beds (Zhu et al., 2008). The Miaohe biota therefore bridges a biological and taphonomical gap between assemblages with impressions of Ediacara-type fossils and carbonaceous compression fossils (Zhu et al., 2008).

Carbonates of the younger Shibantan Member comprise a 'classical' Ediacaran fossil association including various Ediacara-type organisms (*Paracharnia dengyingensis*; Ding Q. and Chen, 1981; Sun, 1986; Dzik, 2002; *Yangtziramulus zhangi*; Xiao et al., 2005; Shen B. et al., 2009; *Hiemalora*, *Pteridinium*, *Rangea*, *Charniodiscus*; Chen Z. et al., 2014; as well as some new forms with circular shape and ribbing which are currently under investigation; Fig. 1.5a-d). Simple horizontal trace fossils (Zhao Z. et al., 1988; Ding L. et al., 1992; Ding Q. et al., 1993; Weber et al., 2007; Chen Z. et al., 2013; Meyer et al., 2014; Fig. 1.5e-f), *Vendotaenia*-like fossils (Ding Q. and Chen, 1981; Sun, 1986; Zhao Z. et al., 1988; Ding Q. et al., 1993; Fig. 1.5g, h), and a new annulated tubular fossil (*Wutubus annularis*; Chen Z. et al., 2014) have also been described. Most of these fossils are closely associated with microbial mats (cf. Xiao et al., 2005; Weber et al., 2007; Shen B. et al., 2009; Chen Z. et al., 2013, 2014; Meyer et al., 2014). The preservational potential of the Shibantan Member is furthermore underlined by findings of organically preserved microbial mat remains (currently under investigation; Fig. 1.6). Together with the Gaojiashan biota (see below), the Shibantan biota has been considered as part of the Nama assemblage (Waggoner, 2003; Narbonne et al., 2012; Chen Z. et al., 2014). However, in contrast to most other settings with Ediacara-type fossils, the Shibantan Member exhibits an almost pure carbonate lithology, thus representing a separate taphonomical window.

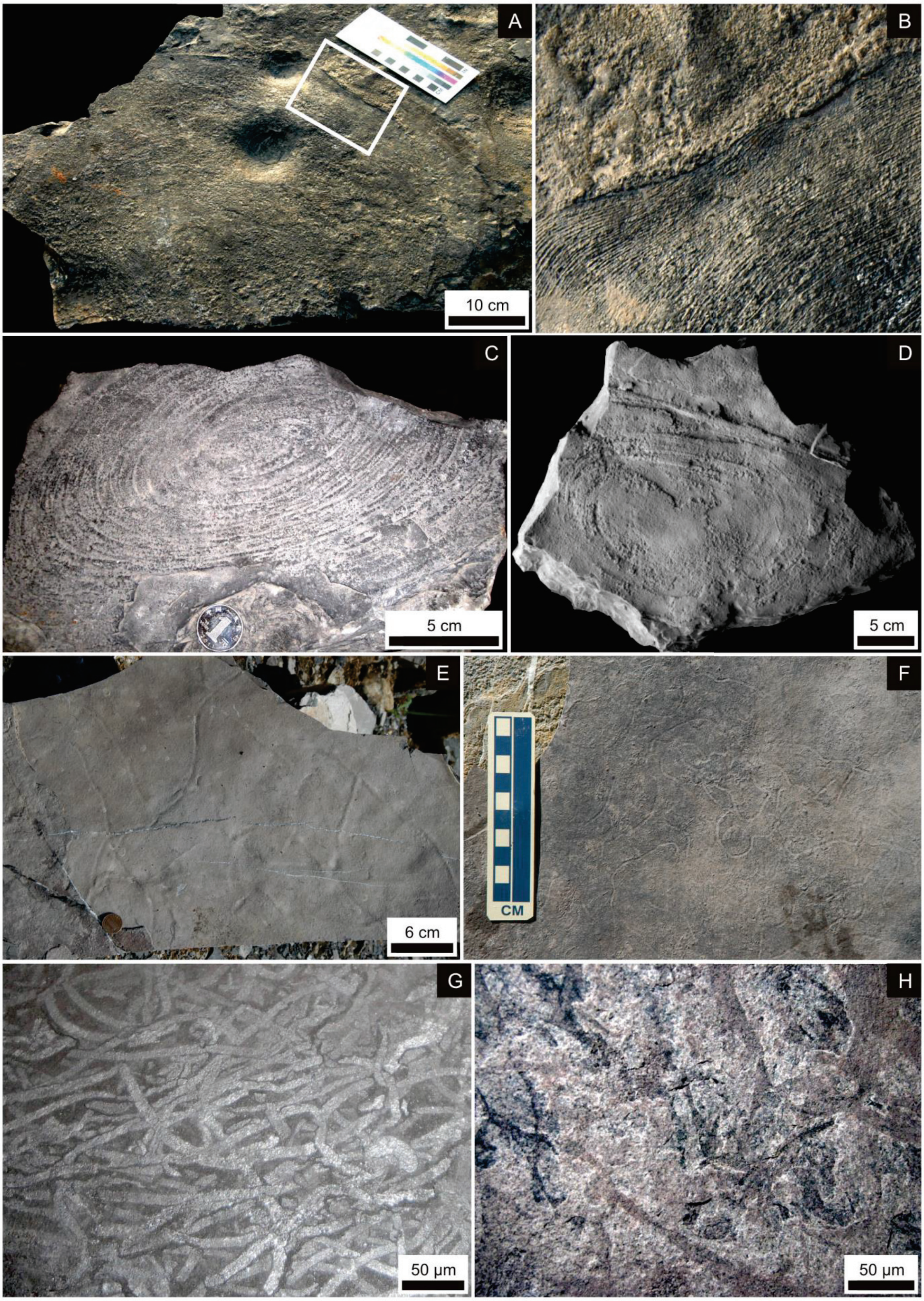

Fig. 1.5 Examples from the Shibantan biota. (A-D) New Ediacara-type fossils (B: detail from A); (E, F) horizontal trace fossils; (G, H) *Vendotaenia*-like fossils.

Another feature of the upper Ediacaran is the onset of biomineralisation, which is commonly explained by (i) detoxification-processes as a response to increasing calcium concentrations in seawater (e.g. Degens et al., 1985; Kaźmierczak et al., 1985; Simkiss, 1989), (ii) the exploration of new benthic niches by faciliating settlement and providing mechanical stability (Cohen, 2005), (iii) a rise of predation-pressure (e.g. Bengtson and Zhao, 1992; Hua et al., 2003) and (iv) substrate competition (Wood, 2011). Of particular interest are calcified fossils such as *Cloudina*, *Namacalathus* and *Namapoikia* which appear at ca. 550 Ma in shallow-water carbonates worldwide and are generally interpreted as metazoans (e.g. Germs, 1972; Grant, 1990; Grotzinger et al., 2000; Hofmann and Mountjoy, 2001; Wood et al., 2002; Wood, 2011; and references therein; Fig. 1.1, 1.4l). The precise biological affinity of *Cloudina* is still ambiguous (Cai et al., 2014), though the genus may relate to annelids and serpulids (Germs, 1972; Glaessner, 1976; Hua et al., 2005) or cnidarians (Grant, 1990; Vinn and Zatón, 2012). Borings in shells of *Cloudina* are interpreted as the earliest evidence for macrophagous predation in the rock record (Bengtson and Zhao, 1992; Hua et al., 2003; Fig. 1.4l). *Namacalathus* has been compared to cnidarians (Grotzinger et al., 2000) while *Namapoikia* has been suspected to be of cnidarian or poriferan affinity (Wood et al., 2002). There are also reports of possible first sponge spicules (e.g. in the Shibantan Member; Steiner et al., 1993), but respective findings are rare and generally contentious (cf. Antcliffe et al., 2014; and references therein). However, like Ediacara-type organisms, the calcified metazoans were intimately associated with benthic microbial mats (e.g. Seilacher, 1999; Grotzinger et al., 2000, 2005; Wood et al., 2002; Wood, 2011) and became extinct at the Precambrian-Cambrian boundary (Amthor et al., 2003).

In south China, various fossils of calcified organisms (*Cloudina, Shaanxilithes*, *Conotubus*, *Gaojiashania*, *Sinotubulites*) occur in the siliciclastic-dominated Gaojiashan Member (therefore commonly referred to as '*Gaojiashan biota*') and the locally overlying dolomitic Beiwan Member (Dengying Formation, respectively) (e.g. Conway Morris et al., 1990; Bengtson and Zhao, 1992; Hua et al., 2003, 2005; Chen Z. et al., 2008; Cai et al., 2010, 2011, 2013; Meyer et al., 2012). Reports of comparable calcified fossils in the Yangtze Gorges area are scarce and restricted to the Baimatuo Member which overlies the Shibantan Member (Chen M. and Wang, 1977; Chen M. et al., 1981; Ding Q. et al., 1993; Chen Z., 1999).

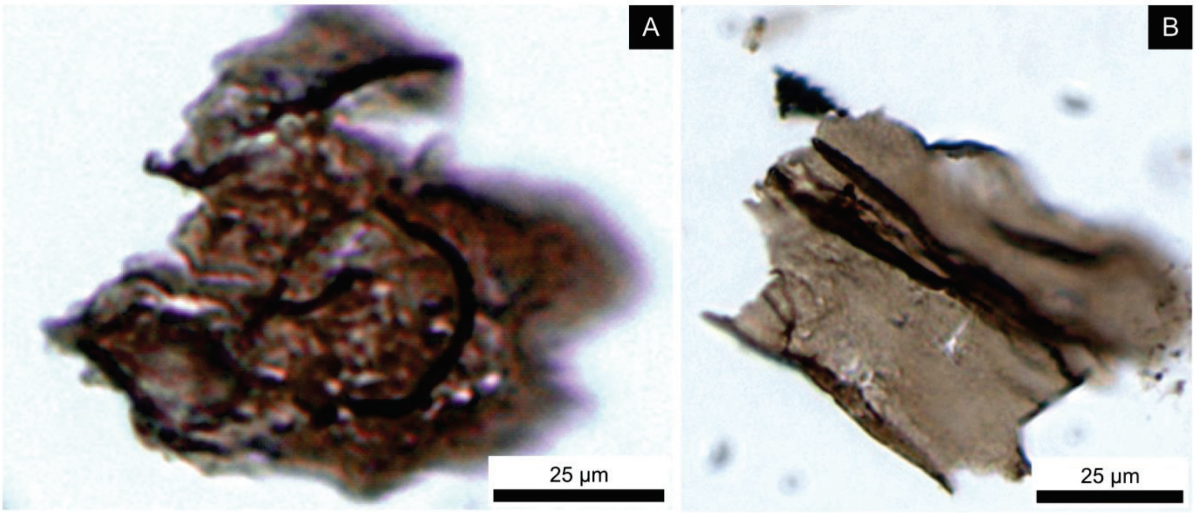

Fig. 1.6 Organically preserved microbial mat remains from the Shibantan Member.

1.3.3 Post-Ediacaran diversification of modern metazoan lineages

In the Cambrian most living metazoan phyla finally appeared in the fossil record (i.e. the '*Cambrian Explosion*' or '*Cambrian Radiation*'; e.g. Knoll and Caroll, 1999; Budd and Jensen, 2000; Valentine, 2002; Budd, 2003; Marshall, 2006; Erwin and Valentine, 2013; Zhang X. et al., 2014; and references therein). Various Cambrian fossil Lagerstätten are characterised by already highly diverse and exceptionally preserved (i.e. including soft-body preservation) fossil associations, with the lower Cambrian Chengjiang biota (Yunnan Province, south China) and the middle Cambrian Burgess Shale biota (British Columbia, Canada) being the most famous examples (e.g. Conway Morris, 1989, 1992; Briggs et al., 1995; Hou et al., 2004; Erwin and Valentine, 2013). The Cambrian diversification was also accompanied by the widespread occurrence of biomineralisation in numerous metazoan lineages (e.g. Bengtson and Conway Morris, 1992; Kouchinsky et al., 2012, and references therein) and the onset of vertical bioturbation by metazoans (i.e. the '*Agronomic Revolution*' or '*Cambrian Substrate Revolution*'; Seilacher and Pflüger, 1994; Bottjer et al., 2000; respectively). Despite the importance of developments in understanding the coevolution of life and Earth, causes and triggers are still poorly understood (cf. e.g. Butterfield, 2011; Kennedy, 2013). South China is particularly well suited in understanding these issues because of the exceptional preservation of various Ediacaran-lower Cambrian fossil Lagerstätten.

1.3.4 The Ediacaran Earth system

During the Cryogenian Period (850-635 Ma; i.e. directly prior to the Ediacaran; Fig. 1.1), the Earth was influenced by at least two prolonged episodes of glaciation (i.e. the Sturtian glaciation at ca. 720-660 Ma and the Marinoan glaciation at ca. 650-635 Ma; Shields-Zhou et al., 2012; and references therein). Some authors proposed that these glaciations were widespread across the globe ('*Snowball Earth*'-hypothesis; Kirschvink, 1992; Hoffman et al., 1998; Hoffman and Schrag, 2002), but this view has been challenged by others (e.g. Hyde et al., 2000; Eyles and Januszczak, 2004; Williams et al., 1998). The following Ediacaran Period, however, was only influenced by several regional and poorly constrained glaciation events such as the Gaskiers Glaciation (ca. 583 Ma; Bowring et al., 2003; Bowring, pers. comm. in Hoffman and Li, 2009; Fig. 1.1). Despite their regional character, these glaciations may have had a profound impact on the evolution of life on Earth. The first occurrence of a moderately diverse Ediacara-fauna, the Avalon Assemblage of Newfoundland (Tab. 1.1), has commonly been related to an oxygenation of deeper marine environments subsequent to the Gaskiers Glaciation (Canfield et al., 2007; Shen Y. et al., 2008; Johnston et al., 2012; Fig. 1.1). However, the relative timing of such evolutionary developments and, more importantly, the oxygenation (commonly referred to as Neoproterozoic Oxygenation Event; Och and Shields-Zhou, 2012), are still unclear (e.g. Och and Shields-Zhou, 2012; Johnston et al., 2013; Macdonald et al., 2013; Lyons et al., 2014). Consequently, a commonly proposed link between the establishment and radiation of complex multicellular life and oxygenation (e.g. Canfield et al., 2007; Shen Y. et al., 2008; Johnston et al., 2012; Och and Shields-Zhou, 2012; Sperling et al., 2013) has been questioned (e.g. Butterfield, 2009, 2011; Lyons et al., 2014). Palaeoecosystems with the earliest metazoan-grade fossils could aid in understanding the inter-relationship between environmental parameters and organisms if biogeochemical proxies are well preserved.

The fundamental change of biogeochemical cycles in the Ediacaran is reflected by the global occurrence of several strongly negative $\delta^{13}C_{carb}$ excursions (Knoll et al., 2004, 2006a; Narbonne et al., 2012; and references therein). For example, basal Ediacaran cap carbonates (i.e. distinct carbonate beds with thicknesses of several metres that sharply overly glacial deposits and surfaces worldwide) are characterised by $\delta^{13}C_{carb}$ values down to ca. -5‰ (Knoll et al., 2004, 2006a; Narbonne et al., 2012;

and references therein). Cap carbonates of the Doushantuo Formation in the working area are special by the local occurrence of $\delta^{13}C_{carb}$ values down to -41.2‰, which could indicate either anaerobic oxidation of methane during deposition (Jiang et al., 2003b, 2006a, b; Wang J. et al., 2008) or a post-depositional overprint by hydrothermal fluids (Bristow et al., 2011). Another profound negative $\delta^{13}C_{carb}$ excursion occurs in slightly younger strata, where $\delta^{13}C_{carb}$ values as high as +6‰ drop down to -12‰ (i.e. the '*Shuram excursion*'; Grotzinger et al., 2011; Narbonne et al., 2012; and references therein). Both excursions are also preserved in strata of the South China Craton (i.e. in the Doushantuo Formation in the working area; see 1.5.1 General stratigraphy) (e.g. Jiang et al., 2003b; Zhou C. et al., 2004; Condon et al., 2005; Jiang et al., 2007; Zhou C. and Xiao, 2007; Zhu et al., 2007; McFadden et al., 2008; Lu et al., 2013).

1.4 Tectonic framework

China consists of the Precambrian Tarim-, North China-, and South China Cratons, bounded by Phanerozoic fold belts (e.g. Zhao G. et al., 2001; Zhao G. and Cawood, 2012; and references therein; Fig. 1.7). The South China Craton is further subdivided into the Yangtze Block in the northwest and the Cathaysia Block in the southeast, separated by the Jiangnan Fold Belt (e.g. Zhao G. et al., 2001; Wang J. and Li, 2003; Zhao G. and Cawood, 2012; and references therein; Fig. 1.7). It is assumed that the Yangtze and Cathaysia Blocks amalgamated in the early to middle Neoproterozoic (i.e. ca. 1.000-800 Ma; e.g. Zhao G. and Cawood, 2012; and references therein), but the exact timing and the process of the collision is controversial. Some authors favour a collision during the Sibao-Jinning Orogeny as a part of the Grenvillian Orogeny (ca. 1000 Ma; Chen J. et al., 1991; Li Z. et al., 1995, 2003, 2008; Li X. et al., 2002; Ling W. et al., 2003; Li W. et al., 2005; Greentree et al., 2006; Ye et al., 2007), while others postulate much younger ages (ca. 870-800 Ma; Zhao G. and Cawood, 1999; Zhou M. et al., 2002a,b; Zhou J. et al., 2004; Zhao J. et al., 2011; Yao et al., 2014).

The general palaeogeography during the Neoproterozoic is still a subject of debate. However, there is consensus that a supercontinent existed during the Neoproterozoic, and most authors favour the 'Rodinia concept' (i.e. Laurentia as centre with all units of continental crust arranged around it; cf. Li Z. et al., 2008; Evans, 2013; and references therein; Fig. 1.8) over other models (e.g. the 'Palaeopangaea concept'; Piper, 2000, 2007). However, the configuration of Rodinia is contentious and the proposed positions of the South China Craton include, amongst others, a position (i) within (Li Z. et al., 1995, 2008, 2013; Li X., 1999; Evans et al., 2000; Greentree et al., 2006), (ii) adjacent to (Zhao G. and Cawood, 1999; Jiang et al., 2003a; Macouin et al., 2004; Cawood et al., 2013), or (iii) close to but isolated from Rodinia (Zhou M. et al., 2002b; Zhang S. et al., 2013).

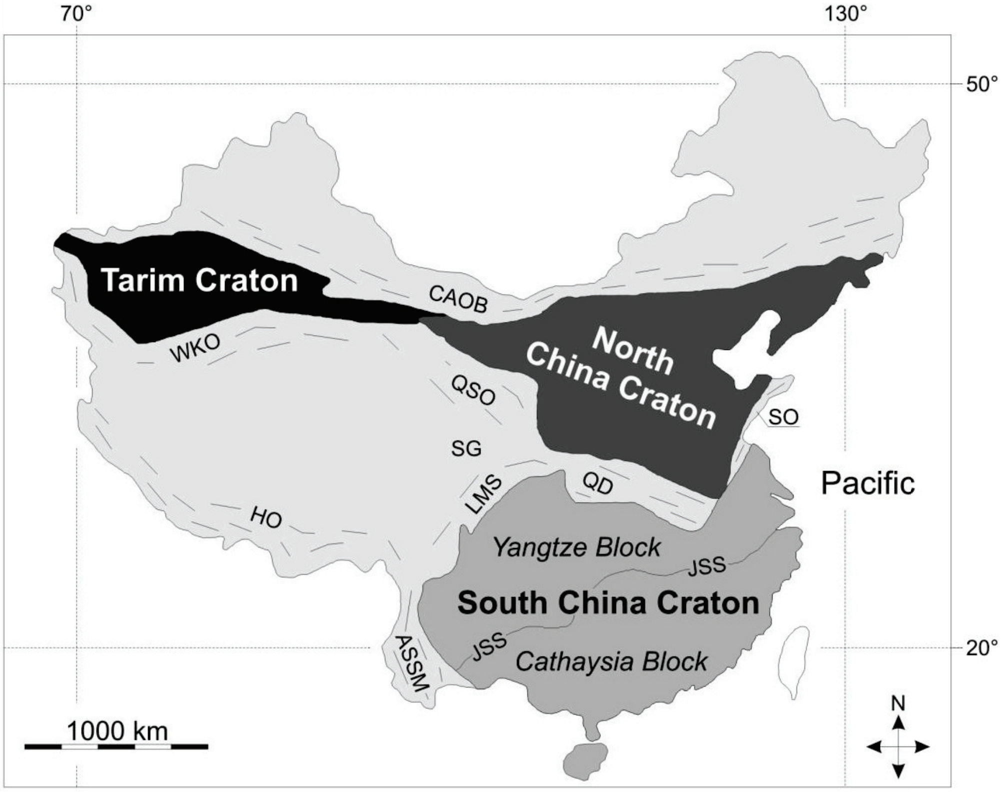

Fig. 1.7 Schematic tectonic map of China. The study area (approximate position marked by the star) is located on the Yangtze Block which is part of the South China Craton. CAOB: Central Asian Orogenic Belt; WKO: Western Kunlun Orogen; QSO: Qilinshan Orogen; HO: Himalayan Orogen; SG: Songpan-Gantze; LMS: Longmenshan; QD: Qinling-Dable; SO: Sulu Orogen; ASSM: Allaoshan-Song Ma; JSS: Jiangshan-Shaoxing suture. Modified after Zhao G. et al. (2001) and Zhao G. and Cawood (2012).

The migration path of the South China Craton is also ambiguously described in the literature. Some evidence shows that the South China Craton was situated at 55-70° N at ca. 800 Ma (Li Z. et al., 2004) but reached a mid-latitude position of 30-40° N by ca. 750 Ma (Liantuo Fm; Evans et al., 2000), being fairly in line with a proposed position of ca. 37° N between ca. 730-670 Ma (Nantuo Fm; Zhang Q. and Piper, 1997). This migration towards lower latitudes may have continued so that the South China Craton was centred at ca. 33° N by ca. 636 Ma (Nantuo Fm; Zhang S. et al., 2013), before it was finally positioned at ca. 3° N in the Ediacaran (Doushantuo Formation; Macouin et al., 2004). Therefore, an equatorial position of the South China Craton can tentatively be assumed during the deposition oft he Dengying Formation, although other reconstructions suggest a position at ca. 30° N (cf. Li Z. et al., 2008; Fig. 1.8).

The South China Craton was possibly affected by four phases of rifting between ca. 820-690 Ma, with the final phase coinciding with the Nantuo Glaciation (Wang J. and Li, 2003). The proposed rifting was potentially linked to the formation of a mantle superplume between ca. 825 Ma and 740 Ma, which caused widespread magmatism including, amongst others, granitoid intrusions such as the Huangling Granite (Li Z. et al., 1999, 2003, 2008; Li X. et al., 2002, 2003; Ling W. et al., 2003). However, other authors interpret the respective igneous rocks as being related to the collision between the Yangtze and Cathaysia Blocks, which would be inconsistent with rifting (Zhou J. et al., 2004; Wang X. et al., 2006). These conflicting interpretations are critical in the understanding of the NE-SW trending Nanhua Basin between the southeastern Yangtze Block and the northwestern Cathaysia Block (Fig. 1.7), which is explained by rifting processes (Wang J. and Li, 2003). Regardless of the different geodynamic interpretations it is generally accepted that the south China Craton became tectonically stable in the Ediacaran and was only influenced by thermal subsidence (Li Z. et al., 2003; Wan, 2010).

530 Ma (lower Cambrian)

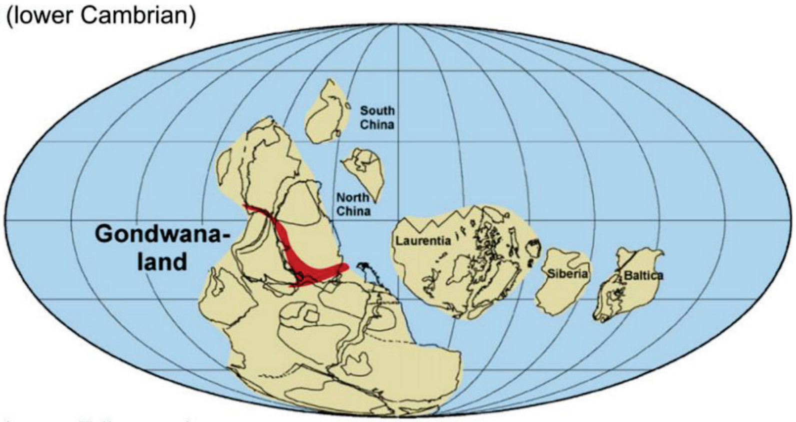

550 Ma (upper Ediacaran)

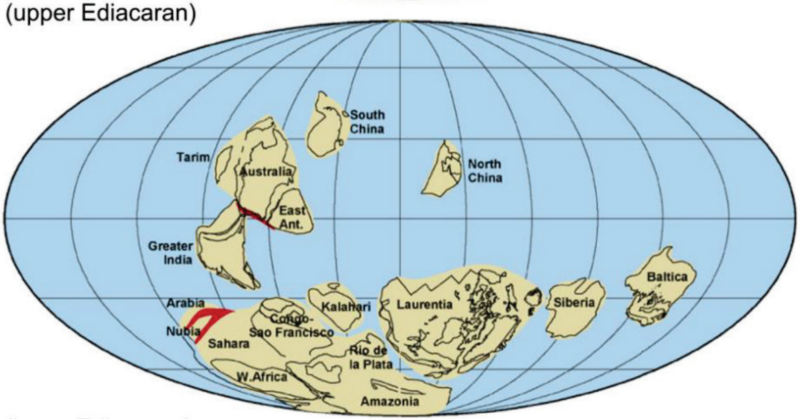

630 Ma (lower Ediacaran)

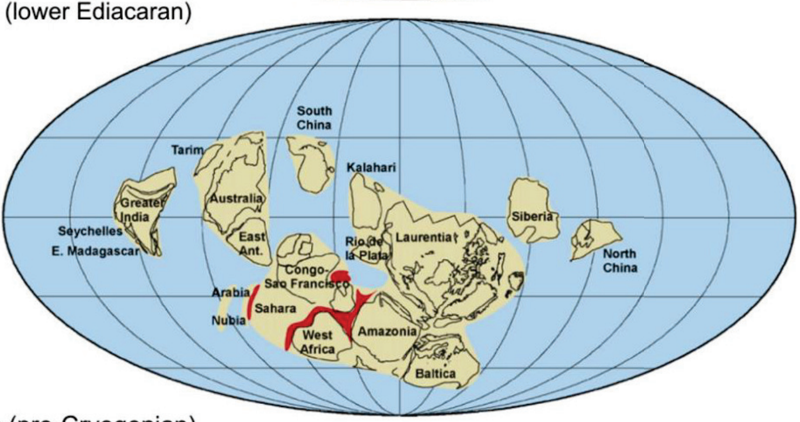

900 Ma (pre-Cryogenian)

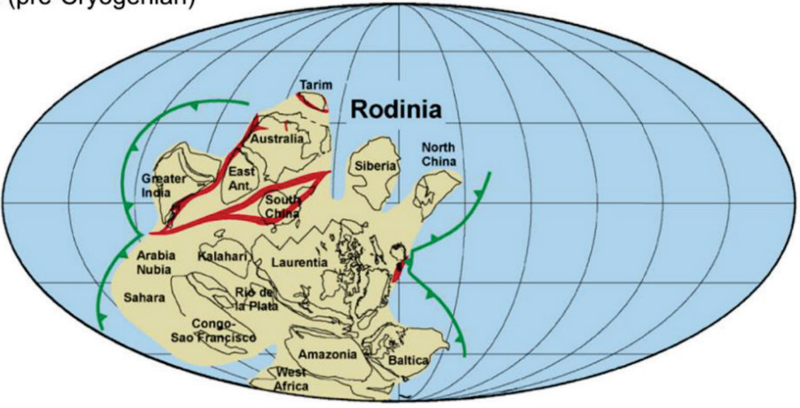

Fig. 1.8 Palaeogeographic reconstructions from pre-Cryogenian to lower Cambrian times including orogenies (red coloured areas) and active margins (green lines; modified after Li Z. et al., 2008).

1.5 Stratigraphy

1.5.1 General stratigraphy

The Huangling Granite is either unconformably overlain by the Cryogenian non-glacial Liantuo Formation (Fig. 1.9) or in tectonic contact to the Palaeoproterozoic amphibolite schists of the Kongling Group (Zhao Z. et al., 1988; Zhou C. et al., 2004; Du et al., 2013). These units are directly overlain by Cryogenian diamictites of the Nantuo Formation, which spread almost entirely over the Yangtze Block and record the Marinoan glaciation (e.g. Zhou C. et al., 2004; Condon et al., 2005; Zhang S. et al., 2008) (Fig. 1.9, 1.10a).

In the Yangtze Gorges area, the Ediacaran is represented by the Doushantuo Formation and the overlying Dengying Formation (e.g. Zhu et al., 2003, 2007; Fig. 1.9). The Doushantuo Formation is generally subdivided into 4 members, with the lowermost Member I (i.e. the cap carbonate; Fig. 1.10b) and the uppermost Member IV (i.e. a black shale containing the Miaohe biota; Fig. 1.10c; see 1.3.2 The Ediacaran biosphere) being particularly well-defined (e.g. Ding L. et al., 1996; Wang X. et al., 1998; Zhu et al., 2003, 2007). In contrast, lithostratigraphic subdivision of the middle part into members is commonly difficult because of substantial lateral facies variations (i.e. no clear or traceable differentiation between carbonate dominated and shale dominated parts; cf. Zhu et al., 2003, 2007). The Dengying Formation

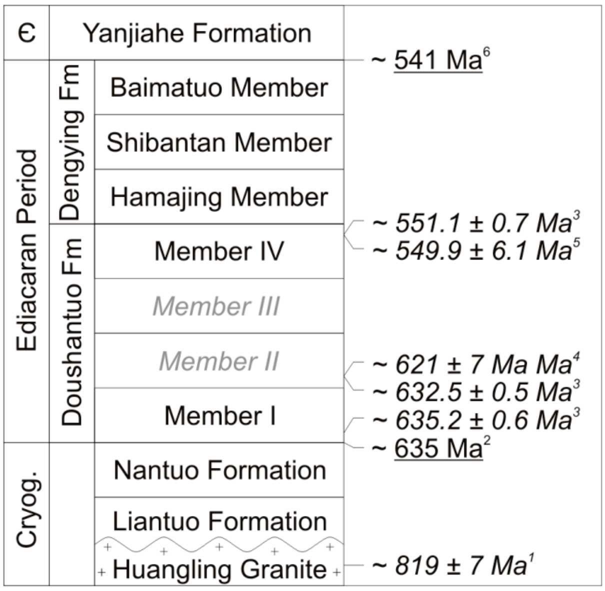

Fig. 1.9 Simplified stratigraphic framework for the Ediacaran in the Yangtze Gorges area (not to scale). Please note that the Palaeoproterozoic Kongling Group and the Cambrian Tianzhushan Member have not been considered, and that the definition of the Members II and III of the Doushantuo Formation is ambiguous because of substantial lateral facies variations (Zhu et al., 2003, 2007). Global boundary ages (underlined) and regional ages (italics) from (1) Ma et al. (1984), (2) Knoll et al. (2006a), (3) Condon et al. (2005), (4) Zhang S. et al. (2005), (5) Yin C. et al. (2005), (6) Peng et al. (2012) and Walker et al. (2013).

represents an extensive shallow water carbonate platform on the Yangtze Block (e.g. Cao et al., 1989; Zhou C. and Xiao, 2007; Jiang et al., 2011). In the working area it is subdivided into (in ascending order) the Ediacaran Hamajing-, Shibantan- and Baimatuo Members (Fig. 1.9), although the Cambrian Tianzhushan Member (only locally present in the eastern flank of the Huangling dome) is commonly integrated as well (e.g. Zhao Z. et al., 1985, 1988; Wang X. et al., 1998; Zhu et al., 2003; 2007; Dong et al., 2009). Other authors exclude the Tianzhushan Member from the Dengying Formation and consider it to be equivalent to the Cambrian Yanjiahe Formation, which overlies the Baimatuo Member in other parts of the Huangling Dome (Zhou C. and Xiao, 2007; Fig. 1.9, 1.10d).

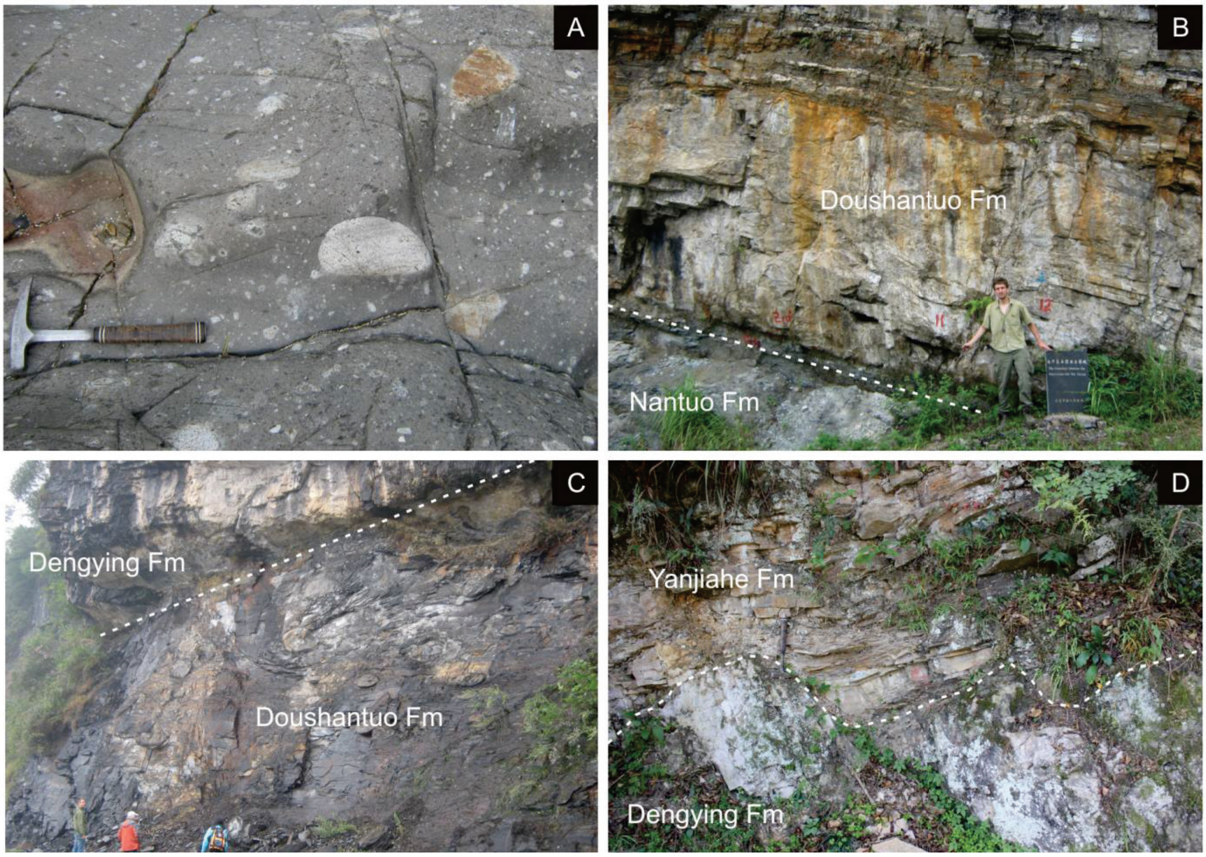

Fig. 1.10 Important stratigraphic units and bed contacts in south China (A in Anhui Province, B-D in the Yangtze Gorges area). (A) Glacial deposits of the Cryogenian Nantuo Formation (represents the Marinoan glaciation), south China. (B) Boundary between the Nantuo Formation (Cryogenian Period) and the Member I of the Doushantuo Formation (i.e. the cap carbonate; Ediacaran Period). (C) Boundary between the Member IV of the Doushantuo Formation and the Hamajing Member of the Dengying Formation. (D) Boundary between the Baimatuo Member of the Dengying Formation (Ediacaran Period) and the Yanjiahe Formation (Cambrian Period).

The Hamajing Member (10-200 m thickness; Zhu et al., 2007) consists of massive and thick-bedded light grey dolomites with intercalations of thin chert bands and concretions (Sun, 1986; Wang X. et al., 1998; Zhu et al., 2003, 2006, 2007; Zhou C. and Xiao, 2007). Large tepee structures, dissolution cavities, birds-eye structures, oolites, oncolites, intraclasts, and cross-bedding indicate a shallow peritidal environment (Wang X. et al., 1998; Zhu et al., 2003, 2007; Xiao et al., 2005; Zhou C. and Xiao, 2007; Shen B. et al., 2009; Chen Z. et al., 2013, 2014; Ling H. et al., 2013; Meyer et al., 2014).

The Shibantan Member (ca. 100-160 m thickness; Zhu et al., 2006, 2007; Zhou C. and Xiao, 2007) crops out very locally in the Yangtze Gorges area close to Yichang (Fig. 1.2), but was also reported from Shimen County (NW Hunan; ca. 140 km linear distance to sections in the Yangtze Gorges area), where it is only ca. 47 m thick (cf. Zhu et al., 2003). The base of the Shibantan Member is a transgressive surface and represents a major sequence boundary, allowing for correlation with the Gaojiashan Member and the Jiuchen Member of the Dengying Formation, which were deposited in small coastal basins on the north-western and south-western platform margins, respectively (Ding L. et al., 1992; Yin J., 1993; Wang X. et al., 1998; Zhu et al., 2003, 2007). In the Yangtze Gorges area, the sequence boundary is accompanied by a shift in $\delta^{13}C_{carb}$ from ca. +3 ‰ in the Hamajing Member to +5 ‰ in the Shibantan Member (Zhu et al., 2007).

The Shibantan Member consists mainly of black to dark grey thin-bedded and locally finely laminated bituminous limestones, including few chert bands and concretions (Sun, 1986; Wang X. et al., 1998; Zhu et al., 2003, 2006, 2007; Zhou C. and Xiao, 2007). The Shibantan Member was deposited in a lower subtidal environment below fair weather wave base (Sun, 1986; Xiao et al., 2005; Shen B. et al., 2009; Ling H. et al., 2013; Chen Z. et al., 2013, 2014), although cross stratification and rip-up clasts may indicate deposition above storm wave-base (Meyer et al., 2014). These preliminary interpretations are only based on insufficient sedimentological data, and many crucial aspects of the palaeoenvironment are still poorly understood. The Shibantan Member is characterised by a complex fossil association (see 1.3.2 The Ediacaran biosphere) and is therefore regarded as the stratigraphical equivalent of the Ediacara Member (Rawnsley Quartzite) in Australia (Sun, 1986; Steiner et al., 1993; Zhu et al., 2007).

The Baimatuo Member (40-570 m thick; Zhu et al., 2006, 2007; Zhou C. and Xiao, 2007) consists of light grey massive dolomites with chert bands or concretions (Sun, 1986; Wang X. et al., 1998).

Cross-stratification, birds-eye structures, as well as abundant evidence for dissolution and brecciation indicate a peritidal environment (Wang X. et al., 1998; Xiao et al., 2005; Zhou C. and Xiao, 2007; Zhu et al., 2007; Shen B. et al., 2009; Ling H. et al., 2013; Chen Z. et al., 2013, 2014; Meyer et al., 2014).

1.5.2 Radiometric ages

The Huangling Granite has a U-Pb zircon age of 819 ± 7 Ma (Ma et al., 1984) thus dating to the Cryogenian (Fig. 1.9). The Global Boundary Stratotype Section and Point (GSSP) of the following Ediacaran Period is placed at the base of the cap carbonate of the Nuccaleena Formation (Flinders Ranges, South Australia), which overlies glacial deposits of the Marinoan glaciation, dated at ca. 635 Ma (Fig. 1.1; Knoll et al., 2004, 2006a; Narbonne et al., 2012; and references therein). The cap carbonate in the lowermost part of the Doushantuo Formation (Fig. 1.10b) is radiometrically constrained by isotope dilution thermal ionisation mass spectrometric (ID-TIMS) and sensitive high resolution ion microprobe (SHRIMP) U-Pb zircon age determinations through ash beds preserved within (635.2 ± 0.6 Ma; Condon et al., 2005) and immediately above the member (632.5 ± 0.5 Ma and 621 ± 7 Ma; Condon et al., 2005; Zhang S. et al., 2005, respectively) (Fig. 1.9). These ages are further confirmed by SHRIMP U-Pb zircon dates of a fallout tuff preserved within the basal layer the glacial Nantuo Formation (636.3 ± 4.9 Ma; Zhang S. et al., 2008) and an ash bed close to the base of the Doushantuo Formation (628.3 ± 5.8 Ma; Yin C. et al., 2005).

The age of the Doushantuo-Dengying boundary (Fig. 1.10c) is constrained by ID-TIMS and SHRIMP U-Pb zircon ages of an ash bed that occurs about 85 cm below the base of the Dengying Formation (551.1 ± 0.7 Ma and 549.9 ± 6.1 Ma; Condon et al., 2005; Yin C. et al., 2005, respectively; Fig. 1.9). These age constraints clearly confirm the biostratigraphic correlation of the Shibantan Member with the Ediacara Member in Australia (Sun, 1986; Steiner et al., 1993; Zhu et al., 2007).

The upper boundary of the Ediacaran Period is defined by the base of the Cambrian (GSSP: placed at the base of the *Trichophycus pedum* ichnozone in the Fortune Head section, Newfoundland) (Brasier et al., 1994; Landing, 1994; Knoll et al., 2004, 2006a). The Precambrian-Cambrian boundary is provisionally dated at ca. 541 Ma (Peng et al., 2012; Walker et al., 2013). The upper boundary of the

Dengying Formation has not been radiometrically dated in the Yangtze Gorges area. However, since the Baimatuo Member of the Dengying Formation is directly overlain by Cambrian strata of a Meishucunian age (Guo et al., 2014; Fig. 1.10d), an age of ca. 541 Ma is tentatively assumed for its upper boundary (Fig. 1.9).

1.6 Methods overview

1.6.1 Sedimentology

Sedimentological data are important to reconstruct sedimentary processes, depositional environments, and the development of the sedimentary system through time. Sedimentological field work included the measurement of a sedimentary section and the documentation of important characteristics such as lithology, sedimentary structures, rock textures and fossils. These issues were complemented by conducting a detailed facies analysis of sample material from certain parts of the sedimentary section. Petrographical tools included observation of polished slabs and thin sections (e.g. reflected-, transmitted- and polarised light microscopy). This was helpful for identifying sedimentary structures and rock textures which are crucial for the interpretation of the facies but indistinctive otherwise. X-ray diffraction (XRD) and staining techniques were used for the differentiation of mineralogies. Staining techniques included the use of Alizarine red S for differentiating dolomite and calcite by staining calcite red, and potassium ferricyanid for differentiating ferroan and non-ferroan carbonates by staining iron-rich calcite and dolomite blueish (Flügel, 2004; and references therein).

1.6.2 Stable isotope signatures in carbonate phases

Stable isotope ratios of oxygen and carbon ($^{18}O/^{17}O$ and $^{13}C/^{12}C$; referred to as $\delta^{18}O$ and $\delta^{13}C$, respectively) are often used for reconstructing the depositional and diagenetic history of carbonate rocks and environmental controls on their formation (Kaufman and Knoll, 1995; Flügel, 2004; and references therein). However, syngenetic isotopic signatures may change in the course of diagenetic processes (e.g. cementation, dissolution and re-precipitation processes), and therefore substantial post-depositional alterations have to be excluded (Kaufman and Knoll, 1995; Flügel, 2004; Hoefs, 2009). This is particularly problematic if bulk samples are analysed since different mineral phases are potentially mixed. However, this was overcome by a precise sampling of selected mineral phases and sediment layers using a micro drill. Stable isotope abundances were measured with conventional gas mass spectrometer techniques.

1.6.3 Organic biomarkers and compound-specific stable isotope signatures

Organic biomarkers are organic molecules that can be unambiguously linked with biological precursor compounds (on geological scales commonly biological lipids); consequently they potentially provide information about present organism (-groups) and environmental conditions (e.g. Brocks and Summons, 2003; Killops and Killops, 2005; Peters et al 2005a, b). Compound-specific $\delta^{13}C$ signatures potentially provide information about biosynthetic pathways and source organisms (e.g. Freeman et al., 1990; Hayes et al., 1990; Hayes, 2001). Therefore, organic biomarkers and compound-specific $\delta^{13}C$ signatures provide the opportunity to gain insight into the geobiology of recent and ancient systems (e.g. Brocks and Summons, 2003; Killops and Killops, 2005; Peters et al 2005a, b).

Organic matter in fossil samples is commonly divided into a fraction which is soluble in organic solvents and a fraction that is insoluble in acids, bases, and organic solvents (bitumen and kerogen, respectively; e.g. Dow, 1977; Vandenbroucke and Largeau, 2007). In the case of the bitumen fraction, the biomarker inventory and compound-specific $\delta^{13}C$ signatures were conventionally analysed with coupled gas chromatography mass spectrometry (GC-MS) and gas chromatography combustion isotope ratio mass spectrometry (GC-C-IRMS), respectively.

The bitumen fraction is generally vulnerable to contamination on geological (i.e. by migrating petroleum-derived fluids) and anthropogenic scales (e.g. during exposure in the outcrop, sampling, storage, preparation, or analyses). Consequently, palaeoenvironmental interpretations are commonly hampered (e.g. Eigenbrode, 2004; Sherman et al., 2007; Brocks et al., 2008; Brocks, 2011). These problems can be overcome by analysing organic molecules that are covalently bound to the kerogen matrix (Fig. 1.11a). Kerogen formation (including the incorporation of biomolecules) is as yet only poorly understood but essentially includes a complex cascade of (poly-) condensation-, defunctionalisation- and insolubilisation reactions, probably modified by microbial processes (cf. e.g. Killops and Killops, 2005; Vandenbroucke and Largeau, 2007; and references therein). However, the kerogen fraction is generally considered to be less prone to contamination and immobile, so that covalently bonded molecular structures are likely syngenetic to the host rock (cf. Brocks et al., 2003).

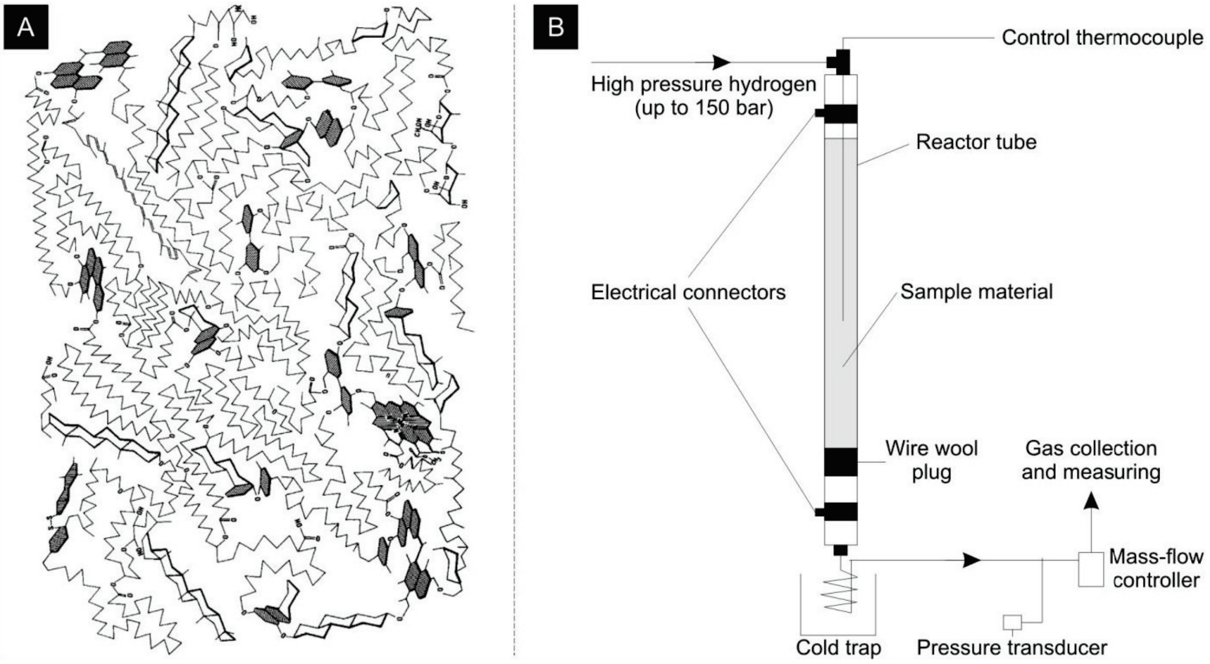

Fig. 1.11 Background information for the kerogen analysis. (A) Chemical model for a Kerogen at the beginning of diagenesis (from Behar and Vandenbroucke, 1987). (B) Sketch of the catalytic hydropyrolysis apparatus (modified after Love et al., 1995).

Catalytic hydropyrolysis (HyPy; Fig. 1.11) is a novel approach which allows for the release of high yields of covalently-bound hydrocarbons from the kerogen and to maintain their biologically-inherited stereochemistry largely intact (Love et al., 1995). Consequently, HyPy was successfully applied for numerous organic biomarker studies on Precambrian rocks (e.g. Brocks et al., 2003; Love et al., 2008; Love et al., 2009). Briefly, isolated kerogens or extraction residues are pyrolysed in a reactor tube by progressive heating from ambient temperature up to 500°C and a constant hydrogen pressure of 150 bar (Fig. 1.11b). Artificial alteration during this step due to oxygenation is inhibited by the hydrogen atmosphere and an admixed sulphided molybdenum catalyst. The constant hydrogen stream also ensures that the successively released hydrocarbons are immediately removed from the hot zone, thus minimising artificial alteration by temperature. The released compounds are subsequently trapped downstream in a dry ice cooled silica gel trap (Fig. 1.11b). This artificial bitumen can then be eluted with organic solvents and analysed as the bitumen fraction (i.e. via GC-MS and GC-C-IRMS; see above), as done in this study.

1.6.4 Trace element analysis of carbonate phases

Trace elemental proxies are well-established tools for the characterisation of environments and have successfully been used to reconstruct the redox state of Ediacaran seawater (e.g. Och and Shields-Zhou 2012; Shields-Zhou and Och, 2011, and references therein). Since mineral-precipitates in microbialites commonly reflect the trace element signature of the surrounding fluid (e.g. seawater) respective data can be used to characterise ancient microbial environments (e.g. Webb and Kamber, 2000, 2011; and references therein). On the other hand, putative microbialites can potentially be discriminated from abiogenic hydrothermal precipitates on this way, which for instance helped to support the biogenicity of ca. 3.5 Ga old stromatolites (Van Kranendonk et al., 2003). A further promising yet still poorly developed step is the possible detection of element-enrichments linked to microbial metabolisms in geological samples, which then could be used as biosignatures for microbial metabolisms (Webb and Kamber, 2004, 2011). However, the mixing of different geochemical signatures is a common problem in trace elemental analyses. This can e.g. be overcome by separating mineral phases by dissolution experiments, but separation of mineral phases or sediment layers sharing the same mineralogy is not possible. Therefore laser ablation inductively coupled plasma mass spectrometry (LA-ICP-MS) was used, allowing for qualitative and quantitative trace element analysis of surfaces with a high spatial resolution (10-120 µm) so that even small areas could be separately analysed.

1.7 Aims of the study and introduction into the following chapters

The Shibantan Member is one of only two known carbonate settings characterised by Ediacara-type fossils. Aim of this study was a comprehensive geobiological characterisation of the Shibantan Member, intergrating both sedimentological and biogeochemical aspects. To meet this aim, the following objectives have been addressed:

I. A detailed sedimentological characterisation of the Shibantan Member to reconstruct depositional environments, sedimentary processes, and the evolution of the depositional system (Chapter 2).
II. A biogeochemical analysis of the Shibantan facies characterised by Ediacara-type fossils to elucidate the interplay between sedimentary and (bio-) geochemical processes (Chapter 3).
III. A critical assessment of the possibilities and limitations of biomarker studies and an evaluation of the direct use of extraction residues for catalytic hydropyrolysis (HyPy) on thermally mature outcrop samples from the Shibantan Member (Chapter 4).

In this way, the complex interplay between tectonic-, sedimentary-, biogeochemical- and biological processes in the Shibantan Member was revealed (Chapter 5). Taken together, the results of this study help to understand the geobiology of palaeoecosystems with Ediacara-type fossils better and have to be considered in future discussions about the early evolution of metazoan life.

References

Albani, A.E., Bengtson, S., Canfield, D.E., Bekker, A., Macchiarelli, R., Mazurier, A., Hammarlund, E.U., Boulvais, P., Dupuy, J.-J., Fontaine, C., Fürsich, F.T., Gauthier-Lafaye, F., Janvier, P., Javaux, E., Ossa, F.O., Pierson-Wickmann, A.-C., Riboulleau, A., Sardini, P., Vachard, D., Whitehouse, M., Meunier, A., 2010. Large colonial organisms with coordinated growth in oxygenated environments 2.1Gyr ago. Nature 466, 100-104.

Amthor, J.E., Grotzinger, J.P., Schröder, S., Bowring, S.A., Ramezani, J., Martin, M.W., Matter, A., 2003. Extinction of Cloudina and Namacalathus at the Precambrian-Cambrian boundary in Oman. Geology 31, 431-434.

Antcliffe, J.B., 2013. Questioning the evidence of organic compounds called sponge biomarkers. Palaeontology 56, 917-925.

Antcliffe, J.B., Callow, R.H.T., Brasier, M.D., 2014. Giving the early fossil record of sponges a squeeze. Biological Reviews n/a, n/a.

Bailey, J.V., Joye, S.B., Kalanetra, K.M., Flood, B.E. and Corsetti, F.A., 2007. Evidence of giant sulphur bacteria in Neoproterozoic phosphorites. Nature 445, 198-201.

Barfod, G.H., Albarède, F., Knoll, A.H., Xiao, S., Télouk, P., Frei, R., Baker, J., 2002. New Lu-Hf and Pb-Pb age constraints on the earliest animal fossils. Earth and Planetary Science Letters 201, 203-212.

Behar, F., Vandenbroucke, M., 1987. Chemical modelling of kerogens. Organic Geochemistry 11, 15-24.

Bengtson, S., Conway Morris, S., 1992. Early Radiation of Biomineralizing Phyla. In: Lipps, J., Signor, P. (Eds.), Origin and Early Evolution of the Metazoa. Springer US, pp. 447-481.

Bengtson, S., Cunningham, J.A., Yin, C., Donoghue, P.C.J., 2012. A merciful death for the ‘earliest bilaterian,’ *Vernanimalcula*. Evolution & Development 14, 421-427.

Bengtson, S., Zhao, Y., 1992. Predatorial Borings in Late Precambrian Mineralized Exoskeletons. Science 257, 367-369.

Bottjer, D.J., Hagadorn, J.W., Dornbos, S.Q., 2000. The Cambrian Substrate Revolution. GSA Today 10, 1-7.

Bowring, S.A., Myrow, P., Landing, E., Ramezani, J. and Grotzinger, J., 2003. Geochronological constraints on terminal Neoproterozoic events and the rise of Metazoan, EGS - AGU - EUG Joint Assembly, Nice.

Brain, C.K.B., Prave, A.R., Hoffmann, K.-H., Fallick, A.E., Botha, A., Herd, D.A., Sturrock, C., Young, I., Condon, D.J., Allison, S.G., 2012. The first animals: ca. 760-million-year-old sponge-like fossils from Namibia. South African Journal of Science 108, 1-8.

Brasier, M., Green, O., Shields, G., 1997. Ediacarian sponge spicule clusters from southwestern Mongolia and the origins of the Cambrian fauna. Geology 25, 303-306.

Brasier, M.D., Cowie, J., Taylor, M., 1994. Decision on the Precambrian-Cambrian boundary stratotype. Episodes 17, 3-8.

Briggs, D.E.G., Erwin, D.H., Collier, F.J., 1995. The Fossils of the Burgess Shale. Smithsonian Books, Washington DC.

Bristow, T.F., Bonifacie, M., Derkowski, A., Eiler, J.M., Grotzinger, J.P., 2011. A hydrothermal origin for isotopically anomalous cap dolostone cements from south China. Nature 474, 68-71.

Brocks, J.J., 2011. Millimeter-scale concentration gradients of hydrocarbons in Archean shales: Live-oil escape or fingerprint of contamination? Geochimica et Cosmochimica Acta 75, 3196-3213.

Brocks, J.J., Grosjean, E., Logan, G.A., 2008. Assessing biomarker syngeneity using branched alkanes with quaternary carbon (BAQCs) and other plastic contaminants. Geochimica et Cosmochimica Acta 72, 871-888.

Brocks, J.J., Love, G.D., Snape, C.E., Logan, G.A., Summons, R.E., Buick, R., 2003. Release of bound aromatic hydrocarbons from late Archean and Mesoproterozoic kerogens via hydropyrolysis. Geochimica et Cosmochimica Acta 67, 1521-1530.

Brocks, J.J., Summons, R.E., 2003. Sedimentary Hydrocarbons, Biomarkers for Early Life. In: Heinrich, D.H., Karl, K.T. (Eds.), Treatise on Geochemistry. Pergamon, Oxford, pp. 63-115.

Budd, G.E., 2003. The Cambrian Fossil Record and the Origin of the Phyla. Integrative and Comparative Biology 43, 157-165.

Budd, G.E., Jensen, S., 2000. A critical reappraisal of the fossil record of the bilaterian phyla. Biological Reviews 75, 253-295.

Butterfield, N., Knoll, A., Swett, K., 1990. A bangiophyte red alga from the Proterozoic of arctic Canada. Science 250, 104-107.

Butterfield, N.J., 2000. *Bangiomorpha pubescens* n. gen., n. sp.: implications for the evolution of sex, multicellularity, and the Mesoproterozoic/Neoproterozoic radiation of eukaryotes. Paleobiology 26, 386-404.

Butterfield, N.J., 2009. Oxygen, animals and oceanic ventilation: an alternative view. Geobiology 7, 1-7.

Butterfield, N.J., 2011. Animals and the invention of the Phanerozoic Earth system. Trends in Ecology & Evolution 26, 81-87.

Cai, Y., Hua, H. and Zhang, X., 2013. Tube construction and life mode of the late Ediacaran tubular fossil *Gaojiashania cyclus* from the Gaojiashan Lagerstätte. Precambrian Research 224, 255-267.

Cai, Y., Hua, H., Schiffbauer, J.D., Sun, B., Yuan, X., 2014. Tube growth patterns and microbial mat-related lifestyles in the Ediacaran fossil *Cloudina*, Gaojiashan Lagerstätte, South China. Gondwana Research 25, 1008-1018.

Cai, Y., Hua, H., Xiao, S., Schiffbauer, J.D., Li, P., 2010. Biostratinomy of the Late Ediacaran Pyritized Gaojiashan Lagerstätte from Southern Shaanxi, South China: Importance of Event Deposits. PALAIOS 25, 487-506.

Cai, Y., Schiffbauer, J.D., Hua, H., Xiao, S., 2011. Morphology and paleoecology of the late Ediacaran tubular fossil *Conotubus hemiannulatus* from the Gaojiashan Lagerstätte of southern Shaanxi Province, South China. Precambrian Research 191, 46-57.

Callow, R.H.T., Brasier, M.D., 2009. Remarkable preservation of microbial mats in Neoproterozoic siliciclastic settings: Implications for Ediacaran taphonomic models. Earth-Science Reviews 96, 207-219.

Canfield, D.E., Poulton, S.W., Narbonne, G.M., 2007. Late-Neoproterozoic Deep-Ocean Oxygenation and the Rise of Animal Life. Science 315, 92-95.

Cao, R., Tang, T., Xue, Y., Yu, C., Yin, L., Zhao, W., 1989. Research on Sinian Strata with ore deposits in the Yangzi (Yangtze) region, China. In: Nanjing Institute of Geology and Palaeontology (Eds.), Upper Precambrian of the Yangzi (Yangtze) Region, China. Nanjing University Press, Nanjing, pp. 1-94.

Cawood, P.A., Wang, Y., Xu, Y., Zhao, G., 2013. Locating South China in Rodinia and Gondwana: A fragment of greater India lithosphere? Geology 41, pp. 903-906.

Chen, D., Dong, W., Zhu, B., Chen, X., 2004. Pb-Pb ages of Neoproterozoic Doushantuo phosphorites in South China: constraints on early metazoan evolution and glaciation events. Precambrian Research 132, 123-132.

Chen, J., Bottjer, D.J., Oliveri, P., Dornbos, S.Q., Gao, F., Ruffins, S., Chi, H., Li, C., Davidson, E.H., 2004. Small Bilaterian Fossils from 40 to 55 Million Years Before the Cambrian. Science 305, 218-222.

Chen, J., Foland, K.A., Xing, F., Xu, X., Zhou, T., 1991. Magmatism along the southeast margin of the Yangtze block: Precambrian collision of the Yangtze and Cathysia blocks of China. Geology 19, 815-818.

Chen, J., Oliveri, P., Gao, F., Dornbos, S.Q., Li, C., Bottjer, D.J., Davidson, E.H., 2002. Precambrian Animal Life: Probable Developmental and Adult Cnidarian Forms from Southwest China. Developmental Biology 248, 182-196.

Chen, J., Oliveri, P., Li, C., Zhou, G., Gao, F., Hagadorn, J.W., Peterson, K.J., Davidson, E.H., 2000. Precambrian animal diversity: Putative phosphatized embryos from the Doushantuo Formation of China. Proceedings of the National Academy of Sciences 97, 4457-4462.

Chen, M., Chen, Y., Qiang, Y., 1981. Some tubular fossils from Sinian-Lower Cambrian boundary sequence, Yangtze Gorges. Tianjin Institute of Geology and Mineral Resources Bulletin 3, 117-124.

Chen, M., Wang, Y., 1977. Note on the tubular metazoan fossils from the Dengying Formation of the upper Sinian System in the Gorge District of the Yangtze River. Chinese Science Bulletin 22, 219-221.

Chen, Y., Jiang, S., Ling, H., Yang, J., 2009. Pb–Pb dating of black shales from the Lower Cambrian and Neoproterozoic strata, South China. Chemie der Erde - Geochemistry 69, 183-189.

Chen, Z., 1999. Late Sinian Metazoan Tubular Fossils from Western Hubei and Southern Shaanxi, China. Nanjing Institute of Geology and Paleontology, Chinese Academy of Science, Nanjing.

Chen, Z., Bengtson, S., Zhou, C.M., Hua, H., Yue, Z., 2008. Tube structure and original composition of *Sinotubulites*: shelly fossils from the late Neoproterozoic in southern Shaanxi, China. Lethaia 41, 37-45.

Chen, Z., Zhou, C., Meyer, M., Xiang, K., Schiffbauer, J.D., Yuan, X. Xiao, S., 2013. Trace fossil evidence for Ediacaran bilaterian animals with complex behaviors. Precambrian Research 224, 690-701.

Chen, Z., Zhou, C., Xiao, S., Wang, W., Guan, C., Hua, H., Yuan, X., 2014. New Ediacara fossils preserved in marine limestone and their ecological implications. Scientific Reports 4, 1-10

Cohen, B.L., 2005. Not armour, but biomechanics, ecological opportunity and increased fecundity as keys to the origin and expansion of the mineralized benthic metazoan fauna. Biological Journal of the Linnean Society 85, 483-490.

Cohen, P.A., Bradley, A., Knoll, A.H., Grotzinger, J.P., Jensen, S., Abelson, J., Hand, K., Love, G., Metz, J., McLoughlin, N., Mesiter, P., Shepard, R., Tice, M., Wilson, J.P., 2009. Tubular Compression Fossils from the Ediacaran Nama Group, Namibia. Journal of Paleontology 83, 110-122.

Condon, D., Zhu, M., Bowring, S., Wang, W., Yang, A., Jin, Y., 2005. U-Pb Ages from the Neoproterozoic Doushantuo Formation, China. Science 308, 95-98.

Conway Morris, S., 1989. Burgess Shale Faunas and the Cambrian Explosion. Science 246, 339-346.

Conway Morris, S., 1992. Burgess Shale-type faunas in the context of the ‘Cambrian explosion’: a review. Journal of the Geological Society 149, 631-636.

Conway Morris, S., Mattes, B.W., Menge, C., 1990. The early skeletal organism *Cloudina*: New occurrences from Oman and possibly China. American Journal of Science 290-A, 245-260.

Degens, E.T., Kaźmierczak, J., Ittekkot, V., 1985. Cellular response to Ca^{2+} stress and its geological implications. Acta Palaeontologica Polonica 30, 115-135.

Ding, L., Li, Y., Hu, X., Xiao, Y., Su, C., Huang, J., 1996. Sinian Miaohe Biota. Geological Publishing House, Beijing

Ding, L., Zhang, L., Li, Y., Dong, J., 1992. The Study of the Late Sinian-Early Cambrian Biota from the Northern Margin of Yangtze Platform. Scientific and Technical Documents Publishing House, Beijing

Ding, Q., Chen, Y., 1981. Discovery of soft metazoan from the Sinian System along eastern Yangtze Gorge, Hubei. Journal of the Wuhan College of Geology 2, 53-57.

Ding, Q., Xing, Y., Wang, Z., Yin, C., Gao, L., 1993. Tubular and Trace Fossils from the Sinian Dengying Formation in the Miaohe-Liantuo Area, Hubei Province. Geological Review 39, 118-123

Dong, L., Xiao, S., Shen, B., Zhou, C., Li, G., Yao, J. 2009. Basal Cambrian Microfossils from the Yangtze Gorges Area (South China) and the Aksu Area (Tarim Block, Northwestern China). Journal of Paleontology 83, 30-44.

Dow, W.G., 1977. Kerogen studies and geological interpretations. Journal of Geochemical Exploration 7, 79-99.

Du, Q., Wang, Z., Wang, J., Qiu, Y., Jiang, X., Deng, Q., Yang, F., 2013. Geochronology and paleoenvironment of the pre-Sturtian glacial strata: Evidence from the Liantuo Formation in the Nanhua rift basin of the Yangtze Block, South China. Precambrian Research 233, 118-131.

Dzik, J., 2002. Possible ctenophoran affinities of the precambrian ‘sea-pen’ *Rangea*. Journal of Morphology 252: 315-334.

Eigenbrode, J., 2004. Late Archean Microbial Ecology: An Integration of Molecular, Isotopic and Lithologic Studies, Department of Geosciences. Pennsylvania State University

Erwin, D.H., Laflamme, M., Tweedt, S.M., Sperling, E.A., Pisani, D., Peterson, K.J., 2011. The Cambrian Conundrum: Early Divergence and Later Ecological Success in the Early History of Animals. Science 334, 1091-1097.

Erwin, D.H., Valentine, J.W., 2013. The Cambrian Explosion: The construction of animal biodiversity. Roberts and Company Publishers Inc., Greenwood Village.

Evans, D.A.D., 2013. Reconstructing pre-Pangean supercontinents. Geological Society of America Bulletin 125, 1735-1751.

Evans, D.A.D., Li, Z.X., Kirschvink, J.L., Wingate, M.T.D., 2000. A high-quality mid-Neoproterozoic paleomagnetic pole from South China, with implications for ice ages and the breakup configuration of Rodinia. Precambrian Research 100, 313-334.

Eyles, N., Januszczak, N., 2004. 'Zipper-rift': a tectonic model for Neoproterozoic glaciations during the breakup of Rodinia after 750 Ma. Earth-Science Reviews 65, 1-73.

Fedonkin, M.A., 1990. Systematic Description of Vendian Metazoa. In: Sokolov, B.S., Iwanowski, A.B. (Eds.), The Vendian System. Springer, Berlin, pp. 71-120.

Fedonkin, M.A., Waggoner, B.M., 1997. The Late Precambrian fossil Kimberella is a mollusc-like bilaterian organism. Nature 388, 868-871.

Flügel, E., 2004. Microfacies of Carbonate Rocks. Analysis, Interpretation and Application., 2nd ed. Springer, Berlin, Heidelberg.

Freeman, K.H., Hayes, J.M., Trendel, J.-M., Albrecht, P., 1990. Evidence from carbon isotope measurements for diverse origins of sedimentary hydrocarbons. Nature 343, 254-256.

Gehling, J.G., Droser, M.L., Jensen, S., Runnegar, B.N., 2005. Ediacaran organisms: relating form to function. In: Briggs, D.E.G. (Ed.), Evolving Form and Function: Fossils and Development. Peabody Museum of Natural History, New Haven, pp. 43-66.

Germs, G.J.B., 1972. New shelly fossils from the Nama Group, South West Africa. American Journal of Science 272, 752-761.

Glaessner, M.F., 1976. Early Phanerozoic annelid worms and their geological and biological significance. Journal of the Geological Society 132, 259-275.

Gnilovskaya, M.B., 1990. Vendian metaphytes. In: Sokolov B.S., Iwanowski, A.B. (Eds.), The Vendian System. Springer, Berlin, pp. 138-147.

Grant, 1990. Shell structure and distribution of Cloudina, a potential index fossil for the terminal Proterozoic. American Journal of Science, 290-A: 261-294.

Grazhdankin, D. 2004. Patterns of distribution in the Ediacaran biotas: facies versus biogeography and evolution. Paleobiology 30, 203-221

Grazhdankin, D.V., Balthasar, U., Nagovitsin, K.E., Kochnev, B.B., 2008. Carbonate-hosted Avalon-type fossils in arctic Siberia. Geology 36, 803-806

Greentree, M.R., Li, Z.-X., Li, X.-H., Wu, H., 2006. Late Mesoproterozoic to earliest Neoproterozoic basin record of the Sibao orogenesis in western South China and relationship to the assembly of Rodinia. Precambrian Research 151, 79-100.

Grotzinger, J., Adams, E.W., Schröder, S., 2005. Microbial–metazoan reefs of the terminal Proterozoic Nama Group (c. 550–543 Ma), Namibia. Geological Magazine 142, 499-517.

Grotzinger, J.P., Fike, D.A., Fischer, W.W., 2011. Enigmatic origin of the largest-known carbon isotope excursion in Earth's history. Nature Geoscience 4, 285-292.

Grotzinger, J.P., Watters, W.A., Knoll, A.H., 2000. Calcified metazoans in thrombolite-stromatolite reefs of the terminal Proterozoic Nama Group, Namibia. Paleobiology 26, 334-359.

Guo, J., Li, Y., Li, G., 2014. Small shelly fossils from the early Cambrian Yanjiahe Formation, Yichang, Hubei, China. Gondwana Research 25: 999-1007.

Hayes, J.M., 2001. Fractionation of Carbon and Hydrogen Isotopes in Biosynthetic Processes. Reviews in Mineralogy and Geochemistry 43, 225-277.

Hayes, J.M., Freeman, K.H., Popp, B.N., Hoham, C.H., 1990. Compound-specific isotopic analyses: A novel tool for reconstruction of ancient biogeochemical processes. Organic Geochemistry 16, 1115-1128.

Hoefs, J., 2009. Stable Isotope Geochemistry, 6 ed. Springer, Berlin, Heidelberg.

Hoffman, P.F., Kaufman, A.J., Halverson, G.P., Schrag, D.P., 1998. A Neoproterozoic Snowball Earth. Science 281, 1342-1346.

Hoffman, P.F., Li, Z.-X., 2009. A palaeogeographic context for Neoproterozoic glaciation. Palaeogeography, Palaeoclimatology, Palaeoecology 277, 158-172.

Hoffman, P.F., Schrag, D.P., 2002. The snowball Earth hypothesis: testing the limits of global change. Terra Nova 14, 129-155.

Hofmann, H.J., 1992. Proterozoic carbonaceous films. In: Schopf, J.W., Klein, C. (Eds.), The Proterozoic biosphere: A multidisciplinary study. Cambridge University Press, Cambridge, pp. 349-357.

Hofmann, H.J., Mountjoy, E.W., 2001. Namacalathus-Cloudina assemblage in Neoproterozoic Miette Group (Byng Formation), British Columbia: Canada's oldest shelly fossils. Geology 29, 1091-1094.

Hofmann, H.J., Narbonne, G.M., Aitken, J.D., 1990. Ediacaran remains from intertillite beds in northwestern Canada. Geology 18, 1199-1202.

Hou, X.-G., Aldridge, R.J., Bergstrom, J., Siveter, D.J., Siveter, D.J., Feng, X.-H., 2004. The Cambrian Fossils of Chengjiang, China: The Flowering of Early Animal Life. Blackwell Publishing, Malden.

Hua, H., Chen, Z., Yuan, X., Zhang, L., Xiao, S., 2005. Skeletogenesis and asexual reproduction in the earliest biomineralizing animal *Cloudina*. Geology 33, 277-280.

Hua, H., Pratt, B.R., Zhang, L.-Y., 2003. Borings in *Cloudina* Shells: Complex Predator-Prey Dynamics in the Terminal Neoproterozoic. PALAIOS 18, 454-459.

Huldtgren, T., Cunningham, J.A., Yin, C., Stampanoni, M., Marone, F., Donoghue, P.C.J., Bengtson, S., 2011. Fossilized Nuclei and Germination Structures Identify Ediacaran ‘Animal Embryos’ as Encysting Protists. Science 334, 1696-1699.

Hyde, W.T., Crowley, T.J., Baum, S.K., Peltier, W.R., 2000. Neoproterozoic 'snowball Earth' simulations with a coupled climate/ice-sheet model. Nature 405, 425-429.

Javaux, E., 2011. 26 - Early eukaryotes in Precambrian oceans. In: Gargaud, M., López-Garcìa, P., Martin, H. (Eds.), Origins and Evolution of Life: An Astrobiological Perspective. Cambridge University Press, Cambridge, pp. 414-449.

Javaux, E.J., Knoll, A.H., Walter, M.R., 2001. Morphological and ecological complexity in early eukaryotic ecosystems. Nature 412, 66-69.

Jensen, S., Droser, M., Gehling, J., 2006. A Critical Look at the Ediacaran Trace Fossil Record. In: Xiao, S., Kaufman, A.J. (Eds.), Neoproterozoic Geobiology and Paleobiology. Topics in Geobiology. Springer Netherlands, pp. 115-157.

Jiang, G., Christie-Blick, N., Kaufman, A.J., Banerjee, D.M., Rai, V., 2003a. Carbonate platform growth and cyclicity at a terminal Proterozoic passive margin, Infra Krol Formation and Krol Group, Lesser Himalaya, India. Sedimentology 50, 921-952.

Jiang, G., Kaufman, A.J., Christie-Blick, N., Zhang, S., Wu, H., 2007. Carbon isotope variability across the Ediacaran Yangtze platform in South China: Implications for a large surface-to-deep ocean δ^{13}C gradient. Earth and Planetary Science Letters 261, 303-320.

Jiang, G., Kennedy, M.J., Christie-Blick, N., 2003b. Stable isotopic evidence for methane seeps in Neoproterozoic postglacial cap carbonates. Nature 426, 822-826.

Jiang, G., Kennedy, M.J., Christie-Blick, N., Wu, H., Zhang, S., 2006a. Stratigraphy, Sedimentary Structures, and Textures of the Late Neoproterozoic Doushantuo Cap Carbonate in South China. Journal of Sedimentary Research 76, 978-995.

Jiang, G., Shi, X., Zhang, S., 2006b. Methane seeps, methane hydrate destabilization, and the late Neoproterozoic postglacial cap carbonates. Chinese Science Bulletin 51, 1152-1173.

Jiang, G., Shi, X., Zhang, S., Wang, Y., Xiao, S., 2011. Stratigraphy and paleogeography of the Ediacaran Doushantuo Formation (ca. 635-551 Ma) in South China. Gondwana Research 19, 831-849.

Johnston, D.T., Poulton, S.W., Goldberg, T., Sergeev, V.N., Podkovyrov, V., Vorob’eva, N.G., Bekker, A., Knoll, A.H., 2012. Late Ediacaran redox stability and metazoan evolution. Earth and Planetary Science Letters 335-336, 25-35.

Johnston, D.T., Poulton, S.W., Tosca, N.J., O’Brien, T.O., Halverson, G.P., Schrag, D.P., Macdonald, F.A., 2013. Searching for an oxygenation event in the fossiliferous Ediacaran of northwestern Canada. Chemical Geology 362, 273-286.

Kaufman, A.J., Knoll, A.H., 1995. Neoproterozoic variations in the C-isotopic composition of seawater: stratigraphic and biogeochemical implications. Precambrian Research 73, 27-49.

Kaźmierczak, J., Ittekkot, V., Degens, E., 1985. Biocalcification through time: environmental challenge and cellular response. Paläontologische Zeitschrift 59, 15-33.

Kelly, A.E., 2009. Hydrocarbon Biomarkers for Biotic and Environmental Evolution through the Neoproterozoic-Cambrian Transition. PhD-thesis Thesis, Massachusetts Institute of Technology, Cambridge, 154 pp.

Kennedy, M., 2013. The Nonlinear Effects of Evolutionary Innovation Biospheric Feedbacks on Qualitative Environmental Change: From the Microbial to Metazoan World. The American Naturalist 181, S100-S111.

Khomentovsky, V.V., 1990. Vendian of the Siberian Platform. In: Sokolov, B.S., Fedonkin, M.A. (Eds.), The Vendian System. Springer, Berlin, pp. 102-183.

Killops, S.D., Killops, V.J., 2005. Introduction to Organic Geochemistry, 2 ed. Wiley-Blackwell.

Kirschvink, J.L., 1992. Late Proterozoic Low-Latitude Global Glaciation: the Snowball Earth. In: Schopf, J.W., Klein, C. (Eds.), The Proterozoic Biosphere: A Multidisciplinary Study. Cambridge University Press, Cambridge, pp. 51-52.

Knoll, A., Walter, M., Narbonne, G.M., Christie-Blick, N., 2006a. The Ediacaran Period: a new addition to the geologic time scale. Lethaia 39, 13-30.

Knoll, A.H., 2000. Learning to tell Neoproterozoic time. Precambrian Research 100, 3-20.

Knoll, A.H., Carroll, S.B., 1999. Early Animal Evolution: Emerging Views from Comparative Biology and Geology. Science 284, 2129-2137.

Knoll, A.H., Grotzinger, J.P., Kaufman, A.J., Kolosov, P., 1995. Integrated approaches to terminal Proterozoic stratigraphy: an example from the Olenek Uplift, northeastern Siberia. Precambrian Research 73, 251-270.

Knoll, A.H., Javaux, E.J., Hewitt, D., Cohen, P., 2006b. Eukaryotic organisms in Proterozoic oceans. Philosophical Transactions of the Royal Society B: Biological Sciences 361, 1023-1038.

Knoll, A.H., Walter, M.R., 1992. Latest Proterozoic stratigraphy and Earth history. Nature 356, 673-678.

Knoll, A.H., Walter, M.R., Narbonne, G.M., Christie-Blick, N., 2004. A New Period for the Geologic Time Scale. Science 305, 621-622.

Kouchinsky, A., Bengtson, S., Runnegar, B., Skovsted, C., Steiner, M., Vendrasco, M., 2012. Chronology of early Cambrian biomineralization. Geological Magazine 149, 221-251.

Landing, E., 1994. Precambrian-Cambrian boundary global stratotype ratified and a new perspective of Cambrian time. Geology 22, 179-182.

Li, C., Chen, J., Hua, T., 1998. Precambrian Sponges with Cellular Structures. Science 279, 879-882.

Li, W., Li, X., Li, Z., 2005. Neoproterozoic bimodal magmatism in the Cathaysia Block of South China and its tectonic significance. Precambrian Research 136, 51-66.

Li, X., 1999. U-Pb zircon ages of granites from the southern margin of the Yangtze Block: timing of Neoproterozoic Jinning: Orogeny in SE China and implications for Rodinia Assembly. Precambrian Research 97, 43-57.

Li, X., Li, Z., Ge, W., Zhou, H., Li, W., Liu, Y., Wingate, M.T.D., 2003. Neoproterozoic granitoids in South China: crustal melting above a mantle plume at ca. 825 Ma? Precambrian Research 122, 45-83.

Li, X., Li, Z., Zhou, H., Liu, Y., Kinny, P.D., 2002. U-Pb zircon geochronology, geochemistry and Nd isotopic study of Neoproterozoic bimodal volcanic rocks in the Kangdian Rift of South China: implications for the initial rifting of Rodinia. Precambrian Research 113, 135-154.

Li, Z., Bogdanova, S.V., Collins, A.S., Davidson, A., De Waele, B., Ernst, R.E., Fitzsimons, I.C.W., Fuck, R.A., Gladkochub, D.P., Jacobs, J., Karlstrom, K.E., Lu, S., Natapov, L.M., Pease, V., Pisarevsky, S.A., Thrane, K., Vernikovsky, V., 2008. Assembly, configuration, and break-up history of Rodinia: A synthesis. Precambrian Research 160, 179-210.

Li, Z., Evans, D.A.D., Halverson, G.P., 2013. Neoproterozoic glaciations in a revised global palaeogeography from the breakup of Rodinia to the assembly of Gondwanaland. Sedimentary Geology 294, 219-232.

Li, Z., Evans, D.A.D., Zhang, S., 2004. A 90° spin on Rodinia: possible causal links between the Neoproterozoic supercontinent, superplume, true polar wander and low-latitude glaciation. Earth and Planetary Science Letters 220, 409-421.

Li, Z., Li, X., Kinny, P.D., Wang, J., 1999. The breakup of Rodinia: did it start with a mantle plume beneath South China? Earth and Planetary Science Letters 173, 171-181.

Li, Z., Li, X., Kinny, P.D., Wang, J., Zhang, S., Zhou, H., 2003. Geochronology of Neoproterozoic syn-rift magmatism in the Yangtze Craton, South China and correlations with other continents: evidence for a mantle superplume that broke up Rodinia. Precambrian Research 122, 85-109.

Li, Z., Zhang, L., Powell, C.M., 1995. South China in Rodinia: Part of the missing link between Australia-East Antarctica and Laurentia? Geology 23, 407-410.

Ling, H., Chen, X., Li, D., Wang, D., Shields-Zhou, G.A., Zhu, M., 2013. Cerium anomaly variations in Ediacaran-earliest Cambrian carbonates from the Yangtze Gorges area, South China: Implications for oxygenation of coeval shallow seawater. Precambrian Research 225, 110-127.

Ling, W., Gao, S., Zhang, B., Li, H., Liu, Y., Cheng, J., 2003. Neoproterozoic tectonic evolution of the northwestern Yangtze craton, South China: implications for amalgamation and break-up of the Rodinia Supercontinent. Precambrian Research 122, 111-140.

Liu, P., Xiao, S., Yin, C., Chen, S., Zhou, C., Li, M., 2014. Ediacaran Acanthomorphic Acritarchs and Other Microfossils From Chert Nodules of the Upper Doushantuo Formation in the Yangtze Gorges Area, South China. Journal of Paleontology 88, 1-139.

Liu, P., Yin, C., Chen, S., Tang, F., Gao, L., 2013. The biostratigraphic succession of acanthomorphic acritarchs of the Ediacaran Doushantuo Formation in the Yangtze Gorges area, South China and its biostratigraphic correlation with Australia. Precambrian Research 225, 29-43.

Love, G., Stalvies, C., Grosjean, E., Meredith, W., Snape, C.E., 2008. Analysis of molecular biomarkers covalently bound within Neoproterozoic sedimentary kerogen. In: Kelley, P.H., Bambach, R.K. (Eds.), From Evolution to Geobiology: Research Questions Driving Paleontology at the Start of a New Century. The Paleontological Society, pp. 67-83.

Love, G.D., Grosjean, E., Stalvies, C., Fike, D.A., Grotzinger, J.P., Bradley, A.S., Kelly, A.E., Bhatia, M., Meredith, W., Snape, C.E., Bowring, S.A., Condon, D.J., Summons, R.E., 2009. Fossil steroids record the appearance of Demospongiae during the Cryogenian period. Nature 457, 718-721.

Love, G.D., Grosjean, E., Stalvies, C., Fike, D.A., Grotzinger, J.P., Bradley, A.S., Kelly, A.E., Bhatia, M., Meredith, W., Snape, C.E., Bowring, S.A., Condon, D.J., Summons, R.E., 2009. Fossil steroids record the appearance of Demospongiae during the Cryogenian period. Nature 457, 718-721.

Love, G.D., Snape, C.E., Carr, A.D., Houghton, R.C., 1995. Release of covalently-bound alkane biomarkers in high yields from kerogen via catalytic hydropyrolysis. Organic Geochemistry 23, 981-986.

Lu, M., Zhu, M., Zhang, J., Shields-Zhou, G., Li, G., Zhao, F., Zhao, X., Zhao, M. (2013). The DOUNCE event at the top of the Ediacaran Doushantuo Formation, South China: Broad stratigraphic occurrence and non-diagenetic origin. Precambrian Research 225, 86-109.

Lyons, T.W., Reinhard, C.T., Planavsky, N.J., 2014. The rise of oxygen in Earth/'s early ocean and atmosphere. Nature 506, 307-315.

Ma, G., Lee, H. and Zhang, Z.F., 1984. An investigation of the age limits of the Sinian System in South China. Bulletin Yichang Institute of Geology and Mineral Ressources 8, 1-29.

Macdonald, F.A., Strauss, J.V., Sperling, E.A., Halverson, G.P., Narbonne, G.M., Johnston, D.T., Kunzmann, M., Schrag, D.P., Higgins, J.A., 2013. The stratigraphic relationship between the Shuram carbon isotope excursion, the oxygenation of Neoproterozoic oceans, and the first appearance of the Ediacara biota and bilaterian trace fossils in northwestern Canada. Chemical Geology 362, 250-272.

Macouin, M., Besse, J., Ader, M., Gilder, S., Yang, Z., Sun, Z., Agrinier, P., 2004. Combined paleomagnetic and isotopic data from the Doushantuo carbonates, South China: implications for the ‘snowball Earth’ hypothesis. Earth and Planetary Science Letters 224, 387-398.

Maloof, A.C., Rose, C.V., Beach, R., Samuels, B.M., Calmet, C.C., Erwin, D.H., Poirier, G.R., Yao, N., Simons, F.J., 2010. Possible animal-body fossils in pre-Marinoan limestones from South Australia. Nature Geoscience 3, 653-659.

Marshall, C.R., 2006. Explaining the Cambrian ‘Explosion’ of Animals. Annual Review of Earth and Planetary Sciences 34, 355-384.

Martin, M.W., Grazhdankin, D.V., Bowring, S.A., Evans, D.A.D., Fedonkin, M.A., Kirschvink, J.L., 2000. Age of Neoproterozoic Bilatarian Body and Trace Fossils, White Sea, Russia: Implications for Metazoan Evolution. Science 288, 841-845.

McCaffrey, M.A., Michael Moldowan, J., Lipton, P.A., Summons, R.E., Peters, K.E., Jeganathan, A., Watt, D.S., 1994. Paleoenvironmental implications of novel C30 steranes in Precambrian to Cenozoic Age petroleum and bitumen. Geochimica et Cosmochimica Acta 58, 529-532.

McFadden, K.A., Huang, J., Chu, X., Jiang, G., Kaufman, A.J., Zhou, C., Yuan, X., Xiao, S., 2008. Pulsed oxidation and biological evolution in the Ediacaran Doushantuo Formation. Proceedings of the National Academy of Sciences 105, 3197-3202.

McFadden, K.A., Xiao, S., Zhou, C., Kowalewski, M., 2009. Quantitative evaluation of the biostratigraphic distribution of acanthomorphic acritarchs in the Ediacaran Doushantuo Formation in the Yangtze Gorges area, South China. Precambrian Research 173, 170-190.

Meyer, M., Schiffbauer, J.D., Xiao, S., Cai, Y., Hua, H., 2012. Taphonomy of the upper Ediacaran engigmatic ribbonlike fossil *Shaanxilithes*. PALAIOS 27, 354-372.

Meyer, M., Xiao, S., Gill, B.C., Schiffbauer, J.D., Chen, Z., Zhou, C., Yuan, X., 2014. Interactions between Ediacaran animals and microbial mats: Insights from Lamonte trevallis, a new trace fossil from the Dengying Formation of South China. Palaeogeography, Palaeoclimatology, Palaeoecology 396, 62-74.

Nagovitsin, K.E., Grazhdankin, D.V., Kochnev, B.B., 2008. Ediacaria in the Siberian hypostratotype of the Riphean. Doklady Earth Sciences 419, 423-427.

Narbonne, G.M., 2005. The Ediacara Biota: Neoproterozoic Origin of Animals and Their Ecosystems. Annual Review of Earth and Planetary Sciences, 421-442.

Narbonne, G.M., Xiao, S., Shields, G.A., Gehling, J.G., 2012. Chapter 18 - The Ediacaran Period. In: Gradstein, F., Ogg, J., Schmitz M., Ogg, G. (Eds.), The Geological Time Scale 2012, Elsevier, Amsterdam, pp. 413-435.

Neuweiler, F., Turner, E.C., Burdige, D.J., 2009a. Early Neoproterozoic origin of the metazoan clade recorded in carbonate rock texture. Geology 37, 475-478.

Neuweiler, F., Turner, E.C., Burdige, D.J., 2009b. Early Neoproterozoic origin of the metazoan clade recorded in carbonate rock texture: REPLY. Geology 37, e196.

Och, L.M., Shields-Zhou, G.A., 2012. The Neoproterozoic oxygenation event: Environmental perturbations and biogeochemical cycling. Earth-Science Reviews 110, 26-57.

Peng, S., Babcock, L.E., Cooper, R.A., 2012. Chapter 19 - The Cambrian Period. In: Gradstein, F., Ogg, J., Schmitz M., Ogg, G. (Eds.), The Geological Time Scale 2012, Elsevier, Amsterdam, pp. 437-488.

Peters, K.E., Walters, C.C., Moldowan, J.M., 2005a. The Biomarker Guide Volume 1: Biomarkers and isotopes in the environment and human history. The Press Syndicate of the University of Cambridge, Cambridge.

Peters, K.E., Walters, C.C., Moldowan, J.M., 2005b. The Biomarker Guide Volume 2: Biomarkers and isotopes in petroleum exploration and earth history. The Press Syndicate of the University of Cambridge, Cambridge.

Peterson, K.J., Butterfield, N.J., 2005. Origin of the Eumetazoa: Testing ecological predictions of molecular clocks against the Proterozoic fossil record. Proceedings of the National Academy of Sciences of the United States of America 102, 9547-9552.

Peterson, K.J., Cotton, J.A., Gehling, J.G., Pisani, D., 2008. The Ediacaran emergence of bilaterians: congruence between the genetic and the geological fossil records. Philosophical Transactions of the Royal Society B: Biological Sciences 363, 1435-1443.

Piper, J.D.A., 2000. The Neoproterozoic Supercontinent: Rodinia or Palaeopangaea? Earth and Planetary Science Letters 176, 131-146.

Piper, J.D.A., 2007. The Neoproterozoic supercontinent Palaeopangaea. Gondwana Research 12, 202-227.

Planavsky, N., 2009. Early Neoproterozoic origin of the metazoan clade recorded in carbonate rock texture: COMMENT. Geology 37, e195.

Reitner, J., Wörheide, G., 2002. Non-Lithistid Fossil Demospongiae - Origins of their Palaeobiodiversity and Highlights in History of Preservation. In: Hooper, J.A., Soest, R.M., Willenz, P. (Eds.), Systema Porifera. Springer US, pp. 52-68.

Retallack, G.J., Dunn, K.L., Saxby, J., 2013. Problematic Mesoproterozoic fossil Horodyskia from Glacier National Park, Montana, USA. Precambrian Research 226, 125-142.

Seilacher, A., 1999. Biomat-related lifestyles in the Precambrian. PALAIOS 14, 86-93.

Seilacher, A., Pflüger, F., 1994. From biomats to benthic agriculture: A biohistoric revolution. In: Krumbein, W.E., Paterson, D.M., Stal, L.J. (Eds.), Biostabilization of Sediments. Bibliotheks und Informationssystem der Carl von Ossietzky Universität Oldenburg, Oldenburg, pp. 97-105.

Shen, B., Xiao, S., Zhou, C., Yuan, X., 2009. *Yangtziramulus zhangi* New Genus and Species, a Carbonate-Hosted Macrofossil from the Ediacaran Dengying Formation in the Yangtze Gorges Area, South China. Journal of Paleontology 83, 575-587.

Shen, Y., Zhang, T., Hoffman, P.F., 2008. On the coevolution of Ediacaran oceans and animals. Proceedings of the National Academy of Sciences 105, 7376-7381.

Sherman, L.S., Waldbauer, J.R., Summons, R.E., 2007. Improved methods for isolating and validating indigenous biomarkers in Precambrian rocks. Organic Geochemistry 38, 1987-2000.

Shields-Zhou, G., Och, L., 2011. The case for a Neoproterozoic Oxygenation Event: Geochemical evidence and biological consequences. GSA Today 21, 4-11.

Shields-Zhou, G.A., Hill, A.C., Macgabhann, B.A., 2012. Chapter 17 - The Cryogenian Period. In: Gradstein, F.M., Ogg, J.G., Schmitz, M.D., Ogg, G.M. (Eds.), The Geologic Time Scale. Elsevier, Boston, pp. 393-411.

Siegl, A., Kamke, J., Hochmuth, T., Piel, J., Richter, M., Liang, C., Dandekar, T., Hentschel, U., 2011. Single-cell genomics reveals the lifestyle of Poribacteria, a candidate phylum symbiotically associated with marine sponges. International Society for Microbial Ecology Journal 5, 61-70.

Simkiss, K., 1989. Biomineralisation in the context of geological time. Earth and Environmental Science Transactions of the Royal Society of Edinburgh 80, 193-199.

Sperling, E.A., Frieder, C.A., Raman, A.V., Girguis, P.R., Levin, L.A., Knoll, A.H., 2013. Oxygen, ecology, and the Cambrian radiation of animals. Proceedings of the National Academy of Sciences 110, 13446-13451

Sperling, E.A., Vinther, J., 2010. A placozoan affinity for Dickinsonia and the evolution of late Proterozoic metazoan feeding modes. Evolution & Development 12, 201-209.

Steiner, M., 1994. Die neoproterozoischen Megaalgen Südchinas. Berliner Geowissenschaftliche Abhandlungen E 15, 1-146.

Steiner, M., Mehl, D., Reitner, J., Erdtmann, B.-D., 1993. Oldest entirely preserved sponges and other fossils from the lowermost Cambrian and a new facies reconstruction of the Yangtze Platform. Berliner Geowissenschaftliche Abhandlungen E, 293-329.

Sun, W., 1986. Late precambrian pennatulids (sea pens) from the eastern Yangtze Gorge, China: *Paracharnia* gen. nov. Precambrian Research 31, 361-375.

Valentine, J.W., 2002. Prelude to the Cambrian explosion. Annual Review of Earth and Planetary Sciences 30, 285-306.

Van Kranendonk, M.J., 2006. Volcanic degassing, hydrothermal circulation and the flourishing of early life on Earth: A review of the evidence from c. 3490-3240 Ma rocks of the Pilbara Supergroup, Pilbara Craton, Western Australia. Earth-Science Reviews 74, 197-240.

Van Kranendonk, M.J., 2007. Chapter 7.2 A Review of the Evidence for Putative Paleoarchean Life in the Pilbara Craton, Western Australia. In: Van Kranendonk, M.J., Smithies, R.H., Bennett, V.C. (Eds.), Earth's Oldest Rocks. Developments in Precambrian Geology 15. Elsevier, pp. 855-877.

Van Kranendonk, M.J., Webb, G.E., Kamber, B.S., 2003. Geological and trace element evidence for a marine sedimentary environment of deposition and biogenicity of 3.45 Ga stromatolitic carbonates in the Pilbara Craton, and support for a reducing Archaean ocean. Geobiology 1, 91-108.

Vandenbroucke, M., Largeau, C., 2007. Kerogen origin, evolution and structure. Organic Geochemistry 38, 719-833.

Vidal, G., 1989. Are late Proterozoic carbonaceous megafossils metaphytic algae or bacteria? Lethaia 22, 375-379.

Vinn, O., Zatón, M., 2012. Inconsistencies in proposed annelid affinities of early biomineralized organism *Cloudina* (Ediacaran): structural and ontogenetic evidences. Carnets de Géologie (Notebooks on Geology), 39-47.

Waggoner, B., 2003. The Ediacaran Biotas in Space and Time. Integrative and Comparative Biology 43, 104-113

Walker, J.D., Geissman, J.W., Bowring, S.A. and Babcock, L.E., 2013. The Geological Society of America Geologic Time Scale. Geological Society of America Bulletin 125, 259-272.

Wan, T., 2010. Tectonics of the Mesoproterozoic, Neoproterozoic and Early Cambrian (1.8 Ga-513 Ma), The Tectonics of China. Springer Berlin Heidelberg, pp. 51-86.

Wang, J., Jiang, G., Xiao, S., Li, Q., Wei, Q., 2008. Carbon isotope evidence for widespread methane seeps in the ca. 635 Ma Doushantuo cap carbonate in south China. Geology 36, 347-350.

Wang, J., Li, Z., 2003. History of Neoproterozoic rift basins in South China: implications for Rodinia break-up. Precambrian Research 122, 141-158.

Wang, X., Erdtmann, B.-D., Chen, X., Mao, X., 1998. Integrated sequence-, bio- and chemostratigraphy of the terminal Proterozoic to Lowermost Cambrian 'black rock series' from central South China. Episodes 21, 178-189.

Wang, X., Zhou, J., Qiu, J., Zhang, W., Liu, X., Zhang, G., 2006. LA-ICP-MS U-Pb zircon geochronology of the Neoproterozoic igneous rocks from Northern Guangxi, South China: Implications for tectonic evolution. Precambrian Research 145, 111-130.

Webb, G., Kamber, B., 2011. Trace Element Geochemistry as a Tool for Interpreting Microbialites. In: Golding, S.D., Glikson, M. (Eds.), Earliest Life on Earth: Habitats, Environments and Methods of Detection. Springer Netherlands, pp. 127-170.

Webb, G.E., Kamber, B.S., 2000. Rare earth elements in Holocene reefal microbialites: a new shallow seawater proxy. Geochimica et Cosmochimica Acta 64, 1557-1565.

Webb, G.E., Kamber, B.S., 2004. Biogenicity inferred from microbialite geochemistry. Microbiology Australia 25, 34-35.

Weber, B., Steiner, M., Zhu, M.Y., 2007. Precambrian - Cambrian trace fossils from the Yangtze Platform (South China) and the early evolution of bilaterian lifestyles. Palaeogeography, Palaeoclimatology, Palaeoecology 254, 328-349.

Williams, D.M., Kasting, J.F., Frakes, L.A., 1998. Low-latitude glaciation and rapid changes in the Earth's obliquity explained by obliquity-oblateness feedback. Nature 396, 453-455.

Willman, S., Moczydłowska, M., 2008. Ediacaran acritarch biota from the Giles 1 drillhole, Officer Basin, Australia, and its potential for biostratigraphic correlation. Precambrian Research 162, 498-530.

Wood, R.A., 2011. Paleoecology of the earliest skeletal metazoan communities: Implications for early biomineralization. Earth-Science Reviews 106, 184-190.

Wood, R.A., Grotzinger, J.P., Dickson, J.A.D., 2002. Proterozoic Modular Biomineralized Metazoan from the Nama Group, Namibia. Science 296, 2383-2386.

Xiao, S., Knoll, A.H., 1999. Fossil preservation in the Neoproterozoic Doushantuo phosphorite Lagerstätte, South China. Lethaia 32, 219-238.

Xiao, S., Knoll, A.H., 2000. Phosphatized Animal Embryos from the Neoproterozoic Doushantuo Formation at Weng'an, Guizhou, South China. Journal of Paleontology 74, 767-788.

Xiao, S., Knoll, A.H., Yuan, X., Pueschel, C.M., 2004. Phosphatized Multicellular Algae in the Neoproterozoic Doushantuo Formation, China, and the Early Evolution of Florideophyte Red Algae. American Journal of Botany 91, 214-227.

Xiao, S., Laflamme, M., 2009. On the eve of animal radiation: phylogeny, ecology and evolution of the Ediacara biota. Trends in ecology & evolution (Personal edition) 24, 31-40.

Xiao, S., Shen, B., Zhou, C., Xie, G., Yuan, X., 2005. A uniquely preserved Ediacaran fossil with direct evidence for a quilted bodyplan. Proceedings of the National Academy of Sciences of the United States of America 102, 10227-10232.

Xiao, S., Yuan, X., Knoll, A.H., 2000. Eumetazoan fossils in terminal Proterozoic phosphorites? Proceedings of the National Academy of Sciences 97, 13684-13689.

Xiao, S., Yuan, X., Steiner, M., Knoll, A.H., 2002. Macroscopic Carbonaceous Compressions in a Terminal Proterozoic Shale: A Systematic Reassessment of the Miaohe Biota, South China. Journal of Paleontology 76, 347-376.

Xiao, S., Zhang, Y., Knoll, A.H., 1998. Three-dimensional preservation of algae and animal embryos in a Neoproterozoic phosphorite. Nature 391, 553-558.

Xiao, S., Zhou, C., Liu, P., Wang, D., Yuan, X., 2014. Phosphatized Acanthomorphic Acritarchs and Related Microfossils from the Ediacaran Doushantuo Formation at Weng'an (South China) and their Implications for Biostratigraphic Correlation. Journal of Paleontology 88, 1-67.

Yao, J., Shu, L., Santosh, M., Zhao, G., 2014. Neoproterozoic arc-related mafic-ultramafic rocks and syn-collision granite from the western segment of the Jiangnan Orogen, South China: Constraints on the Neoproterozoic assembly of the Yangtze and Cathaysia Blocks. Precambrian Research 243, 39-62.

Ye, M.-F., Li, X.-H., Li, W.-X., Liu, Y., Li, Z.-X., 2007. SHRIMP zircon U-Pb geochronological and whole-rock geochemical evidence for an early Neoproterozoic Sibaoan magmatic arc along the southeastern margin of the Yangtze Block. Gondwana Research 12, 144-156.

Yin, C., Liu, P., Awramik, S.M., Chen, S., Tang, F., Gao, L., Wang, Z., Riedman, L.A., 2011. Acanthomorph Biostratigraphic Succession of the Ediacaran Doushantuo Formation in the East Yangtze Gorges, South China. Acta Geologica Sinica - English Edition 85, 283-295.

Yin, C., Tang, F., Liu, Y., Gao, L., Liu, P., Xing, Y., Yang, Z., Wan, Y., Wang, Z., 2005. U-Pb zircon age from the base of the Ediacaran Doushantuo Formation in the Yangtze Gorges, South China: constraint on the age of Marinoan glaciation. Episodes 28, 48-49.

Yin, J., 1993. Geological Evolution and Mineralization from the Surrounding Areas of Sichuan Basin and its Vicinal Regions during the Sinian Subera. Press of Chengdu University of Science and Technology, Chengdu.

Yin, L., Zhu, M., Knoll, A.H., Yuan, X., Zhang, J., Hu, J., 2007. Doushantuo embryos preserved inside diapause egg cysts. Nature 446, 661-663.

Yin, Z., Zhu, M., Tafforeau, P., Chen, J., Liu, P., Li, G., 2013. Early embryogenesis of potential bilaterian animals with polar lobe formation from the Ediacaran Weng'an Biota, South China. Precambrian Research 225, 44-57.

Yuan, X., Chen, Z., Xiao, S., Zhou, C., Hua, H., 2011. An early Ediacaran assemblage of macroscopic and morphologically differentiated eukaryotes. Nature 470, 390-393.

Yuan, X., Jun, L.I., Ruiji, C.A.O., 1999. A diverse metaphyte assemblage from the Neoproterozoic black shales of South China. Lethaia 32, 143-155.

Zhang, Q., Piper, J.D.A., 1997. Palaeomagnetic study of Neoproterozoic glacial rocks of the Yangzi Block: palaeolatitude and configuration of South China in the late Proterozoic Supercontinent. Precambrian Research 85, 173-199.

Zhang, S., Evans, D.A.D., Li, H., Wu, H., Jiang, G., Dong, J., Zhao, Q., Raub, T.D., Yang, T., 2013. Paleomagnetism of the late Cryogenian Nantuo Formation and paleogeographic implications for the South China Block. Journal of Asian Earth Sciences 72, 164-177.

Zhang, S., Jiang, G., Han, Y., 2008. The age of the Nantuo Formation and Nantuo glaciation in South China. Terra Nova 20, 289-294.

Zhang, S., Jiang, G., Zhang, J., Song, B., Kennedey, M.J., Christie-Blick, N., 2005. U-Pb sensitive high-resolution ion microprobe ages from the Doushantuo Formation in south China: Constraints on late Neoproterozoic glaciations. Geology 33, 473-476.

Zhang, X., Hua, H., Reitner, J., 2006. A new type of Precambrian megascopic fossils: the Jinxian biota from northeastern China. Facies 52, 169-181.

Zhang, X., Shu, D., Han, J., Zhang, Z., Liu, J., Fu, D., 2014. Triggers for the Cambrian explosion: Hypotheses and problems. Gondwana Research 25, 896-909.

Zhang, Y., Yuan, X., Yin, L., 1998. Interpreting Late Precambrian Microfossils. Science 282, 1783.

Zhao, G., Cawood, P.A., 1999. Tectonothermal evolution of the Mayuan Assemblage in the Cathaysia Block; implications for Neoproterozoic collision-related assembly of the South China Craton. American Journal of Science 299, 309-339.

Zhao, G., Cawood, P.A., 2012. Precambrian geology of China. Precambrian Research 222-223, 13-54.

Zhao, G., Wilde, S.A., Cawood, P.A., Sun, M., 2001. Archean blocks and their boundaries in the North China Craton: lithological, geochemical, structural and P-T path constraints and tectonic evolution. Precambrian Research 107, 45-73.

Zhao, J., Zhou, M., Yan, D., Zheng, J., Li, J., 2011. Reappraisal of the ages of Neoproterozoic strata in South China: No connection with the Grenvillian orogeny. Geology 39, 299-302.

Zhao, Y., He, M., Chen, M., Peng, J., Yu, M., Wang, Y., Yang, R., Wang, P., Zhang, Z., 2004. Discovery of a Miaohe-type biota from the Neoproterozoic Doushantuo Formation in Jiangou County, Guizhou Province, China. Chinese Science Bulletin 49, 1916-1918.

Zhao, Z., Xing, Y., Ding, Q., Liu, G., Zhao, Y., Zhang, S., Meng, X., Yin, C., Ning, B., Han, P., 1988. The Sinian System of Hubei. China University of Geosciences Press, Wuhan.

Zhao, Z., Xing, Y., Ma, G., Chen, Y., 1985. Biostratigraphy of the Yangtze Gorges area, 1 Sinian. Geological Publishing House, Beijing.

Zhou, C., Tucker, R., Xiao, S., Peng, Z., Yuan, X., Chen, Z., 2004. New constraints on the ages of Neoproterozoic glaciations in south China. Geology 32, 437-440.

Zhou, C., Xiao, S., 2007. Ediacaran $\delta^{13}C$ chemostratigraphy of South China. Chemical Geology 237, 89-108.

Zhou, J., Wang, X., Qiu, J., Gao, J., 2004. Geochemistry of Meso- and Neoproterozoic mafic-ultramafic rocks from northern Guangxi, China: Arc or plume magmatism? Geochemical Journal 38, 139-152.

Zhou, M., Kennedy, A.K., Sun, M., Malpas, J., Lesher, M., 2002a. Neoproterozoic Arc-Related Mafic Intrusions along the Northern Margin of South China: Implications for the Accretion of Rodinia. The Journal of Geology 110, 611-618

Zhou, M., Yan, D., Kennedy, A.K., Li, Y., Ding, J., 2002b. SHRIMP U-Pb zircon geochronological and geochemical evidence for Neoproterozoic arc-magmatism along the western margin of the Yangtze Block, South China. Earth and Planetary Science Letters 196, 51-67.

Zhu, M., Gehling, J.G., Xiao, S., Zhao, Y., Droser, M.L., 2008. Eight-armed Ediacara fossil preserved in contrasting taphonomic windows from China and Australia. Geology 36, 867-870.

Zhu, M., Xiao, S., Yin, C., 2006. The Cryogenian and Ediacaran of South China: Ice Ages, Animal Embryos, Acritarchs, and Algae. The Second International Paleontological Congress Pre-Meeting Field Trip A8.

Zhu, M., Zhang, J., Steiner, M., Yang, A., Li, G., Erdtmann, B.D., 2003. Sinian-Cambrian stratigraphic framework for shallow- to deep-water environments of the Yangtze Platform: an integrated approach. Progress in Natural Science 13, 951-960.

Zhu, M., Zhang, J., Yang, A., 2007. Integrated Ediacaran (Sinian) chronostratigraphy of South China. Palaeogeography, Palaeoclimatology, Palaeoecology 254, 7-61.

- Chapter 2 -

Depositional dynamics of a bituminous carbonate facies in a tectonically-induced intra-platform basin: The Shibantan Member (Dengying Formation, Ediacaran Period)

(Submitted to *Carbonates and Evaporites*)

Jan-Peter Duda, Maoyan Zhu, Joachim Reitner

Abstract

The Shibantan Member (Dengying Formation, Ediacaran Period) is one of only a few carbonate units with Ediacara-type fossils worldwide, but little is known about its sedimentology. A detailed sedimentological characterisation revealed that the Shibantan Member was deposited on a carbonate ramp system linked to an intra-platform basin. Evaporitic dolomites of the Hamajing Member (representing sub- to supratidal inner-ramp environments above fair weather wave base) are sharply overlain by black laminated limestones of the lower Shibantan Member, representing a subtidal lower- to middle ramp environment close to the storm wave base. This facies-shift implies a sudden local deepening event, probably due to a tectonically-induced increase in subsidence. The Shibantan basin was subsequently filled as evidenced by the gradual transition into dark wavy dolomites deposited in a subtidal middle-ramp environment (i.e. between storm- and fair weather wave base) and, eventually, the upper Dengying Formation (i.e. the Baimatuo Member), which represents the same depositional environments as the Hamajing Member. Sedimentation in the Shibantan basin was highly dynamic as evidenced by a distinct slumping horizon and mass-flow deposits, partly possibly due to synsedimentary tectonic processes. A microbial-mat associated biota which includes Ediacara-type fossils is restricted to the lower Shibantan Member. The close spatial relationship between allochthonous event deposits and autochthonous fossil associations in this setting implies that the event deposits were not only important for the preservation of fossils, but probably also for the supply of nutrients.

Keywords

Ediacaran, Yangtze platform, Ediacara biota, sedimentary facies, depositional environment

2.1 Introduction

The Ediacaran Period (635-541 million years; Ma) spanned the time between the terminal Neoproterozoic global glaciation ('Marinoan') and the Cambrian biological radiation (Knoll et al., 2004, 2006; Narbonne et al., 2012; Walker et al., 2013). This interval is characterised by the establishment of complex organisms of partly metazoan affinity (Ediacara-type fossils or Vendobionta; 575-541 Ma), the first potential trace fossils of bilateralian organisms, and the advent of biomineralisation and predation (*Cloudina* community) (e.g. Germs, 1972; Bengtson and Zhao, 1992; Grotzinger et al., 2000; Knoll et al., 2004, 2006; Narbonne, 2005; Jensen et al., 2006). This transition from a Precambrian 'microbial world' to a Phanerozoic 'multicellular eukaryotic world' clearly resulted from the complex interaction between the geo- and biosphere, but causes and triggers for this shift are still enigmatic (cf. Butterfield, 2011; Kennedy, 2013).

The well-developed and exposed Ediacaran sedimentary successions of the Yangtze Platform in South China are an important archive for these developments since they contain numerous fossil Lagerstätten. The Shibantan Member of the Dengying Formation (Fig. 2.1) is particularly interesting since it is characterised by a complex fossil association including *Vendotaenia* sp. (Ding and Chen, 1981; Sun, 1986; Zhao et al., 1988; Ding et al., 1993), simple horizontal trace fossils (Zhao et al., 1988; Ding et al., 1992; Ding et al., 1993; Weber et al., 2007; Chen et al., 2013; Meyer et al., 2014), Ediacara-type organisms (*Paracharnia dengyingensis*; Ding and Chen, 1981; Sun, 1986; Dzik, 2002; *Yangtziramulus zhangi*; Xiao et al., 2005; Shen et al., 2009; *Hiemalora*, *Pteridinium*, *Rangea*, *Charniodiscus*; Chen et al., 2014), and a new annulated tubular fossil (*Wutubus annularis*; Chen et al., 2014). Most of these fossils are closely associated with microbial mats (Xiao et al., 2005; Weber et al., 2007; Shen et al., 2009; Chen et al., 2013, 2014; Meyer et al., 2014). Furthermore there are few reports of acritarchs (Sun, 1986; Wang et al., 1998) and sponge spicules (Steiner et al., 1993). Despite this high biological diversity, however, little is known about the palaeoenvironments in which these organisms thrived.

Another important characteristic of the Shibantan Member is its carbonate lithology. Palaeoecosystems with Ediacara-type fossils are usually preserved in siliciclastic and volcaniclastic environments (e.g. Narbonne, 2005, and references therein). Worldwide, the Shibantan Member (e.g. Ding and Chen, 1981; Sun, 1986; Steiner et al., 1993; Dzik, 2002; Xiao et al., 2005; Zhu et al., 2007;

Shen et al., 2009; Chen et al., 2013, 2014) and the Khatyspyt Formation in Siberia (e.g. Fedonkin, 1990; Khomentovsky, 1990; Knoll et al., 1995; Grazhdankin, 2004; Grazhdankin et al., 2008) are the only known pure carbonates containing Ediacara-type fossils. In contrast to their siliciclastic and volcaniclastic counterparts, however, the sedimentology of these settings is as yet only poorly known. This study provides a detailed sedimentological characterisation of the Shibantan Member with respect to its depositional environments and sedimentary processes. Based on the findings a depositional model is proposed and the similarities and differences compared to other settings with Ediacara-type fossils are discussed.

2.2 Geological framework

The Dengying Formation (551-541 Ma; Condon et al., 2005; Walker et al., 2013) represents a shallow-water carbonate platform (e.g. Cao et al., 1989; Zhou and Xiao, 2007; Jiang et al., 2011), referred to as Dengying platform in the following. In the Yangtze Gorges area, it is subdivided into (from base to top) the Hamajing, the Shibantan and the Baimatuo Members (Zhao et al., 1985, 1988) (Fig. 2.1). The Shibantan Member is stratigraphically equivalent to the Ediacara Member in Australia (Sun, 1986; Steiner et al., 1993; Zhu et al., 2007).

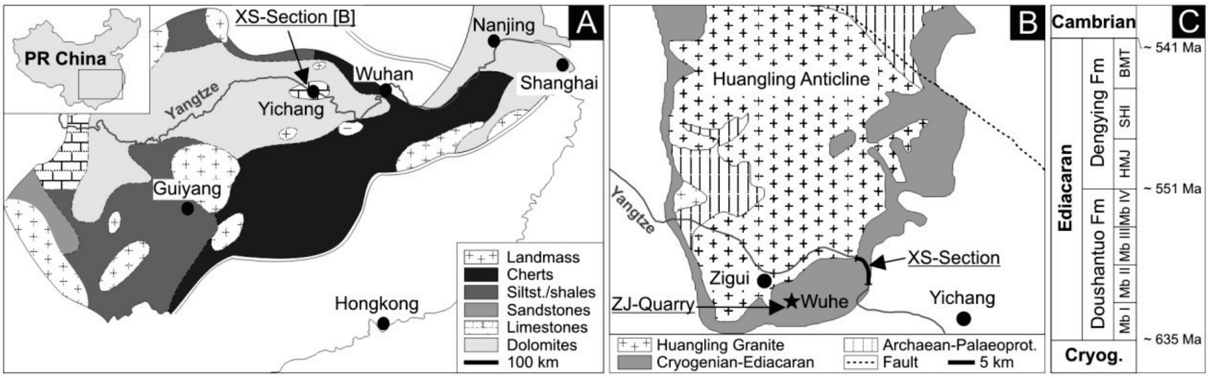

Fig. 2.1 Geological context of the Shibantan Member. A: Facies distribution on the Dengying platform at the time of deposition. The study area is located in the direct vicinity of Yichang (see arrow). B (detail from A): Precise location of the Xinshipai- (XS-) section and Zhoujia'ao- (ZJ-) Quarry in the southern part of the Huangling Anticline. C: Stratigraphic framework of the Ediacaran strata in the study area (not to scale). HMJ = Hamajing Member; SHI = Shibantan Member; BMT = Baimatuo Member. A: modified after Zhu et al. (2007); B: modified after Chen et al. (2013); ages in C from Condon et al. (2005) and Walker et al. (2013).

The Hamajing Member (10-200 m thickness; e.g. Zhu et al., 2007) consists of massive and medium-to thick-bedded light grey dolomites intercalated with thin chert bands and -concretions towards the top (e.g. Sun, 1986; Wang et al., 1998; Zhu et al., 2003, 2007; Zhou and Xiao, 2007). Large tepee structures, dissolution cavities, birds-eye structures, oolites, oncolites, intraclasts, and cross-bedding indicate a shallow peritidal environment (Wang et al., 1998; Zhu et al., 2003, 2007; Xiao et al., 2005; Zhou and Xiao, 2007; Shen et al., 2009; Chen et al., 2013, 2014; Ling et al., 2013; Meyer et al., 2014).

The Shibantan Member (ca. 100-160 m thickness; e.g. Zhou and Xiao, 2007; Zhu et al., 2007) crops out very locally in the area of Yichang (Hubei), but was also reported in Shimen County (NW Hunan) where it is only ca. 47 m thick (cf. Zhu et al., 2003). The member consists mainly of black to dark grey thin- to medium-bedded and locally finely-laminated bituminous limestones, including some chert bands and -concretions (Sun, 1986; Wang et al., 1998; Zhou and Xiao, 2007; Zhu et al., 2003, 2007). The Shibantan Member was probably deposited in a lower subtidal environment below fair weather wave base (FWB) (Sun, 1986; Xiao et al., 2005; Shen et al., 2009; Ling et al., 2013; Chen et al., 2013, 2014), though cross stratification and rip-up clasts were taken as evidence for deposition above storm wave-base (SWB) (Meyer et al., 2014). In addition to the sedimentary facies, however, the evolution of the depositional system and sedimentary dynamics are still poorly understood.

The Baimatuo Member (40-570 m thick; e.g. Zhou and Xiao, 2007; Zhu et al., 2007) consists of light grey massive and medium- to thick-bedded dolomites with chert bands and -concretions (Sun, 1986; Wang et al., 1998). Cross-stratification, birds-eye structures, as well as abundant evidence for dissolution and brecciation indicate a peritidal environment (Wang et al., 1998; Xiao et al., 2005; Zhou and Xiao, 2007; Zhu et al., 2007; Shen et al., 2009; Ling et al., 2013; Chen et al., 2013, 2014; Meyer et al., 2014).

2.3 Methods and location

The studied section is exposed along a road-cut on the south-western bank of the Yangtze River on the eastern rim of the Huangling anticline in the vicinity of Yichang (base of the section: ca. 30°49'25.57"N, 111° 9'52.21"E; top of the section: ca. 30°48'48.64"N; 111° 9'58.61"E) (Fig. 2.1). The location of the section is approximately equal to the Shipai section which is the type-section for the Dengying Formation and requires a boat for access (Zhao et al., 1988; Zhu et al., 2006). In order avoid confusion the section investigated herein is referred to as the Xinshipai- (XS) section ('xīn' = Chinese for 'new').

This work is mainly based on sedimentological field methods. Additionally, polished slabs and petrographical thin-sections were investigated with respect to sedimentary structures and rock textures. Mineralogies were differentiated by using staining techniques (alizarine red S for differentiating dolomite and calcite; potassium ferricyanid for differentiating ferroan and non-ferroan carbonates; see Flügel, 2004; and references therein).

2.4 Results and discussion

2.4.1 Sedimentary section (Fig. 2.2)

A distinct black limestone unit is interbedded within the upper part of the Hamajing Member (Fig. 2.2). The upper surface of the Hamajing Member is nodular and the lithostratigraphic boundary between the Hamajing Member and the Shibantan Member is distinct. The transitions between all distinct facies following up-section from the boundary, including the boundary between the Shibantan Member and the Baimatuo Member, are gradual.

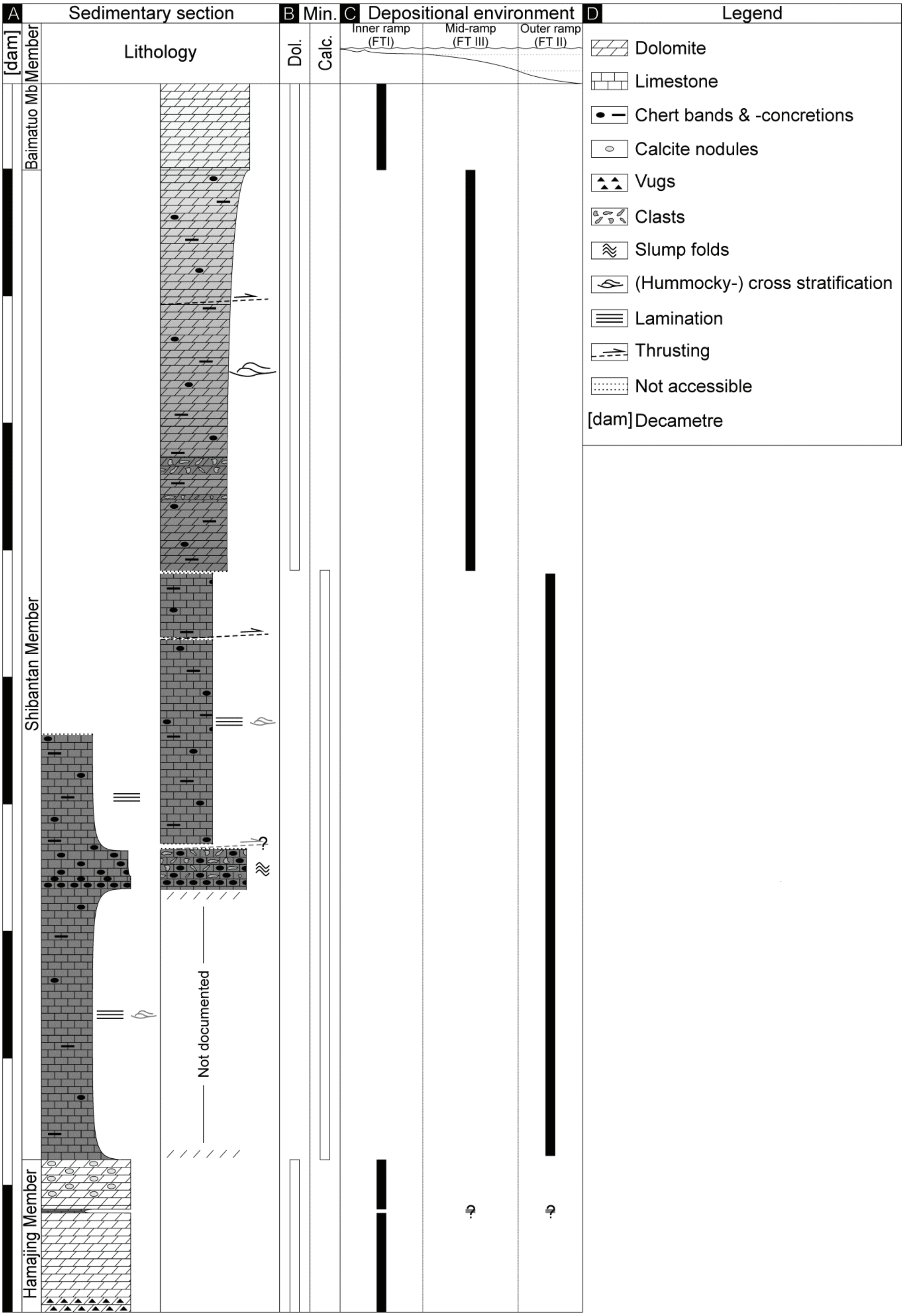

Fig. 2.2 The Xinshipai-section in Yichang. A: Vertical facies distribution. B: Mineralogy. C: Depositional environments. D: Legend.

2.4.2 Facies analysis (Fig. 2.3-2.6)

Based on lithology and sedimentary structures, 3 facies-types (FTs) can be distinguished.

2.4.2.1 FT I Evaporitic dolomites (Hamajing Member, Baimatuo Member) (Fig. 2.3)

Description: Generally this facies comprises light grey (locally pinkish-reddish stained), massive to well-bedded dolomites. Beds are not always continuous and their appearance ranges from wavy to even. In places, larger-scale cross stratification and brecciation of distinct mm-thick layers can be observed (Fig. 2.3a, b). Other important features are mm- to cm-sized angular to rectangular open vugs, in some cases with thin cement-rims at the edges, and locally associated with clasts (Fig. 2.3c, d). Mm- to dm-sized white calcite and chert nodules of different shapes 'floating' in the sediment can be locally observed (Fig. 2.3e, f). The dolomites are micro- to fine crystalline and peloidal and locally exhibit mm-sized calcite pseudomorphs after gypsum crystals (Fig. 2.3g, h).

Interpretation: Brecciation and cross-stratification point to a shallow-water high-energy environment. Given the presence of calcite pseudomorphs after gypsum crystals, the white calcite and chert nodules are tentatively interpreted as calcite pseudomorphs after gypsum or anhydrite whereas the vugs may have resulted from wholesale dissolution of former evaporite minerals. This is in accordance with other reports of evaporite occurrences on the Dengying platform (Xi, 1987; Siegmund and Erdtmann, 1994; Steiner, 2001; Zhu et al., 2007; Lu et al., 2013; see 2.4.3). Taken together, a sub- to supratidal inner ramp environment above FWB is evident.

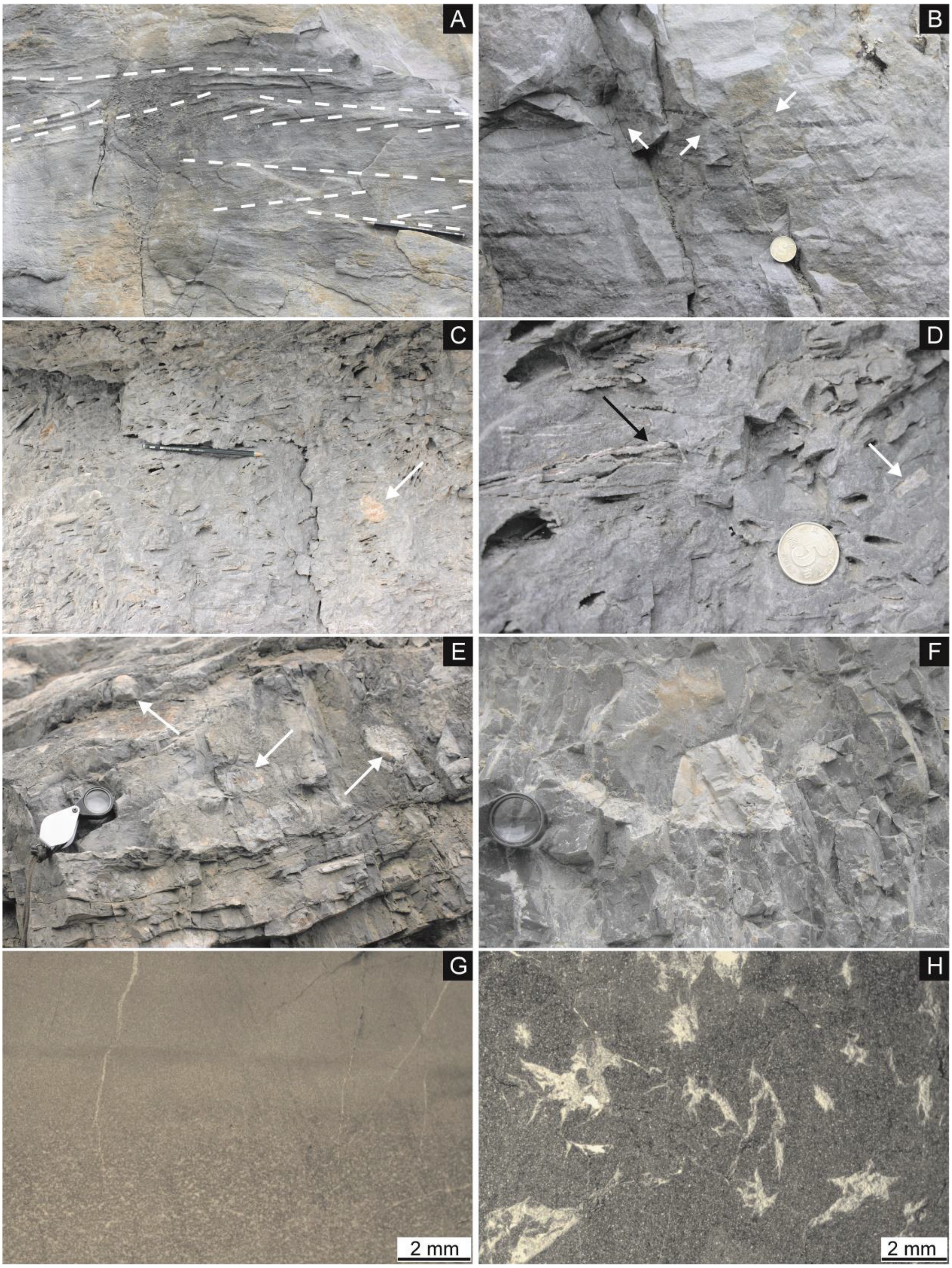

Fig. 2.3 FT I Evaporitic dolomites. A: Larger-scale cross stratification (see dashed lines for orientation; pencil as scale); B: Brecciated mm-thick layers (see arrows); C, D: Dissolution vugs of former evaporite-minerals, note clasts (white arrows) and cement rims (black arrows); E, F: White nodules (see arrows in E), probably pseudomorphs after gypsum or anhydrite. G: Micro- to fine crystalline dolomite with peloidal texture at the base. H: Calcite pseudomorphs after gypsum crystals Photos A, B, F, G, H: slightly above the section shown in Fig. 2.2.

2.4.2.2 FT II Black laminated limestones (lower Shibantan Member) (Fig. 2.4, 2.5)

Description: Generally this facies comprises black and finely laminated limestone with a strong sulphidic smell. The lamination of this facies is due to an alternation of mm- to cm-thick black limestone layers and mm-thick brownish laminae (Fig. 2.4a). The brownish layers are characterised by an indistinct clotted mudstone texture (Fig. 2.4b). Also present are common wrinkled surfaces, horizontal trace fossils and *Vendotaenia*-like fossils (often rather resembling disrupted microbial mats) on top (Fig. 2.4c-d). These features can be particularly well observed at other places in the area (e.g. the Zhoujia'ao-Quarry close to Wuhe, Fig. 2.1). The black limestone beds reveal locally (hummocky-) cross-stratification which become more prominent up-section (Fig. 2.4e-g). The beds have mud- to fine grainstone textures, and individual beds are locally graded (fining upward). In some cases erosional boundaries, lenticular bedding, load casts and dewatering structures are observed, pointing to periodic reworking, transportation and deposition. The dewatering structures could also reflect seismic activities. Chert bands and -concretions become more prominent up-section. These are evidently early diagenetic in origin since (i) bedding features can be traced across boundaries between the chert and the carbonate and (ii) layers are less compacted in the cherts than in the surrounding carbonate sediments (Fig. 2.4h).

Within this FT a distinct level characterised by highly abundant chert nodules occurs. This horizon is locally characterised by sedimentary folds on a metre-scale (Fig. 2.5a), whereas the material is brecciated with unsorted mm- to cm-sized clasts in other places (Fig. 2.5b, c).

Interpretation: In view of the observed sedimentary structures, the black limestone beds are interpreted as allochthonous event deposits whereas the brownish beds are interpreted as autochthonous microbial mats. It should be noted, however, that this discrimination is commonly only possible because of characteristic surface structures of the microbial mat layers. Obviously, this depositional setting was temporarily affected by storm reworking, indicating a subtidal lower- to middle ramp environment close to the SWB. Since the distinct horizon within this FT shows evidence for ductile deformation of semi-consolidated material (slump folds) as well as brittle deformation of consolidated material (brecciation), mass transport by slumping appears likely.

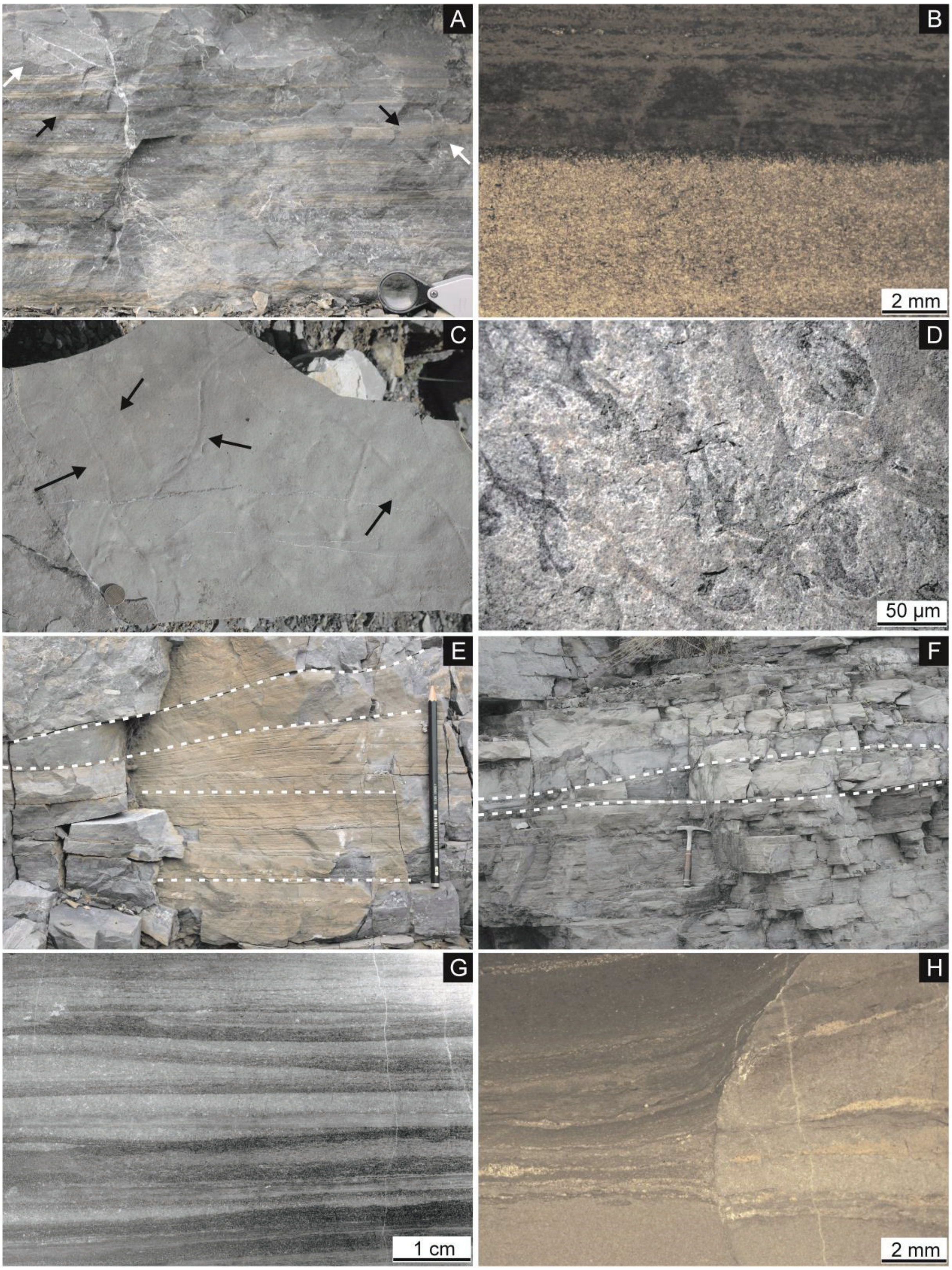

Fig. 2.4 FT II Black laminated limestones. A: Alternation of black limestone beds (white arrows; event deposits) and mm-thick brownish layers (black arrows; microbial mats); B: Microbial mat with clotted mudstone texture overlying an event deposit with fine grainstone-texture. C: Microbial mat surface with horizontal traces (see arrows); D: *Vendotaenia*-like fossils/disrupted microbial mats. E-F: Hummocky cross stratification (dashed lines for orientation); G: Small-scale cross stratification; H: Early diagenetic chert concretion. C, D, G: Zhoujia'ao-Quarry (close to Wuhe; Fig. 2.1).

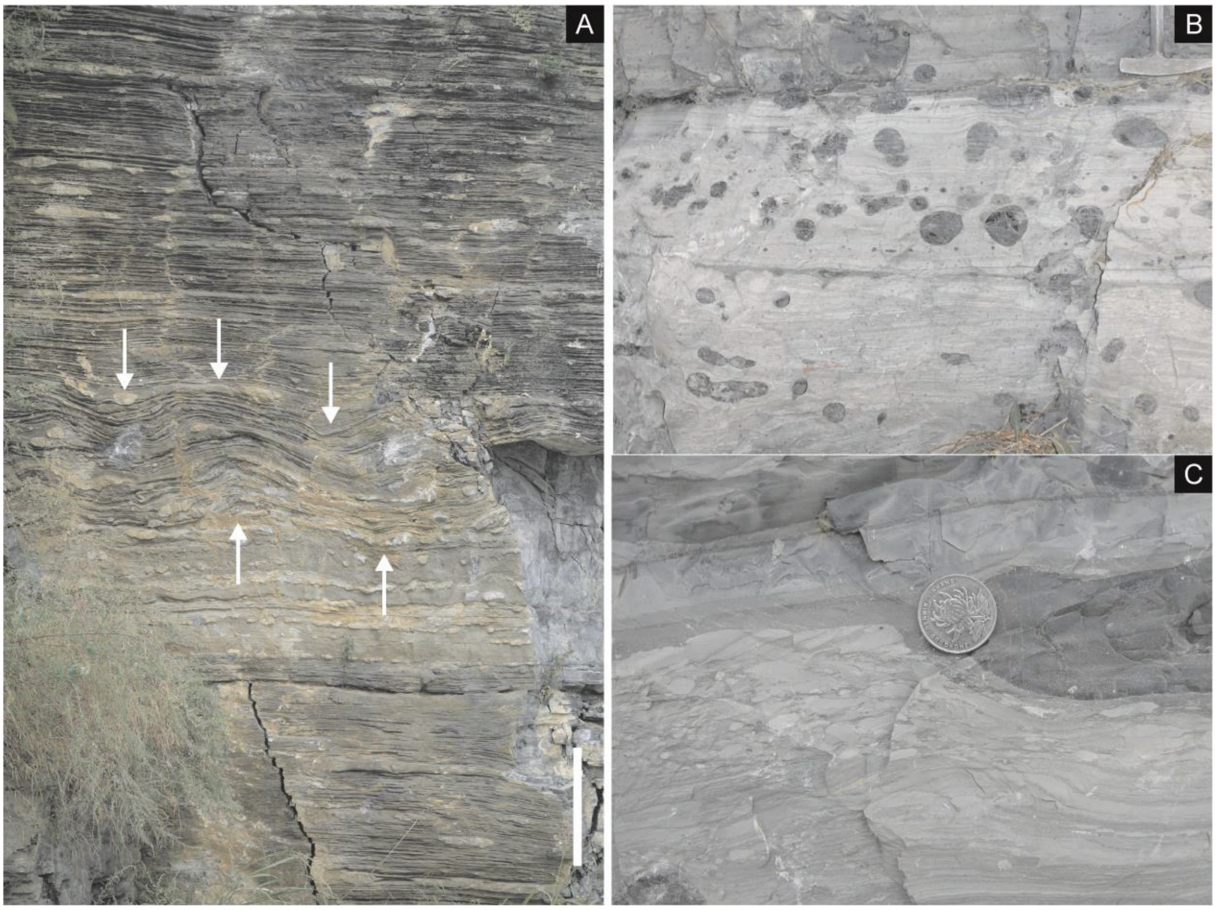

Fig. 2.5 Slumping horizon in the lower Shibantan Member. A: Slump folds (see arrows; scale bar = 1 m); B, C: Brecciation textures (C is detail from B).

2.4.2.3 FT III Dark wavy dolomites (upper Shibantan Member) (Fig. 2.6)

Description: The FT III comprises dark-greyish dolomites characterised by a sulphidic smell. Beds of this facies are very wavy (Fig. 2.6a) and reveal prominent hummocky cross stratification on different scales that increase in abundance and dimensions upwards (Fig. 2.6b). Chert bands and -concretions are concentrated in some horizons. Lateral pinching out of beds is observed towards the top of the section (Fig. 2.6c). Distinct beds in the lower part of the section contain larger-sized clasts but lack sedimentary structures such as cross bedding (Fig. 2.6d).

Interpretation: The wavy character of beds and the prominent hummocky cross stratification point to an environment frequently affected by storms and indicate a subtidal middle-ramp environment between SWB and FWB. The distinct beds in the lower part of the section are interpreted as mass-flow deposits.

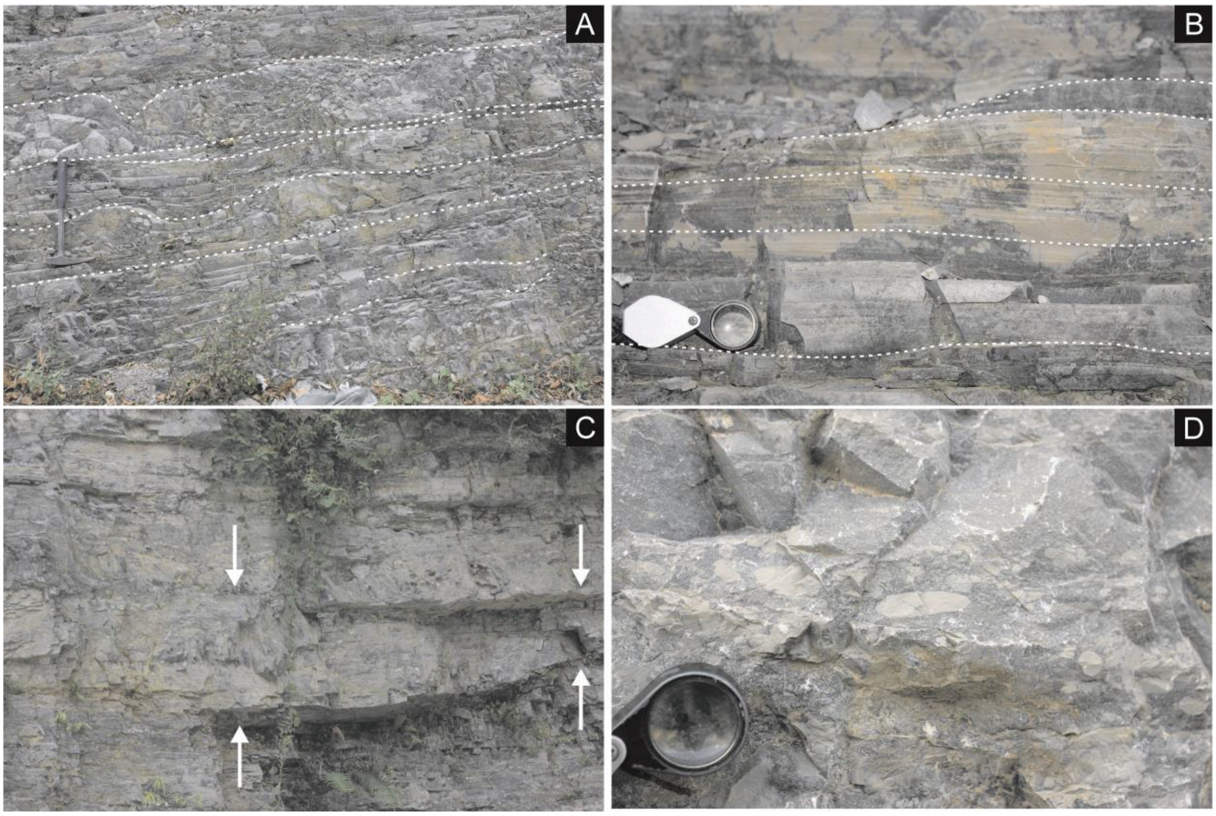

Fig. 2.6 FT III Dark wavy dolomites. A: Wavy character of beds (dashed lines for orientation); B: Hummocky cross stratification (dashed lines for orientation); C: Lateral pinching out bed (see arrows; max. thickness of the bed ca 50 cm); D: Mass-flow bed with larger-sized clasts.

2.4.3 Depositional environments and facies development

The depositional system of the Shibantan Member can generally be described with a carbonate ramp model (Fig. 2.2, 2.7) with facies types ranging from sub- to supra-tidal inner-ramp environments above FWB (FT I Evaporitic dolomites) to subtidal lower- to middle-ramp environments close to the SWB (FT II Black laminated limestones). Problematically, the depth of wave-reworking can alternate within the same depositional setting so that FWB and SWB are artificial terms (Aigner, 1985). However, the discussion of possible smaller cycles is beyond the scope of this paper and the classical ramp model is considered appropriate to understand the general sedimentary development of the Shibantan basin.

The occurrence of calcite pseudomorphs after evaporite minerals as well as of dissolution vugs in the XS-section is in good accordance with contemporaneous evaporites elsewhere on the platform (Xi, 1987; Siegmund and Erdtmann, 1994; Steiner, 2001; Zhu et al., 2007; Lu et al., 2013). For instance, the lower Dengying Formation in eastern Yunnan (i.e. the Donglongtang Member) exhibits pseudo-crystals of gypsum and stromatolitic structures, indicating deposition in a coastal tidal flat (Zhu et al., 2007; Lu et al., 2013). Likewise, primary interbedding of evaporites and dolomites (now brecciated by dissolution of evaporites), dissolution vugs as well as features of meteoric diagenesis and karstification were observed in the Dengying Formation in Sansha (Hunan), indicating deposition in a restricted lagoonal environment that was repeatedly interrupted by periods of subaerial exposure (Siegmund and Erdtmann, 1994). Furthermore, thick dolomites with anhydrite and up to 200 m halite were deposited the Changnin Basin in south Sichuan (Xi, 1987). The restricted conditions required to form evaporites were possibly caused by a temporarily rimmed morphology of the Ediacaran Yangtze platform (Zhu et al., 2003, 2007; Vernhet and Reijmer, 2010; Jiang et al., 2011) or the Jiangnan Uplift, which was situated between the platform in the east and the basin in the west (Xi, 1987; Siegmund and Erdtmann, 1994). However, the regional formation of evaporitic basins was possibly also controlled by fault-related subsidence (Xi, 1987; Vernhet, 2007; Vernhet et al., 2007; see 2.4.4).

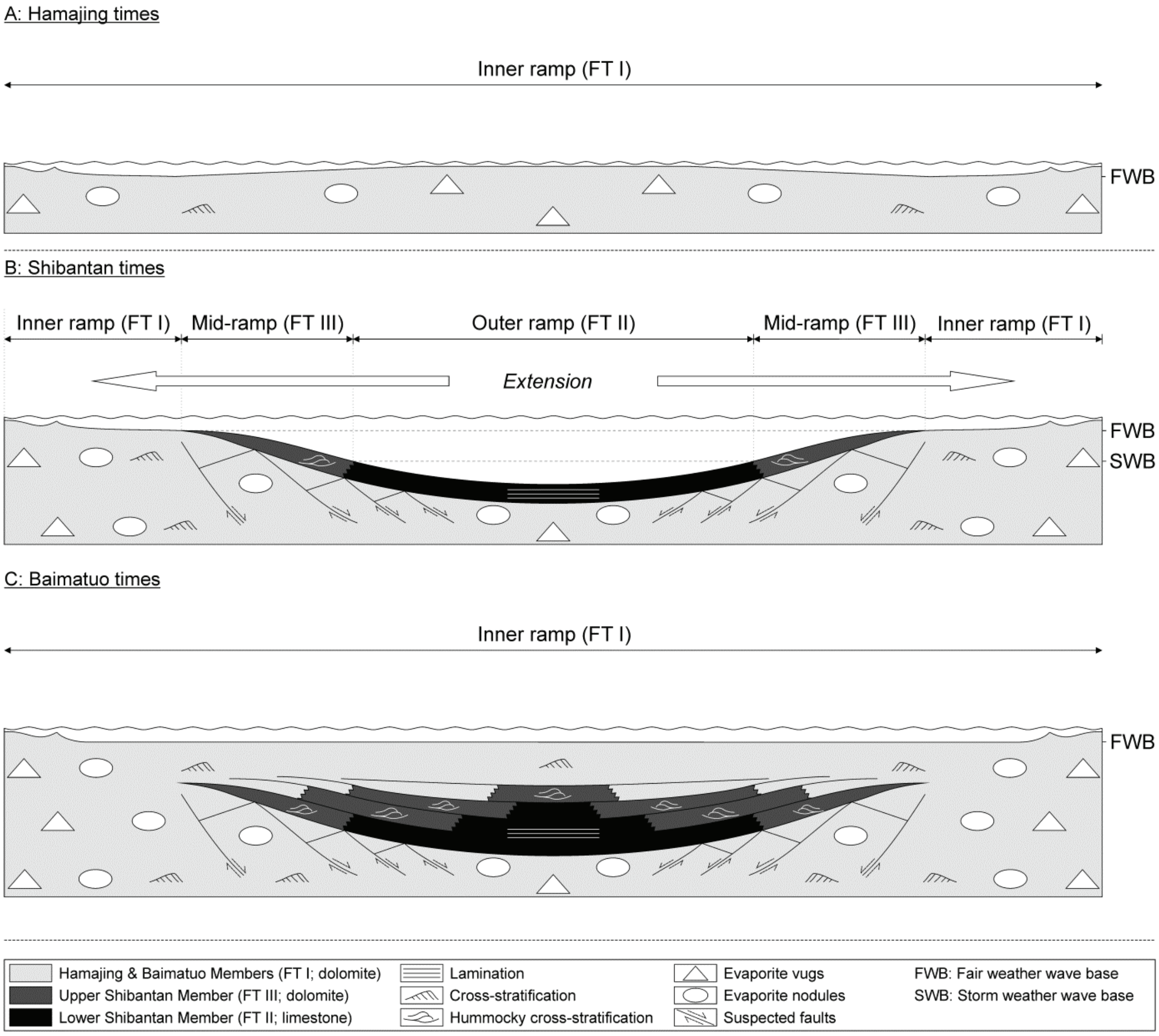

Fig. 2.7 Hypothetical geodynamic evolution of the Shibantan basin within the Dengying carbonate platform. The Xinshipai-section represents the central part of the basin. A: The Dengying platform was tectonically stable and solely characterized by an inner-ramp facies during Hamajing times in the Yichang area. B: Sudden increase of local subsidence (probably due to the reactivation of old faults by regional extensional processes) led to the formation of the Shibantan basin which was then successively filled by carbonate ramp systems. C: Widespread inner-ramp settings were re-established during Baimatuo times. Please note that the depicted faults are only suspected and the tectonic processes responsible for the formation of the Shibantan Member are still unclear.

Within the FT I, the successive transition from non-bedded deposits with vugs into dm-thick beds and a massive part with white chert nodules in the uppermost Hamajing Member (Fig. 2.2) may reflect a slight deepening of the environment. The distinct black limestone bed intercalated into the topmost Hamajing Member possibly represents an interim deepening pulse preceding the actual Shibantan Member or, alternatively, may results from lateral facies variability in the otherwise very shallow-marine environments of the Dengying Formation. However, the boundary between the Hamajing

Member and the Shibantan Member is generally unconformable and represents a major sequence boundary (Wang et al., 1998; Zhu et al., 2003, 2007). Possible causes are (i) a sea-level change or (ii) a tectonic event (Zhu et al., 2003) and/or (iii) increased subsidence of the protected basin (Steiner et al., 1993). The deepening must have been rapid since no progressive crossing of single facies belts is observed and the surface of the Hamajing Member does not show any evidence for erosion. At the same time, the local character of the Shibantan Member and the contemporary occurrence of small coastal basins on the north-western and south-western margins of the platform (represented by the Gaojiashan and Jiuchen Members, respectively; Zhu et al., 2003) implies that the deepening was restricted to certain areas on the platform (see 2.4.4).

The FT II (Black laminated limestones) is vertically continuous over at least 40 m without a prominent change in its characteristics. Therefore, the sedimentation rate probably did not exceed the subsidence and *vice versa*. However, the chert bands and -concretions occurring in this FT could reflect periods of condensed sedimentation. In Phanerozoic deposits, carbonate concretions and cemented-beds (i.e. hardgrounds) are formed by various processes but they usually grow during times of reduced sedimentation (e.g. Bathurst, 1975; Raiswell, 1988; Fürsich et al., 1992). In Precambrian sedimentary rocks, including the Shibantan Member, the predominance of chert bands and -concretions can be plausibly explained by (i) the lack of biological sinks for silica, leading to higher concentrations of dissolved silica in seawater (e.g. Knoll, 1985; Maliva et al., 1989; Siever, 1992) and (ii) the absence of vertical bioturbation, causing higher concentrations of silica ions within very shallow depths of the sediments (e.g. McIlroy and Logan, 1999; Callow and Brasier, 2009). Furthermore, high contents of organic matter within the Shibantan carbonates (providing nucleation sites) may have favoured early diagenetic silica precipitation (cf. Knoll, 1985; Siever, 1992; and references therein). Thus, the observed chert bands and -concretions may be interpreted in similar ways to early diagenetic carbonate concretions in Phanerozoic strata and would be in line with a carbonate platform environment characterised by comparably low sedimentation rates that may have even decreased section upwards.

Starting with the FT III (i.e. Dark wavy dolomites) the basin became successively filled. This trend is not only evident by means of sedimentary structures and textures but is also expressed by a change in mineralogy from calcite to dolomite. In the course of the proceeding shallowing, facies belts are progressively crossed as evident by gradual transitions. Important, however, is that the entire facies is characterised by wavy beds and hummock cross stratification, underlining the constant impact of storm waves on the middle ramp environment. Ultimately, the FT III grades back into evaporitic dolomites deposited in a sub- to supra-tidal inner-ramp environment above FWB (i.e. the FT I). Accordingly, the facies of the overlying Baimatuo Member strongly resembles that of the Hamajing Member.

2.4.4 Development of the Shibantan basin

As discussed before (see 2.4.3) the depositional environments of the Shibantan Member can plausibly be explained with a carbonate ramp model (Fig. 2.2, 2.7). Ramps occur consistently in tectonic regimes characterised by gentle flexural subsidence (Burchette and Wright, 1992). Given the restriction of the Shibantan Member to the Yangtze Gorges area and its geological context it appears that the ramp system was linked to an intra-platform basin (Fig. 2.7). Intra-platform basins are shallow (mostly < 200 m deep), relatively short-lived structures that are known to develop within major carbonate platforms by tectonic processes or the diapiric uplift of salt (Burchette and Wright, 1992). Their typical size is up to a few hundred kilometres across (Burchette and Wright, 1992) which is in good accordance with the dimension on the Shibantan basin.

However, though significant evaporite deposits were reported for other areas of the Dengying platform (Xi, 1987; Siegmund and Erdtmann, 1994; Steiner, 2001; Zhu et al., 2007; see 2.4.3) there is no evidence for significant amounts of evaporites in the area of Yichang. This implies that tectonic processes may have been crucial for the development of the Shibantan Member. Following a final rift phase related to the breakup of Rodinia during the Nantuo glaciation (i.e. ≥ 690 Ma), South China became tectonically stable and sedimentation was mainly controlled by thermal subsidence (Wang and Mo, 1995; Wang and Li, 2003; Li et al., 2008; Wan, 2010). On the other hand, small (< 10 km) isolated basins related to old (i.e. Meso- to Neoproterozoic) fault systems existed during Doushantuo- to lower Dengying times in Yichang and other areas of the platform (Xi, 1987; Vernhet, 2007). Further evidence on the tectonic impact on the sedimentation of the Shibantan Member could be provided by the slumping structures since the respective processes are commonly related with seismic activity (e.g. Flügel, 2004). Sediment-slumping during Dengying time is also known from other areas on the platform (Steiner, 2001). The mass-flows in contrast occur in a middle ramp environment frequently affected by storm waves (Fig. 2.2, 2.6) and were therefore probably caused by storms, though a tectonic trigger cannot be excluded. Taken together, however, a relation of the Shibantan basin to faults that have been induced or reactivated by regional extensional processes appears highly plausible, but further detailed structural geological studies are necessary for a detailed understanding of the tectonic framework.

2.4.5 Palaeoecological implications

The microbial-mat associated biota in the Shibantan Member (i.e. Ediacara-type fossils, horizontal traces, vendotaenids) can clearly be attributed to the FT II (Black laminated limestones) and thus to an environment close to the SWB. The Ediacara-type organisms are probably autochthonous and their preservation was facilitated by episodic deposition of silty sediments, comparable to volcanic ash-masking in the Avalon Assemblage of Newfoundland (Sun, 1986; Xiao et al., 2005; Shen et al., 2009). Though it is not clear whether clay minerals in the preserving beds in the Shibantan Member are detrital and/or authigenic in origin (e.g. Chen et al., 2013; Meyer et al., 2014), the interrelationship between allochthonous event deposits and autochthonous fossil associations is conspicuous in the Shibantan Member.

Event beds have also been important for the preservation of fossils in the contemporary Gaojiashan Member, which was deposited on the north-western margin of the platform and can be correlated with the Shibantan Member owing to the presence of a basal transgressive surface and the preserved biota (Ding et al., 1992; Yin, 1993; Zhu et al., 2003, 2007). The Gaojiashan Member generally represents a siliciclastic-dominated shallowing-upward sequence, encompassing environments beneath the SWB to above the FWB. Tubular fossils (e.g. *Conotubus* and *Gaojiashania*; Cai et al., 2011, 2013) were buried in situ by distal event deposits below the average SWB (Cai et al., 2010). Thus, the general facies development, sedimentary processes and the habitats of the biota are fairly in line with the Shibantan

Member. However, the lithology (siliciclastic-dominated vs. carbonate) and fauna (*Cloudina* community vs. Ediacara-type fossil community) are strikingly different, and this is probably due to the different position on the Dengying platform (coastal basin vs. offshore basin; Zhu et al., 2003). In these respects, the Shibantan Member is more comparable to the Khatyspyt Formation in north-eastern Siberia which consists of bituminous carbonates deposited in a deep-water carbonate ramp setting below SWB and contains Ediacara-type fossils (e.g. Fedonkin, 1990; Khomentovsky, 1990; Knoll et al., 1995; Grazhdankin et al., 2008). The Ediacara community in the Khatyspyt Formation is attributed to the Avalon Assemblage of Newfoundland by some authors (Grazhdankin, 2004; Grazhdankin et al., 2008; but see Waggoner, 2003 and Narbonne, 2005 for a different interpretation) which also occurred in deep-water environments below SWB (Waggoner, 2003; Wood et al., 2003; Narbonne, 2005). Assuming that the distribution of these assemblages was controlled by palaeoecological conditions (Grazhdankin, 2004) rather than by biogeography (Waggoner, 2003) or taphonomy (Narbonne, 2005), the importance of event deposits in the Shibantan Member reinforces the idea that the supply of nutrients by sedimentary processes was crucial for microbial mats and associated organisms in deeper water environments (Narbonne, 2005). This is also in line with the suspected utilisation of the sedimentary substrate and/or the ambient seawater by Ediacara-type organisms (Gehling et al., 2005; Xiao et al., 2005; Sperling et al., 2007; Shen et al., 2009; Meyer et al., 2014). Therefore, both the palaeoenvironment as well as sedimentary processes were probably crucial for the early evolution of complex life in Ediacaran palaeoecosystems.

2.5 Conclusions

The depositional system of the Ediacaran Shibantan Member in South China is explained with a carbonate ramp model linked to an intra-platform basin. The Dengying carbonate platform is generally characterised by sub- to supratidal inner ramp environments (above FWB; i.e. FT I Evaporitic dolomites). After a sudden local deepening event, probably due to a tectonically-induced increase in subsidence, a subtidal lower- to middle ramp environment (close to SWB; i.e. FT II Black laminated limestones) was established. Sedimentation was probably condensed as evidenced by early diagenetic chert bands and -concretions. In this environment the microbial mat associated biota in the Shibantan Member (i.e. Ediacara-type fossils, horizontal traces and vendotaenids) flourished. The basin became subsequently filled as indicated by a gradual transition to a subtidal middle-ramp environment (between SWB and FWB; i.e. FT III Dark wavy dolomites) and, ultimately, back to the FT I (see above). A distinct slump horizon as well as mass-flow deposits provide evidence that sedimentation in the Shibantan basin was highly dynamic, partly due to wave effect and, most likely, tectonic processes.

The close interrelationship between allochthonous event deposits and autochthonous fossil associations in the FT II is conspicuous in the Shibantan Member, and the situation is in some regards comparable to the contemporaneous Gaojiashan Member in the north-western part of the Dengying carbonate platform and the Khatyspyt Formation in north-eastern Siberia. The event deposits were probably important for the supply of nutrients to the microbial mats and associated organisms, as well as for the preservation of fossils.

Acknowledgements

Axel Hackmann, Anna Kral and Patrick Kunath are acknowledged for technical support. Marta Rodriguez-Martinez, Soo Yeun Ahn and Cui Luo are thanked for help and fruitful discussions during field-work. Martin Blumenberg, Volker Thiel, Filiz Afşar and Sebastián Oriolo are acknowledged for critical discussions and Lixia Li for helping with Chinese literature.

This work was financially supported by the Deutsche Forschungsgemeinschaft (DFG) (grant BL971/1-3), the National Basic Research Program of China (2013CB835006), the National Natural Science Foundation of China, the Courant Research Centre of the University Göttingen, and the German Academic Exchange Service.

References

Aigner, T., 1985. Strom Depositional Systems. Dynamic Stratigraphy in Modern and Ancient Shallow-Marine Sequences. Lecture Notes in Earth Sciences. Springer, Berlin, Heidelberg.

Bathurst, R.G.C., 1975. Carbonate sediments and their diagenesis. Developments in sedimentology, 12. Elsevier, Amsterdam.

Bengtson, S., Zhao, Y., 1992. Predatorial Borings in Late Precambrian Mineralized Exoskeletons. Science 257, 367-369.

Burchette, T.P., Wright, V.P., 1992. Carbonate ramp depositional systems. Sedimentary Geology 79, 3-57.

Butterfield, N.J., 2011. Animals and the invention of the Phanerozoic Earth system. Trends in Ecology & Evolution 26, 81-87.

Cai, Y., Hua, H., Xiao, S., Schiffbauer, J.D., Li, P., 2010. Biostratinomy of the Late Ediacaran Pyritized Gaojiashan Lagerstätte from Southern Shaanxi, South China: Importance of Event Deposits. PALAIOS 25, 487-506.

Cai, Y., Schiffbauer, J.D., Hua, H., Xiao, S., 2011. Morphology and paleoecology of the late Ediacaran tubular fossil *Conotubus hemiannulatus* from the Gaojiashan Lagerstätte of southern Shaanxi Province, South China. Precambrian Research 191, 46-57.

Callow, R.H.T., Brasier, M.D., 2009. Remarkable preservation of microbial mats in Neoproterozoic siliciclastic settings: Implications for Ediacaran taphonomic models. Earth-Science Reviews 96, 207-219.

Cao, R., Tang, T., Xue, Y., Yu, C., Yin, L., Zhao, W., 1989. Research on Sinian Strata with ore deposits in the Yangzi (Yangtze) region, China. In: Nanjing Institute of Geology and Palaeontology (Eds.), Upper Precambrian of the Yangzi (Yangtze) Region, China. Nanjing University Press, Nanjing, pp. 1-94.

Chen, Z., Zhou, C., Meyer, M., Xiang, K., Schiffbauer, J.D., Yuan, X., Xiao, S., 2013. Trace fossil evidence for Ediacaran bilaterian animals with complex behaviors. Precambrian Research 224, 690-701.

Chen, Z., Zhou, C., Xiao, S., Wang, W., Guan, C., Hua, H., Yuan, X., 2014. New Ediacara fossils preserved in marine limestone and their ecological implications. Scientific Reports 4, 4180.

Condon, D., Zhu, M., Bowring, S., Wang, W., Yang, A., Jin, Y., 2005. U-Pb Ages from the Neoproterozoic Doushantuo Formation, China. Science 308, 95-98.

Ding, L., Zhang, L., Li, Y., Dong, J., 1992. The Study of the Late Sinian-Early Cambrian Biota from the Northern Margin of Yangtze Platform. Scientific and Technical Documents Publishing House, Beijing

Ding, Q.X., Chen, Y.Y., 1981. Discovery of soft metazoan from the Sinian System along eastern Yangtze Gorge, Hubei. Journal of the Wuhan College of Geology 2, 53-57.

Ding, Q.X., Xing, Y.S., Wang, Z.Q., Yin, C.Y., Gao, L.Z., 1993. Tubular and Trace Fossils from the Sinian Dengying Formation in the Miaohe-Liantuo Area, Hubei Province. Geological Review 39, 118-123

Dzik, J., 2002. Possible ctenophoran affinities of the precambrian "sea-pen" *Rangea*. Journal of Morphology 252, 315-334.

Fedonkin, M.A., 1990. Systematic Description of Vendian Metazoa. In: Sokolov, B.S., Iwanowski, A.B. (Eds.), The Vendian System. Springer, Berlin, pp. 71-120.

Flügel, E., 2004. Microfacies of Carbonate Rocks. Analysis, Interpretation and Application. Springer, Berlin, Heidelberg

Fürsich, F.T., Oschmann, W., Singh, I.B., Jaitly, A.K., 1992. Hardgrounds, reworked concretion levels and condensed horizons in the Jurassic of western India: their significance for basin analysis. Journal of the Geological Society 149, 313-331.

Gehling, J.G., Droser, M.L., Jensen, S., Runnegar, B.N., 2005. Ediacaran organisms: relating form to function. In: Briggs, D.E.G. (Ed.), Evolving Form and Function: Fossils and Development. Peabody Museum of Natural History, New Haven, pp. 43-66.

Germs, G.J.B., 1972. New shelly fossils from the Nama Group, South West Africa. American Journal of Science 272, 752-761.

Grazhdankin, D., 2004. Patterns of distribution in the Ediacaran biotas: facies versus biogeography and evolution. Paleobiology 30, 203-221.

Grazhdankin, D.V., Balthasar, U., Nagovitsin, K.E., Kochnev, B.B., 2008. Carbonate-hosted Avalon-type fossils in arctic Siberia. Geology 36, 803-806.

Grotzinger, J.P., Watters, W.A., Knoll, A.H., 2000. Calcified metazoans in thrombolite-stromatolite reefs of the terminal Proterozoic Nama Group, Namibia. Paleobiology 26, 334-359.

Jensen, S., Droser, M., Gehling, J., 2006. A Critical Look at the Ediacaran Trace Fossil Record. In: Xiao S., Kaufman, A.J. (Eds.), Neoproterozoic Geobiology and Paleobiology. Topics in Geobiology. Springer Netherlands, pp. 115-157.

Jiang, G., Shi, X., Zhang, S., Wang, Y., Xiao, S., 2011. Stratigraphy and paleogeography of the Ediacaran Doushantuo Formation (ca. 635-551 Ma) in South China. Gondwana Research 19, 831-849.

Kennedy, M., 2013. The Nonlinear Effects of Evolutionary Innovation Biospheric Feedbacks on Qualitative Environmental Change: From the Microbial to Metazoan World. The American Naturalist 181, S100-S111.

Khomentovsky, V.V., 1990. Vendian of the Siberian Platform. In: Sokolov B.S., Fedonkin, M.A. (Eds.), The Vendian System. Springer, Berlin, pp. 102-183.

Knoll, A., Walter, M., Narbonne, G.M., Christie-Blick, N., 2006. The Ediacaran Period: a new addition to the geologic time scale. Lethaia 39, 13-30.

Knoll, A.H., 1985. Exceptional Preservation of Photosynthetic Organisms in Silicified Carbonates and Silicified Peats. Philosophical Transactions of the Royal Society of London. B, Biological Sciences 311, 111-122.

Knoll, A.H., Grotzinger, J.P., Kaufman, A.J., Kolosov, P., 1995. Integrated approaches to terminal Proterozoic stratigraphy: an example from the Olenek Uplift, northeastern Siberia. Precambrian Research 73, 251-270.

Knoll, A.H., Walter, M.R., Narbonne, G.M., Christie-Blick, N., 2004. A New Period for the Geologic Time Scale. Science 305, 621-622.

Li, Z., Bogdanova, S.V., Collins, A.S., Davidson, A., De Waele, B., Ernst, R.E., Fitzsimons, I.C.W., Fuck, R.A., Gladkochub, D.P., Jacobs, J., Karlstrom, K.E., Lu, S., Natapov, L.M., Pease, V., Pisarevsky, S.A., Thrane, K., Vernikovsky, V., 2008. Assembly, configuration, and break-up history of Rodinia: A synthesis. Precambrian Research 160, 179-210.

Ling, H.-F., Chen, X., Li, D., Wang, D., Shields-Zhou, G.A., Zhu, M., 2013. Cerium anomaly variations in Ediacaran–earliest Cambrian carbonates from the Yangtze Gorges area, South China: Implications for oxygenation of coeval shallow seawater. Precambrian Research 225, 110-127.

Lu, M., Zhu, M., Zhang, J., Shields-Zhou, G., Li, G., Zhao, F., Zhao, X., Zhao, M. (2013). The DOUNCE event at the top of the Ediacaran Doushantuo Formation, South China: Broad stratigraphic occurrence and non-diagenetic origin. Precambrian Research 225, 86-109.

Maliva, R.G., Knoll, A.H., Siever, R., 1989. Secular Change in Chert Distribution: A Reflection of Evolving Biological Participation in the Silica Cycle. PALAIOS 4, 519-532.

McIlroy, D., Logan, G.A., 1999. The Impact of Bioturbation on Infaunal Ecology and Evolution during the Proterozoic-Cambrian Transition. PALAIOS 14, 58-72.

Meyer, M., Xiao, S., Gill, B.C., Schiffbauer, J.D., Chen, Z., Zhou, C., Yuan, X., 2014. Interactions between Ediacaran animals and microbial mats: Insights from Lamonte trevallis, a new trace fossil from the Dengying Formation of South China. Palaeogeography, Palaeoclimatology, Palaeoecology 396, 62-74.

Narbonne, G.M., 2005. The Ediacara Biota: Neoproterozoic Origin of Animals and Their Ecosystems, Annual Review of Earth and Planetary Sciences. Annual Review of Earth and Planetary Sciences, 421-442.

Narbonne, G.M., Xiao, S., Shields, G.A., Gehling, J.G., 2012. Chapter 18 - The Ediacaran Period. In: Gradstein, F., Ogg, J., Schmitz M., Ogg, G. (Eds.), The Geological Time Scale 2012, Elsevier, Amsterdam, pp. 413-435.

Raiswell, R., 1988. Chemical model for the origin of minor limestone-shale cycles by anaerobic methane oxidation. Geology 16, 641-644.

Shen, B., Xiao, S., Zhou, C., Yuan, X., 2009. *Yangtziramulus zhangi* New Genus and Species, a Carbonate-Hosted Macrofossil from the Ediacaran Dengying Formation in the Yangtze Gorges Area, South China. Journal of Paleontology 83, 575-587.

Siegmund, H., Erdtmann, B.-D., 1994. Facies and diagenesis of some upper proterozoic dolomites of South China. Facies 31, 255-263.

Siever, R., 1992. The silica cycle in the Precambrian. Geochimica et Cosmochimica Acta 56, 3265-3272.

Sperling, E.A., Pisani, D., Peterson, K.J., 2007. Poriferan paraphyly and its implications for Precambrian palaeobiology. Geological Society London Special Publications 286, 355-368.

Steiner, M., 2001. Die fazielle Entwicklung und Fossilverbreitung auf der Yangtze Plattform (Südchina) im Neoproterozoikum / frühesten Kambrium. Freiberger Forschungshefte C 492, 1-26.

Steiner, M., Mehl, D., Reitner, J., Erdtmann, B.-D., 1993. Oldest entirely preserved sponges and other fossils from the Lowermost Cambrian and a new facies reconstruction of the Yangtze Platform. Berliner Geowissenschaftliche Abhandlungen E, 293-329.

Sun, W., 1986. Late precambrian pennatulids (sea pens) from the eastern Yangtze Gorge, China: *Paracharnia* gen. nov.. Precambrian Research 31, 361-375.

Vernhet, E., Reijmer, J.J.G., 2010. Sedimentary evolution of the Ediacaran Yangtze platform shelf (Hubei and Hunan provinces, Central China). Sedimentary Geology 225, 99-115.

Vernhet, E., 2007. Paleobathymetric influence on the development of the late Ediacaran Yangtze platform (Hubei, Hunan, and Guizhou provinces, China). Sedimentary Geology 197, 29-46.

Vernhet, E., Heubeck, C., Zhu, M.Y., Zhang, J.M., 2007. Stratigraphic reconstruction of the Ediacaran Yangtze platform margin (Hunan province, China) using a large olistolith. Palaeogeography, Palaeoclimatology, Palaeoecology 254, 123-139.

Waggoner, B., 2003. The Ediacaran Biotas in Space and Time. Integrative and Comparative Biology 43, 104-113.

Walker, J.D., Geissman, J.W., Bowring, S.A., Babcock, L.E., 2013. The Geological Society of America Geologic Time Scale. Geological Society of America Bulletin 125, 259-272.

Wan, T., 2010. The Tectonics of China. Springer Berlin Heidelberg

Wang, H., Mo, X., 1995. An outline of the tectonic evolution of China. Episodes 18, 6-16.

Wang, J., Li, Z.-X., 2003. History of Neoproterozoic rift basins in South China: implications for Rodinia break-up. Precambrian Research 122, 141-158.

Wang, X., Erdtmann, B.-D., Chen, X., Mao, X., 1998. Integrated sequence-, bio- and chemostratigraphy of the terminal Proterozoic to Lowermost Cambrian "black rock series" from central South China. Episodes 21, 178-189.

Weber, B., Steiner, M., Zhu, M.Y., 2007. Precambrian - Cambrian trace fossils from the Yangtze Platform (South China) and the early evolution of bilaterian lifestyles. Palaeogeography, Palaeoclimatology, Palaeoecology 254, 328-349.

Wood, D.A., Dalrymple, R.W., Narbonne, G.M., Gehling, J.G., Clapham, M.E., 2003. Paleoenvironmental analysis of the late Neoproterozoic Mistaken Point and Trepassey formations, southeastern Newfoundland. Canadian Journal of Earth Sciences 40, 1375-1391.

Xi, X., 1987. Characteristics and environments of Sinian evaporite in Southern Sichuan, China. Earth Sciences 13, 23-29.

Xiao, S., Shen, B., Zhou, C., Xie, G., Yuan, X., 2005. A uniquely preserved Ediacaran fossil with direct evidence for a quilted bodyplan. Proceedings of the National Academy of Sciences of the United States of America 102, 10227-10232.

Yin, J., 1993. Geological Evolution and Mineralization from the Surrounding Areas of Sichuan Basin and its Vicinal Regions during the Sinian Subera. Press of Chengdu University of Science and Technology, Chengdu.

Zhao, Z., Xing, Y., Ding, Q., Liu, G., Zhao, Y., Zhang, S., Meng, X., Yin, C., Ning, B., Han, P., 1988. The Sinian System of Hubei. China University of Geosciences Press, Wuhan.

Zhao, Z., Xing, Y., Ma, G., Chen, Y., 1985. Biostratigraphy of the Yangtze Gorges area, 1 Sinian. Geological Publishing House, Beijing.

Zhou, C., Xiao, S., 2007. Ediacaran $\delta^{13}C$ chemostratigraphy of South China. Chemical Geology 237, 89-108.

Zhu, M., Zhang, J., Steiner, M., Yang, A., Li, G., Erdtmann, B. D., 2003. Sinian-Cambrian stratigraphic framework for shallow- to deep-water environments of the Yangtze Platform: an integrated approach. Progress in Natural Science 13, 951-960.

Zhu, M., Xiao, S., Yin, C., 2006. The Cryogenian and Ediacaran of South China: Ice Ages, Animal Embryos, Acritarchs, and Algae. The Second International Paleontological Congress Pre-Meeting Field Trip A8

Zhu, M., Zhang, J., Yang, A., 2007. Integrated Ediacaran (Sinian) chronostratigraphy of South China. Palaeogeography, Palaeoclimatology, Palaeoecology 254, 7-61.

- Chapter 3 -

Geobiology of an Ediacaran palaeoecosystem: The Shibantan Member (Dengying Formation, South China)

(*Precambrian Research; in revision*)

Jan-Peter Duda, Martin Blumenberg, Volker Thiel, Klaus Simon, Maoyan Zhu, Joachim Reitner

Abstract

The Shibantan Member (Dengying Formation, Ediacaran Period) is one of only few pure carbonate settings with Ediacara-type organisms worldwide and its lithology promises an excellent preservation of sedimentary facies and biogeochemical signatures. Here we provide the first comprehensive geobiological investigation of the Shibantan Member, addressing the interplay between sedimentary and (bio-) geochemical processes. Facies analyses revealed that carbonate and organic matter were autochthonously formed by biogeochemical processes linked to microbial mats. However, the material was frequently reworked and re-deposited within the same setting (i.e. para-autochthonous) as evidenced by e.g. erosional contacts, cross stratification and microbial chips. Negative Ce anomalies (Ce/Ce*) and low V/Cr ratios demonstrate that molecular O_2 was present in the water column, while characteristic Ni/Co-, V/(V+Ni), and V/Sc ratios suggest the presence of sub- to anoxic water. Taken together, our results imply a temporarily stratified water body frequently mixed and ventilated by storms. ^{13}C-enrichments in the Shibantan carbonates ($\delta^{13}C$ = +3.3 to +4.0‰, VPDB) together with ^{13}C-depletions of syngenetic *n*-alkanes cleaved from the extraction residue using catalytic hydropyrolysis (HyPy; $\delta^{13}C$ = -31.7 to -36.3‰, VPDB) indicate a significant withdrawal of ^{12}C by primary producers that thrived within the mats. At the same time, sulphurised biomarkers in the bitumen and HyPy-treated extraction residue hint at organic matter decomposition and concomitant sulphide production by sulphate-reducing bacteria. When oxygen was available at the sediment-water interface due to mixing by storms, sulphide oxidising bacteria were possibly temporarily favoured, supporting a respective interpretation of vendotaenid fossils in the Shibantan Member. It appears that the palaeoecosystem was highly dynamic due to a complex interplay of biological and geological processes. This has to be considered in future discussions about the evolution of metazoan life in Ediacara palaeoecosystems.

Keywords

Ediacaran, Ediacara-type organisms, sedimentary facies, biomarkers, stable carbon isotopes, trace elements, biogeochemical environment

Referred to by Chapter 6: ‘Reconsiderations and corrigenda’

3.1 Introduction

The Ediacaran Period (635-541 million years ago; Ma) spanned the time between the last Neoproterozoic global glaciation (Marinoan) and the Cambrian Explosion (Knoll et al., 2004, 2006; Walker et al., 2013). This period is generally regarded as a critical interval because of the strong influence of the Gaskiers glaciation (~580 Ma), the establishment of architecturally complex organisms of partly metazoan affinity (Ediacara-type fossils or Vendobionta; 575-541 Ma), the first potential trace fossils of bilateralian organisms, and the advent of biomineralisation and predation (*Cloudina* community) (e.g. Germs, 1972; Bengtson and Zhao, 1992; Grotzinger et al., 2000; Knoll et al., 2004, 2006; Narbonne, 2005; Jensen et al., 2006). Thus, the Ediacaran Period is characterised by one of the most dramatic revolutions of the Earth's biosphere with consequences for the entire Earth's system. Despite the importance of Ediacara palaeoecosystems for the early evolution of metazoans (e.g. Narbonne, 2005, and references therein), only little is known about their geobiology. Preservational and analytical issues make the use of biogeochemical proxies on sedimentary rocks from these settings often difficult. For instance, Ediacara palaeoecosystems are usually restricted to volcanic and siliciclastic sediments with a low preservational potential (Narbonne, 2005; Callow and Brasier, 2009) and therefore, with one exception from the Ediacaran White Sea setting (Kelly, 2009), biomarkers are not preserved in these environments. Carbonate systems may be more promising to fill this major preservational gap and contain more information about Ediacaran environments and -biology. However, only few pure carbonate settings with Ediacara-type organisms exist that can be considered as stratigraphical equivalents of the Ediacaran Member: the Khatyspyt Formation in Siberia and the Shibantan Member in South China (e.g. Sun, 1986, 1989; Fedonkin, 1990; Knoll et al., 1995; Xiao et al., 2005; Fedonkin and Vickers-Rich, 2007; Grazhdankin et al., 2008; Shen et al., 2009; Chen et al., 2013, 2014).

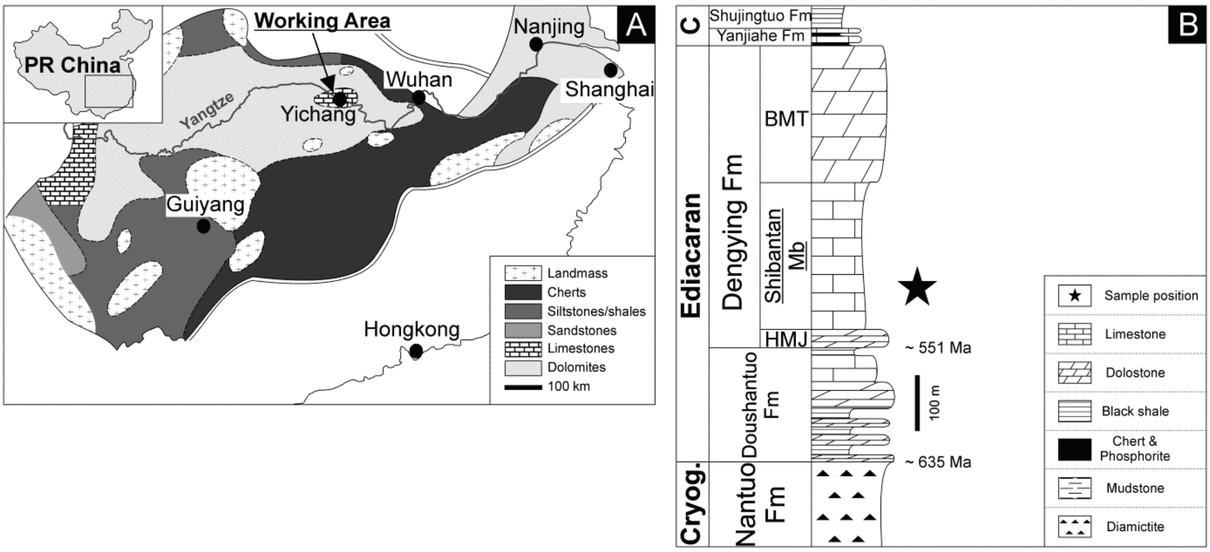

Fig. 3.1 Geological context of the Shibantan Member. A: Facies distribution on the Yangtze platform at time of deposition, the working area is located in the direct vicinity of Yichang (see arrow). B: Ediacaran- to Cambrian stratigraphy in the working area (Wuhe-Yanjiahe section), sample position marked by the star. C = Cambrian; HMJ = Hamajing Member; BMT = Baimatuo Member. A modified after Zhu et al. (2007); B modified after Chen et al. (2013) with ages from Condon et al. (2005).

The Shibantan Member (Dengying Formation, ca. 551-541 Ma; Zhu et al., 2003, 2007; Condon et al., 2005) exhibits dark, organic-rich limestones deposited in a distal offshore basin situated within the Yangtze carbonate platform (e.g. Wang et al., 1998; Steiner, 2001; Zhu et al., 2003, 2007; Ling et al., 2013; Fig. 3.1). It contains an exceptional fossil association (Xilinxia Biota; Chen et al., 1981; Ding et al., 1992) with putative algal or bacterial colonies (*Vendotaenia antiqua*; e.g. Sun, 1986; Zhao et al., 1988; Steiner, 1994; Weber et al., 2007; Zhu et al., 2007; Anderson et al., 2011), clear Ediacara-type fossils (*Paracharnia dengyingensis*; Ding and Chen, 1981; Sun, 1986; Dzik, 2002; *Yangtziramulus zhangi*; Xiao et al., 2005; Shen et al., 2009; *Hiemalora*, *Pteridinium*, *Rangea*, *Charniodiscus*; Chen et al., 2014) as well as the first trace fossils of mobile benthic animals on the Yangtze Platform (e.g. Zhao et al., 1988; Weber et al., 2007; Zhu et al., 2007; Chen et al., 2013; Meyer et al., 2014). Furthermore, a new annulated tubular fossil (*Wutubus annularis*; Chen et al., 2014) has been described. Further studies reported on occurrences of early sponge spicules (Steiner et al., 1993) and suggested specimens of the tubular fossil *Sinotubulites baimatuoensis* (Chen et al., 1981; Zhao et al., 1988). The Shibantan Member thus comprises a unique Ediacara fossil Lagerstätte, but almost nothing is known about the palaeoenvironment in which all of these organisms thrived.

Here we provide the first comprehensive geobiological investigation of the Shibantan Member as an Ediacara palaeoecosystem, addressing both sedimentological and biogeochemical issues. Facies, stable isotopes, trace elements (including rare earth elements), and organic biomarkers were analysed for a representative sample characterised by an Ediacara-type organism. Our study was aimed at elucidating the interplay between sedimentary and (bio-) geochemical processes in the Shibantan Member, which potentially has implications for other palaeoecosystems with Ediacara-type organisms.

3.2 Material and methods

3.2.1 Samples

Petrographical analyses were performed on various samples from the Shibantan Member in the Yichang area (Fig. 3.1). Additionally, comprehensive petrographical and biogeochemical analyses were conducted on the middle part of a representative sample block characterised by an Ediacara-type fossil on top (Fig. 3.2a, b). All samples were collected in the Zhoujia'ao Quarry, stratigraphically positioned in the lower part of the Shibantan Member (Fig. 3.1).

3.2.2 Bulk analyses

3.2.2.1 C/N/S

Bulk total inorganic carbon and N/S analysis was performed with a Hekatech Euro EA CNS instrument.

Total organic carbon (TOC) was measured with a Leco SC-632 instrument and T_{max} data were obtained with a standard Rock-Eval 6 instrument (APT Norway). For TOC analyses, the temperature program started with 300°C (3 min.) before temperature was raised by 25°C/min. to 650°C (0 min.).

3.2.2.2 Mineralogy

The mineralogical composition was determined by X-ray diffraction (XRD) analysis of whole-rock powder using a Philips X Pert MPD equipped with a PW3050 Goniometer (Cu as anode material). Data were collected from 4° to 69.5°2θ with a step size of 0.02°2θ and a scan step time of 2 seconds.

3.2.3 Stable isotopes ($\delta^{13}C$, $\delta^{18}O$)

For carbon and oxygen stable isotope measurements, carbonates were drilled from individual beds using a high precision drill (KaVo Dental GmbH, Biberach/Riß, Germany). Carbonate powders were reacted with 100% phosphoric acid (density > 1.95) at 70°C using a Thermo Kiel VI carbonate preparation line connected to a Finnigan Delta plus mass spectrometer. $\delta^{13}C$ values are reported in per mil relative to VPDB, while $\delta^{18}O$ values are reported in per mil relative to SMOW. Reproducibility was checked by replicate analysis of laboratory standards and was better than ±0.02‰ for $\delta^{13}C$ and ±0.03‰ (1σ) for $\delta^{18}O$.

3.2.4. Organic geochemistry

3.2.4.1 Extractable biomarkers (bitumen)

For biomarker analyses, all glassware and silica gel were heated to 500°C for 3h. A parallel prepared and analysed laboratory blank was run to keep track of laboratory contaminations. Sample surfaces including several dm of rock material were removed during several cutting steps with a pre-cleaned rock saw and, finally, a cleaned high precision saw (Buehler; Isomet 1000, Germany). The resulting sample was carefully crushed and powdered using a pebble mill (Retsch MM 301, Germany) and extracted with 100 ml each of dichloromethane (DCM), DCM/*n*-hexane (1/1; v/v) and *n*-hexane using ultrasonication (15 min.). Extracts were combined, desulphurised with active copper, and dried in a pre-cleaned rotary evaporator followed by N_2. The extraction residue was Soxhlet-extracted (DCM/methanol, 9:1, v:v) over 24h, decalcified with HCl (~3 mol/l), and again rigorously extracted using a solvent sequence as above. The solid residue was then further processed with catalytic hydropyrolysis (HyPy; see below).

3.2.4.2 Non-extractable biomarkers (HyPy-treated extraction residue)

Precambrian biomarkers are commonly problematic due to maturity and contamination issues, which have also been demonstrated for the Shibantan Member (Kelly, 2009). In addition to the bitumen fraction we therefore analysed the non-extractable macromolecular organic matter (i.e. the extraction residue after decalcification of silica lean rock material, therefore assumed to represent the kerogen) using HyPy. The kerogen is (1) much less susceptible to contamination than the bitumen, (2) immobile and thus endogenous to the host rock, and (3) tends to be less affected by thermal maturation than bitumen (e.g. Love et al., 1995, 2005, 2008; Brocks et al., 2003b; Marshall et al., 2007). Hence, HyPy has been successfully used for studying biomarkers in Precambrian rocks (Brocks et al., 2003b; Love et al., 2008, 2009; Marshall et al., 2007). In our study the samples were pyrolysed using a HyPy system from Strata Ltd. (Nottingham, UK) following Snape et al. (1989) and Love et al. (1995). Briefly, samples were heated in the presence of a sulphided molybdenum catalyst (ambient temperature to 250°C at 50°C min^{-1}; 250°C to 500°C at 8°C min^{-1}) under a hydrogen pressure of 150 bar and a flow of 5 L min^{-1}. The hydrocarbons released from the extraction residue were trapped downstream on silica powder cooled with dry ice (see Meredith et al., 2004). The pyrolysate was eluted from the silica trap with *n*-hexane. Elemental sulphur was removed with activated copper.

3.2.4.3 Combined gas chromatography–mass spectrometry (GC–MS) and gas chromatography combustion isotope ratio-mass spectrometry (GC-C-IRMS)

Extracts of the bitumen and the HyPy-treated extraction residue were subsequently fractionated into a saturated (F1), an aromatic (F2) and a polar fraction (cf. Blumenberg et al., 2012). Fractions 1 and 2 were analysed by GC–MS using a Varian CP-3800 GC coupled to a Varian1200L triple quadrupole MS. The GC was equipped with a deactivated retention gap (internal diameter (i.d.) 0.53 mm) connected to a fused silica capillary column (Phenomenex Zebron ZB-5MS, 30 m, 0.32 mm i.d., 0.25

µm film thickness). He was used as carrier gas. The GC oven was programmed from 80°C (held for 3 min) to 310°C (4°C/min; held for 25 min.). Fractions were injected on column. The ion source in the MS was operated at 200°C in electron ionisation mode at 70 eV. Biomarkers were identified by comparing mass spectra and retention times with published data and/or reference compounds. For relative quantification of compounds, selected ion monitoring (SIM) analyses were used because of better peak resolutions.

Thermal maturity was assessed by calculating a computed vitrinite reflectance equivalent based on the methylphenanthrene index MPI-1 (Radke and Welte, 1983) and phenanthrene/methylphenanthrene ratios (Phen/MP) (Brocks et al., 2003a).

δ^{13}C-values of hydrocarbons were analysed (two replicates) using a Thermo Scientific Trace GC coupled to a Delta Plus isotope-ratio MS. The combustion reactor contained CuO, Ni and Pt and was operated at 940°C. The GC was equipped with a Zebron ZB-5MS (30 m; 0.25 µm film thickness, 0.32 mm i.d.) and runs using a temperature program identical to that described above. δ^{13}C values are reported in per mil relative to VPDB. Reproducibility was checked by replicate analysis of laboratory standards. Standard deviations were generally better than ±2.3 (mean ±0.9).

3.2.5 Element-geochemistry

Trace elements including rare earth elements and yttrium (REE + Y) were analysed with laser ablation inductively coupled plasma mass spectrometry (LA-ICPMS) using a Perkin-Elmer SCIEX Elan DRII coupled to a laser ablation system from Lamda Physik (operating conditions: 27 kV, 7 Hz; pit Ø 120 µm). In order to minimise analytical errors, 17 spots were measured on different layers. NBS610 was used as internal standard, and ablation yields were corrected by referencing to ^{43}Ca. Anomalies were calculated based on shale normalised values (PAAS; McLennan, 1989) using published formulae for Eu/Eu*, Ce/Ce*, Pr/Pr*, Gd/Gd* (e.g. Bau and Dulski, 1996) and La/La* (e.g. Alibo and Nozaki, 1999).

3.3 Results

3.3.1 Petrography

The biogeochemically analysed sample was characterised by a poorly preserved Ediacara-type organism with circular ribs on top (Fig. 3.2a). Thin sections perpendicular to bedding from beneath this structure revealed fine grained calcite and organic material, while detrital (i.e. volcanic or siliciclastic) material was absent. These observations were confirmed by XRD, which showed exclusively calcite. The organic material was present in the form of horizontally orientated filaments within beds and laminae. Bed thicknesses were up to 2 cm and varied slightly. In places, gradation within the beds, cross bedding and lenticular bedding (Fig. 3.2c, d) were observed. Individual beds can be differentiated by crystal sizes as well as by the abundance and frequency of horizontally orientated organic filaments. In some cases, dark-brown laminae could hardly be differentiated from pressure solution rims. Load casts are a common feature, and contacts between beds are often erosional (Fig. 3.2e). An autochthonous microbial mat facies is another important characteristic of the Shibantan Member (Fig. 3.2f) and abundant organic remains are still preserved therein (Fig. 3.2g, h).

Sparite-filled, irregularly shaped voids were concentrated within certain layers of the samples (e.g. the lower part in Fig. 3.2e). The sizes of most of these voids were ≤ 1.8 mm in length and ≤ 0.25 mm in height. These structures are common features of the Shibantan carbonates as evidenced by other samples from the same quarry and previous reports (‘lensoidal pockets of spar’ in Xiao et al., 2005; ‘lensoidal calcspar’ in Shen et al., 2009).

Fig. 3.2 Biogeochemically analysed sample and sedimentology of the Shibantan Member. A: Top view with possible Ediacara-type fossil. B: Sketch of the analysed sample block (side view of Fig. 3.2a). C-E: Structures related to erosion and re-deposition (C: Cross bedding; D: Lenticular bedding, E: Erosional boundaries (black arrows) and microbial chips (white arrows)). F: Microbial mat facies (coin as scale). G, H: Organic remains of microbial mats.

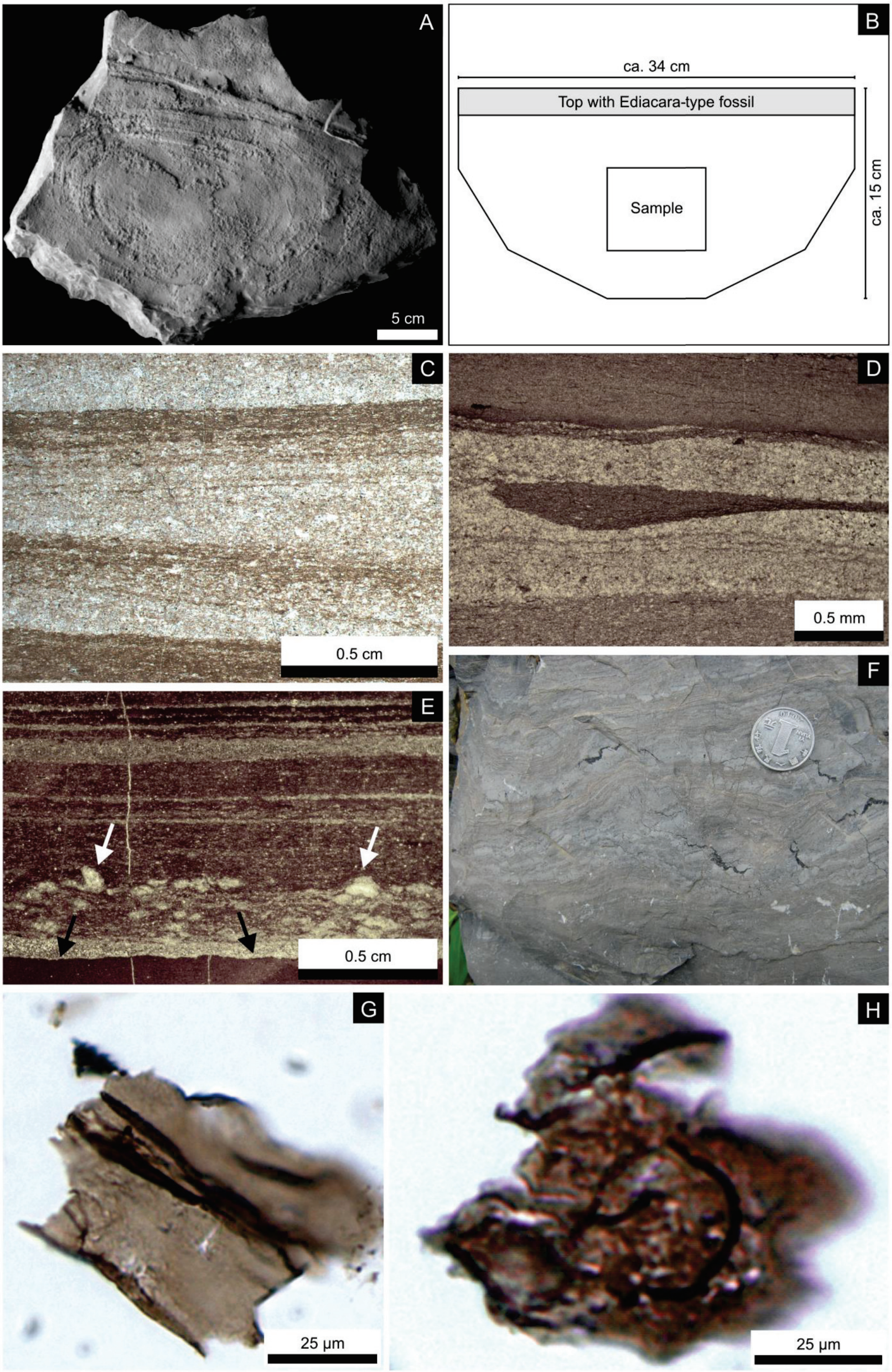
A
5 cm
B
ca. 34 cm
Top with Ediacara-type fossil
Sample
ca. 15 cm
C
0.5 cm
D
0.5 mm
E
0.5 cm
F
G
25 µm
H
25 µm

3.3.2 Stable isotope signatures in carbonate phases

Stable carbon isotope ratios ($\delta^{13}C_{carbonate}$) in different sample layers had generally a narrow range between +3.3 and +4.0‰ (Fig. 3.3). Stable oxygen isotope ratios ($\delta^{18}O_{carbonate}$) ranged between +25.6 and +26.8‰ (Fig. 3.3).

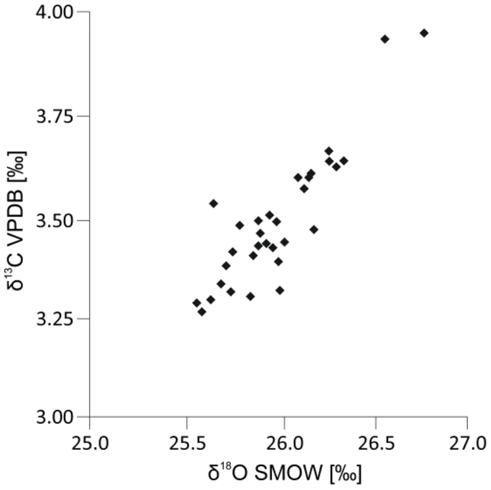

Fig. 3.3 $\delta^{13}C$ and $\delta^{18}O$ values of individual carbonate beds.

3.3.4 Organic geochemistry

The Shibantan Member has relatively high contents of total organic carbon (TOC = 0.6%). The organic matter (OM) was found to be highly mature ($T_{max} \geq 500°C$; HI = 125 mg HC/g TOC), but MPIs point to the late oil window ($MPI\text{-}1_{Bitumen} = 1.42$; $MPI\text{-}1_{Kerogen} = 1.38$) since the Phen/MP ratios of the organic matter are < 1 ($Phen/MP_{Bitumen} = 0.74$; $Phen/MP_{Kerogen} = 0.50$). Contents of sulphur (= 0.1 wt.-%) and nitrogen (= 0.05 wt.-%) as well as calculated C/N (= 12.5) and C/S (= 5.4) ratios are low.

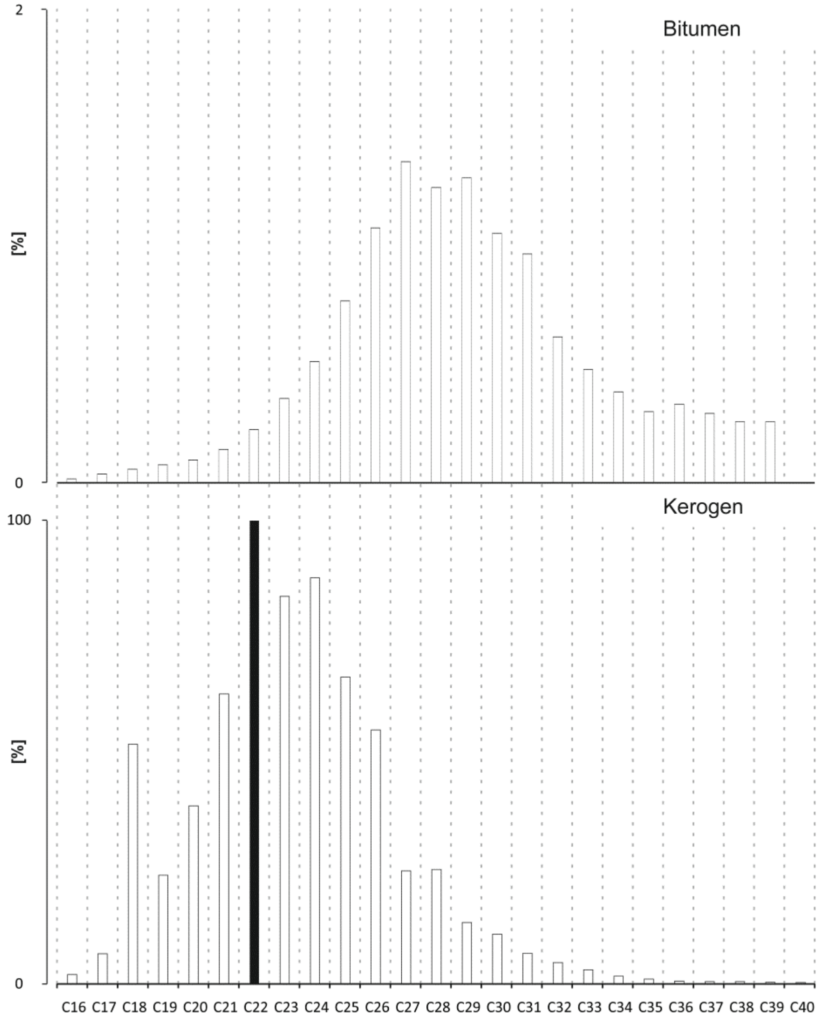

Fig. 3.4 Comparison of yields of *n*-alkanes in bitumen and HyPy-treated extraction residue relative to main compound (i.e. the C_{22} *n*-alkane in kerogen; indicated by black bar).

In the bitumen, *n*-alkanes ranged from C_{16} to C_{39} and had a bimodal distribution with maxima at C_{27} and (minor) at C_{36} (Fig. 3.4). Pristane and phytane were absent. Steranes and hopanes were only detected in trace concentrations too low for reliable interpretations. The bitumen was rich in polyaromatic hydrocarbons (PAHs) and contained abundant organic sulphur compounds. Major constituents were various thiophenes like dibenzothiophenes (DBTP; see Tab. 3.1 for abbreviations) and methylated dibenzothiophenes (MDBTP, DMDBTP), but also non-sulphur bearing PAHs such as (methyl-) phenanthrenes (PA, MPA) (Fig. 3.5).

The *n*-alkanes from the HyPy-treated extraction residue had carbon chain lengths from C_{16} to C_{40} and a bimodal distribution with a major maximum at C_{22} and a second maximum at C_{18} (Fig. 3.4). Concentrations of acyclic (i.e. pristane and phytane) and cyclic (i.e. steranes and hopanes) isoprenoid biomarkers were, similar to the bitumen, too low for interpretations. The extraction residue was also rich in PAHs (Fig. 3.5). Thiophenes like e.g. DBTP MDBTP, DMDBTP (Tab. 3.1) were also detected, though they were much less abundant than in the bitumen.

Compound	Abbr.	m/z
Phenanthrene	PA	178
Dibenzothiophene	DBTP	184
Methylphenanthrene	MPA	192
Methyldibenzothiophene	MDBTP	198
Dimethyldibenzothiophene	DMDBTP	212
Pyrene	PYR	202
Perylen	P	252

Tab. 3.1 Names, abbreviations, and molecular weights of aromatic hydrocarbons.

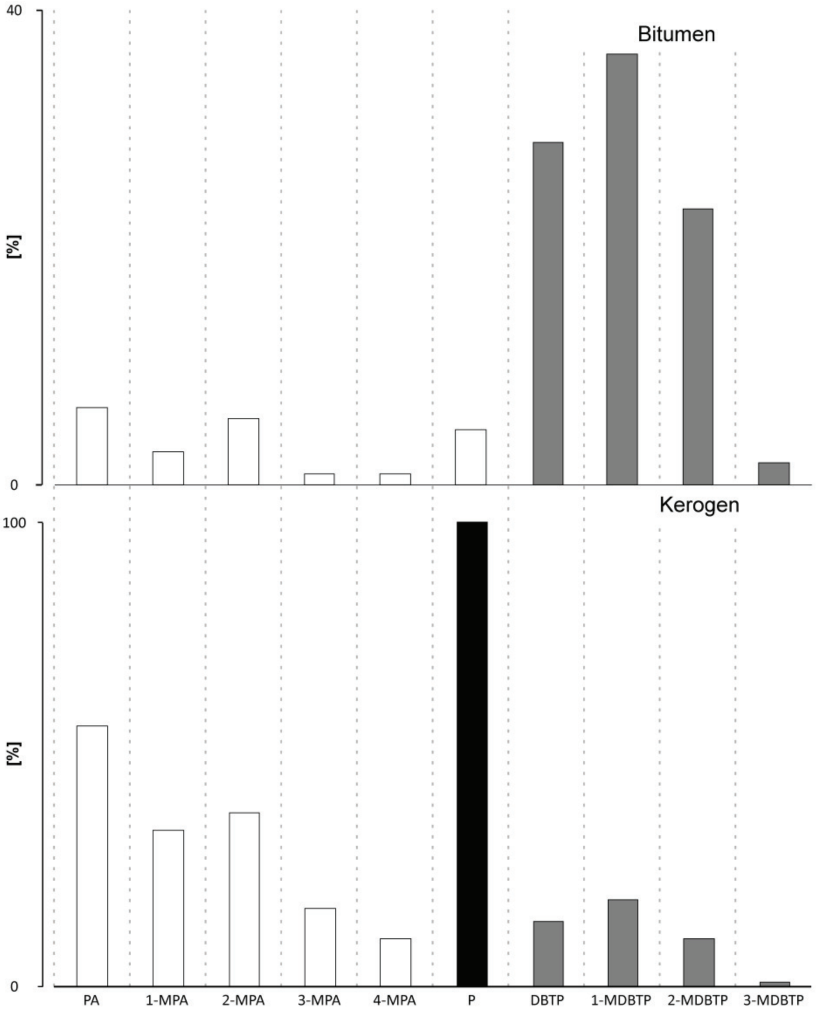

Fig. 3.5 Comparison of yields of selected aromatic compounds in bitumen and HyPy-treated extraction residue relative to main compound (i.e. P in HyPy-treated extraction residue; indicated by black bar). See Tab. 3.1 for abbreviations of compounds.

The $\delta^{13}C$ values of *n*-alkanes in the bitumen ranged from -28.5 to -32.1‰. $\delta^{13}C$ values of *n*-alkanes released from the extraction residue after applying HyPy were lower and ranged from -31.7 to -36.3‰ (Fig. 3.6).

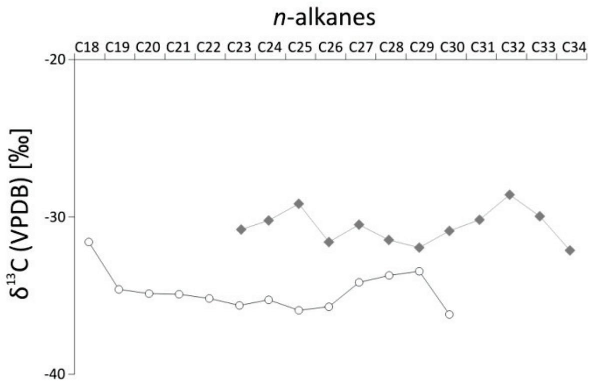

Fig. 3.6 Compound specific $\delta^{13}C$ values of organic matter in the bitumen (grey squares) and HyPy-treated extraction residue (white dots).

3.3.5 Element-geochemistry

Concentrations of measured main and trace elements are given in Tab. 3.2, and REE + Y concentrations are provided in Tab. 3.3. Calculated ratios and indexes are provided in Tab. 3.4. Because trace element concentrations are extremely low and partly close to detection limit in the Shibantan carbonate (Tab. 3.2, 3.3; see also Och, 2011), calculated mean values and standard-deviations are given in addition to values for each measuring point (n = 17). REE + Y concentration patterns of the individual point measurements are coherent (Fig. 3.7).

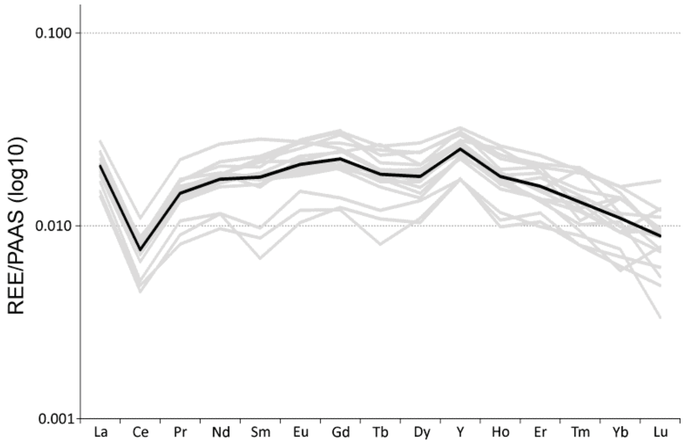

Fig. 3.7 REE + Y pattern of the analysed sample. Grey lines represent single measurements, the black line represents the calculated mean value.

	Main- and trace elements													
MP	Al	Si	P	S	Mn	Fe	Ni	Ti	Cu	Mo	Sc	V	Cr	Co	Th
1	18.7	2280	434	546	3.68	51.1	0.87	11.7	0.10	0.11	0.13	3.30	7.57	0.06	0.06
2	10.5	2190	272	576	3.58	52.9	0.76	9.08	0.08	0.12	0.15	2.85	8.19	0.07	0.04
3	34.6	3040	448	502	3.31	48.8	0.74	16.29	0.14	0.11	0.14	3.73	6.82	0.04	0.08
4	6.57	2420	140	526	3.06	26.4	0.71	5.79	0.19	0.11	0.07	2.13	1.80	0.04	0.03
5	3.25	980	72.9	281	3.16	51.4	0.66	5.75	0.26	0.04	0.07	2.02	2.83	0.06	0.01
6	8.18	844	88.3	299	2.74	20.5	0.50	5.25	0.191	0.07	0.07	1.96	1.46	0.03	0.02
7	11.6	2150	178	344	2.88	45.7	0.67	6.96	0.30	0.06	0.06	2.33	2.11	0.04	0.04
8	9.78	1698	208	450	3.06	36.3	0.75	8.60	0.19	0.09	0.09	3.06	2.37	0.04	0.04
9	11.6	2070	249	1029	3.61	39.2	0.83	9.17	0.18	0.09	0.06	3.19	3.90	0.04	0.04
10	4.64	2100	190	388	3.28	32.7	0.66	7.19	0.17	0.09	0.03	2.47	2.30	0.03	0.02
11	6.39	1580	224	401	3.54	40.4	0.75	7.49	0.09	0.08	0.05	2.18	3.18	0.04	0.02
12	3.81	1205	70.6	227	2.71	59.0	0.45	5.37	0.13	0.02	0.02	2.28	2.44	0.05	0.01
13	4.60	9420	101	238	2.44	16.7	0.41	4.92	0.05	0.03	0.06	2.41	2.36	0.03	0.01
14	6.34	5910	138	255	2.62	22.8	0.43	7.10	0.11	0.03	0.03	2.16	3.69	0.02	0.01
15	5.14	6320	124	295	2.64	23.1	0.56	4.10	0.07	0.03	0.07	2.67	5.72	0.03	0.01
16	7.46	2450	152	452	4.89	145	0.73	5.86	0.07	0.08	0.07	2.68	6.03	0.07	0.02
17	15.4	4150	439	652	4.26	161	2.03	6.66	0.55	0.22	0.16	5.05	6.56	0.06	0.06
Mean (n = 17)	9.91	2989	208	439	3.26	51.4	0.74	7.49	0.17	0.08	0.08	2.73	4.08	0.04	0.03
Std-Derivation	7.39	2195	122	193	0.61	39.2	0.35	2.86	0.12	0.05	0.04	0.75	2.16	0.01	0.02

Tab. 3.2 Major- and trace element concentrations (excluding REE + Y) of selected elements (in ppm). MP = Measuring point.

	REE + Y														
MP	La	Ce	Pr	Nd	Sm	Eu	Gd	Tb	Dy	Y	Ho	Er	Tm	Yb	Lu
1	0.77	0.70	0.14	0.63	0.12	0.03	0.13	0.02	0.11	0.83	0.02	0.06	0.008	0.04	0.004
2	0.80	0.65	0.15	0.69	0.11	0.03	0.15	0.02	0.10	0.84	0.02	0.06	0.008	0.05	0.005
3	0.93	0.67	0.14	0.60	0.10	0.02	0.10	0.01	0.08	0.66	0.02	0.04	0.008	0.03	0.005
4	0.74	0.61	0.13	0.57	0.10	0.02	0.10	0.02	0.10	0.72	0.02	0.05	0.006	0.04	0.004
5	0.85	0.63	0.13	0.61	0.10	0.02	0.09	0.01	0.07	0.62	0.02	0.04	0.005	0.03	0.003
6	0.73	0.58	0.13	0.63	0.10	0.02	0.09	0.01	0.07	0.61	0.02	0.04	0.004	0.03	0.002
7	0.80	0.62	0.13	0.62	0.12	0.02	0.11	0.02	0.10	0.71	0.02	0.05	0.006	0.03	0.003
8	0.77	0.61	0.14	0.59	0.10	0.03	0.11	0.02	0.10	0.74	0.02	0.04	0.005	0.03	0.004
9	0.79	0.62	0.14	0.63	0.12	0.03	0.14	0.02	0.11	0.80	0.02	0.06	0.005	0.04	0.004
10	0.73	0.56	0.12	0.56	0.10	0.02	0.10	0.01	0.08	0.69	0.02	0.04	0.006	0.03	0.004
11	0.70	0.52	0.12	0.54	0.09	0.02	0.10	0.01	0.07	0.60	0.02	0.04	0.004	0.02	0.003
12	0.64	0.41	0.09	0.39	0.05	0.02	0.07	0.01	0.06	0.47	0.01	0.03	0.003	0.02	0.002
13	0.57	0.39	0.07	0.33	0.05	0.01	0.06	0.01	0.05	0.47	0.01	0.03	0.003	0.02	0.003
14	0.54	0.36	0.08	0.39	0.04	0.01	0.06	0.01	0.05	0.47	0.01	0.03	0.004	0.02	0.001
15	0.91	0.67	0.15	0.73	0.13	0.03	0.12	0.02	0.10	0.75	0.03	0.05	0.004	0.04	0.004
16	0.92	0.67	0.15	0.64	0.10	0.02	0.10	0.01	0.09	0.64	0.02	0.04	0.005	0.03	0.005
17	1.05	0.87	0.19	0.90	0.16	0.03	0.14	0.02	0.13	0.87	0.03	0.07	0.008	0.05	0.007
Mean (n = 17)	0.78	0.60	0.13	0.59	0.10	0.02	0.10	0.01	0.08	0.67	0.02	0.05	0.005	0.03	0.004
Std-Derivation	0.12	0.12	0.03	0.13	0.01	0.01	0.03	0.004	0.02	0.12	0.004	0.01	0.002	0.01	0.001
PAAS	38.200	79.600	8.830	33.900	5.550	1.080	4.660	0.774	4.680	27.000	0.991	2.850	0.405	2.820	0.433
Normalized	0.020	0.008	0.015	0.017	0.018	0.021	0.022	0.019	0.018	0.025	0.018	0.016	0.013	0.011	0.009

Tab. 3.3 REE + Y concentrations (in ppm). MP = Measuring point. PAAS after McLennan (1989).

	Ratios & Indexes												
MP	Y/Ho	Nd/Yb	La/La*	Ce/Ce*	Pr/Pr*	Gd/Gd*	Eu/Eu*	Dy/Sm	V/Cr	Ni/Co	V/(V+Ni)	V/Sc	∑REE+Y
1	35.80	1.24	0.06	0.49	1.14	1.12	1.09	0.90	0.44	14.63	0.79	25.04	3.61
2	43.09	1.28	0.06	0.43	1.21	1.49	1.09	0.87	0.35	11.29	0.79	18.55	3.66
3	36.67	1.54	0.08	0.42	1.23	1.22	0.95	0.79	0.55	19.04	0.83	26.97	3.43
4	39.89	1.20	0.07	0.45	1.18	1.11	1.05	0.86	1.19	20.36	0.75	30.33	3.21
5	36.47	1.93	0.07	0.43	1.14	1.14	0.98	0.72	0.71	11.11	0.75	30.55	3.22
6	34.66	1.77	0.06	0.43	1.13	1.23	1.27	0.74	1.34	14.88	0.80	30.06	3.05
7	43.58	1.63	0.07	0.44	1.15	1.23	0.94	0.77	1.11	15.60	0.78	36.83	3.35
8	39.26	1.89	0.07	0.43	1.24	1.01	1.07	0.93	1.29	18.05	0.80	33.61	3.30
9	36.15	1.32	0.06	0.43	1.21	1.30	0.98	0.93	0.82	23.30	0.79	51.22	3.51
10	36.44	1.68	0.07	0.43	1.16	1.19	0.93	0.76	1.08	19.90	0.79	96.79	3.08
11	38.96	2.72	0.07	0.41	1.19	1.24	1.05	0.81	0.68	16.98	0.74	45.41	2.85
12	44.15	1.87	0.08	0.38	1.27	1.24	1.27	1.17	0.93	8.74	0.83	96.69	2.28
13	48.37	1.40	0.09	0.43	1.10	1.47	1.16	1.07	1.02	14.49	0.85	37.59	2.08
14	40.43	1.52	0.07	0.39	1.12	1.31	1.08	1.29	0.58	19.15	0.83	65.04	2.07
15	30.20	1.55	0.06	0.41	1.13	1.22	1.14	0.72	0.47	19.24	0.83	38.86	3.72
16	38.90	2.03	0.07	0.41	1.28	1.23	0.92	0.88	0.44	10.81	0.79	39.79	3.44
17	33.77	1.66	0.06	0.44	1.17	1.15	0.93	0.81	0.77	31.82	0.71	32.29	4.50
Mean (n = 17)	38.63	1.66	0.07	0.43	1.18	1.23	1.05	0.88	0.81	17.02	0.79	43.27	0.21
Std-Derivation	4.29	0.36	0.01	0.02	0.05	0.12	0.11	0.16	0.31	5.35	0.04	22.09	0.60

Tab. 3.4 Calculated element-geochemical ratios/indexes (∑REE + Y in ppm). MP = Measuring point.

3.4 Discussion

3.4.1 Sedimentary facies of the Shibantan Member

Cross stratification (Fig. 3.2c), lenticular bedding (Fig. 3.2d), erosive boundaries (Fig. 3.2e), and load casts point to transportation and thus a partly allochthonous source of the Shibantan carbonates. These features support a depositional environment below fair weather base but above storm weather base, as suggested by Xiao et al. (2005).

Interesting in this regard is the presence of autochthonous microbial mat facies in the Shibantan Member (Fig. 3.2f). At the same time disrupted resistant organic remains of microbial mats indicate reworking and subsequent re-sedimentation of mat-related material (Fig. 3.2g, h). Pflüger and Gresse (1996) described non-actualistic ‘microbial sand chips’ in sedimentary rocks deposited in storm-influenced nearshore marine environments below fair weather base (i.e. < 30-50 m water depth). The respective environments were inhabited by microbial mats which were eroded during major storms so that marginally rounded microbial sand chips were formed. The voids in the Shibantan carbonates probably have a similar origin, and are therefore termed ‘microbial chips’ in the following. Undeniably, this interpretation requires that a temporal and spatial linkage to well-developed mats can be demonstrated. According to Pflüger and Gresse (1996) the presence of biogenic mats is e.g. indicated by (1) refractory organic matter in the laminated parent sediment, (2) high concentrations of pyrite associated with sandy intraclasts indicating the presence of organic matter in the clasts, as well as (3) plastic deformation of the clasts during the erosive event. With the exception of pyrite occurrences, these criteria are in line with the voids observed in the material studied and are further evidenced by microbial facies and organic remains in other samples from the Zhoujia’ao Quarry (Fig. 3.2e-h). The lack of pyrite within clasts can be plausibly explained by the lack of reactive detrital iron minerals (cf. Pflüger and Gresse, 1996), probably due to the isolated position on the Shibantan carbonate platform (see Fig. 3.1a; Zhu et al., 2007).

While the combination of mat-binding, storm reworking and re-deposition is in good accordance with other observed features such as erosive boundaries and load casts (Fig. 3.2e), it is likely that carbonate precipitation within the voids occurred early after erosion and re-deposition of microbial mat fragments, i.e. when the organic remains were still cohesive and elastic (Pflüger and Gresse, 1996). In such a scenario, cementation may have been induced by increasing alkalinities due to sulphate reduction (cf. e.g. Canfield and Raiswell, 1991; Vasconcelos et al., 1995; Castanier et al., 2000) or carbonate nucleation on dead cell material (cf. Bosak and Newman, 2003).

The re-deposited material including the putative microbial mat fragments probably derived from the Shibantan Member itself (i.e. para-autochthonous) for several reasons. Firstly, a nearby source of the re-deposited material is indicated by the general absence of reworked shallow-water compounds derived from surrounding environments (e.g. ooids, oncolites, extraclasts). Second, the high frequency of microbial chips in some samples from the Shibantan Member is in line with the model of Pflüger and Gresse (1996), where microbial sand chips are formed by erosion of a microbial mat during storm events, but are re-deposited in shallow depressions with only very little actual transport. Third, a para-autochthonous origin of the carbonate sediment is further evidenced by the presence of almost intact autochthonous mats (Fig. 3.2f-h). Lastly, no scattering or incongruences of stable carbon isotopes (carbonate and organic material, respectively) and individual elemental redox-proxies were observed, suggesting that no major mixing of carbonates from different sources occurred. Taken together, all these characteristics clearly point to a para-autochthonous sediment, and a microbial mat environment that was frequently affected by erosion and re-deposition. The findings also suggest that the authigenic geochemical signals were not appreciably affected by allochthonous material.

3.4.2 Stable isotopes in carbonate phases

Analysis of $\delta^{13}C$ and $\delta^{18}O$ can help to decipher the depositional and diagenetic history of carbonate rocks and environmental controls on their formation, but post-depositional alterations of the $\delta^{13}C$ values need to be carefully considered (Kaufman and Knoll, 1995). However, thin sections of the Shibantan carbonates revealed no indications of major diagenetic alteration, and the number of cracks was very low (sampling over the few existing cracks was avoided by the use of a micro drill). Furthermore, carbonates are expected to retain the $\delta^{13}C$ values of original seawater if the Mn/Sr ratios are lower than 10 (Kaufman and Knoll, 1995) so that a Mn/Sr ratio of only about 0.01 indicates a minor impact of diagenetic fluids on the Shibantan sample. If referred to VPDB, the $\delta^{18}O$ values of the Shibantan carbonate range between -4.0 and -5.8‰ (mean of -4.8‰) and can thus be assumed to be valid as $\delta^{18}O$ values below -10‰ indicate significant alteration unacceptable for valid interpretations of $\delta^{13}C$ (cf. Kaufman and Knoll, 1995).

The measured $\delta^{13}C_{carbonate}$ values (Fig. 3.3) are in good agreement with contemporaneous sedimentary rocks (cf. Jacobsen and Kaufman, 1999). Interestingly, it was already noted that diverse Ediacaran organisms first appeared in sediments that document this rise in $\delta^{13}C_{carbonate}$ which was explained by globally high rates of organic matter burial associated with high levels of primary productivity (Knoll et al., 1986; Kaufman and Knoll, 1995). In the Hamajing Member of the Dengying Formation $\delta^{13}C_{carbonate}$ values remain relatively constant at +3‰ before increasing up to +5‰ in the Shibantan Member (Zhu et al., 2007). Because of the carbonate lithology of the Shibantan Member this additional enrichment in ^{13}C cannot be explained by dolomitisation. However, $\delta^{13}C$ values of syngenetic *n*-alkanes in the HyPy-treated extraction residue (Fig. 3.6) correspond with biomass from extant autotrophic organisms (down to ca. -35‰; cf. Schidlowski, 1988). Thus, a preferential withdrawal of ^{12}C by primary producers (e.g. cyanobacteria and/or algae) and an effective burial of the resulting ^{13}C-depleted biomass can plausibly explain the enrichment of ^{13}C in the Shibantan carbonate. This is in good agreement with the sedimentary facies, implying that burial and preservation of organic matter was much more effective in the Shibantan Member than in the shallower water areas represented by the underlying Hamajing Member. This is probably due to the absence of constant wave agitation and thus effective re-suspension and re-mineralisation of organic matter. In addition, a more effective burial of organic matter in the Shibantan Member may have been caused by low concentrations of molecular O_2 in the deeper water layers (see below), and by the steady growth of benthic ‘mat grounds’ that were only occasionally disturbed by storms. Indeed, mat grounds have been proposed as effective carbon sinks and their existence has been considered as an important mechanism for burying organic matter in the terminal Proterozoic (Gehling, 1999).

3.4.3 Organic matter

3.4.3.1 Organic matter (maturity, syngeneity)

Surface contamination is known to particularly affect mature and biomarker-lean rock samples from the Precambrian (Brocks et al., 2008), including the Shibantan Member (Kelly, 2009). Thus, the data quality has to be critically assessed and the syngeneity of organic compounds has to be demonstrated before Precambrian ecosystems can be reliably interpreted.

The high T_{max} is inconsistent with the calculated MPI-1 values as well as with the low C/N and C/S ratios, and as yet we do not have a plausible explanation for this. However, the extraordinarily low amounts of typical oil biomarkers in both bitumen and extraction residue, despite fairly high TOC values, correspond with a high thermal maturity of the organic matter. The high maturity is in line with the burial depth of the Ediacaran strata in Yichang (basal Ediacaran units max. about 4 km prior to Silurian orogeny; Jiang et al., 2006), but may also possibly have been influenced by post-depositional hydrothermal processes in the working area (Bristow et al., 2011; Derkowski et al., 2013).

Potential contamination can be critically assessed by comparing biomarkers from the bitumen with those released from the kerogen (cf. Brocks et al., 2003b). Compared to the kerogen-derived *n*-alkanes from the HyPy-treated extraction residue, those in the bitumen are systematically enriched in ^{13}C and have a quite different chain-length distribution (Fig. 3.4, 3.6), suggesting a non-endogenous source for these biomarkers. However, the bitumen did not show the characteristic preference of long-chain, odd-numbered *n*-alkanes derived from the cuticular waxes of higher land plants (Tissot and Welte, 1984). Therefore, a contribution from modern higher land plant material appears unlikely. More probably, the sample was contaminated with fossil (i.e. already matured) bitumen which may include natural (migrated) as well as anthropogenic compounds. The aromatic fractions of the bitumen and HyPy-treated extraction residue are generally characterised by the same key compounds (PA, DBTP, MPA, MDBTP). Differences in the distribution patterns (higher thiophene/PAH ratio in the bitumen) are most likely due to changes induced by the HyPy cracking (Fig. 3.5) and the aromatic compounds are therefore interpreted as being syngenetic. Taken together, our results indicate that maturity and contamination severely affected the bitumen inventory of the Shibantan Member, which is in line with results published elsewhere (Kelly, 2009). Nevertheless, aromatic hydrocarbons in the bitumen as well as aliphatic and aromatic hydrocarbon moieties in the kerogen appear to be largely syngenetic and can therefore be used for the reconstruction of the palaeoenvironment.

3.4.3.2 n-Alkanes

Though not specific, syngenetic *n*-alkanes cleaved from the extraction residue of the Shibantan carbonate are generally in line with a predominantly algal or bacterial source. An autotrophic metabolism can be inferred based on the $\delta^{13}C$ values of the single *n*-alkanes cleaved from the extraction residue (Fig. 3.6) and the concurrent enrichment of ^{13}C in the Shibantan carbonate (Fig. 3.3; see above).

3.4.3.3 Aromatics

Studies of kerogens indicate that Precambrian sedimentary organic matter tends to be aromatic in nature and yields relatively low amounts of aliphatic hydrocarbons (e.g. Summons et al., 1994; Brocks and Summons, 2003; Brocks et al., 2003b). The causes, however, are still unclear (Imbus et al., 1992; Brocks et al., 2003b; Marshall et al., 2007). One explanation is that Precambrian source organisms (e.g. acritarchs; Arouri et al., 2000), produced predominantly biodegradation-resistant (cyclised) biopolymers (Brocks et al., 2003b). A similarly high aromaticity is known from Mesoproterozoic bitumens of Mauritania, and has been explained by inputs of highly aromatic biopolymers and exopolymeric substances of microbial mats (Blumenberg et al., 2012). In the Shibantan Member, organic-walled fossils roughly comparable to ones reported from the Ediacaran White Sea setting (Steiner and Reitner, 2001) are preserved (Fig. 3.2g, h), implying the possible presence of resistant biopolymers. Furthermore, $\delta^{13}C$ values of *n*-alkanes in the HyPy-treated extraction residue (Fig. 3.6) are in line with $\delta^{13}C$ values of probably mat-related organic matter in Precambrian strata elsewhere (e.g. Blumenberg et al., 2012), making a similar origin of the organic matter in the Shibantan Member plausible. Therefore, organic geochemical characteristics point at microbial mats as main sources of organic matter in the Shibantan Member.

3.4.3.4 Organically bound sulphur

Organically bound sulphur is typically produced by reactions between organic matter and excess sulphide during early diagenesis (Sinninghe Damsté and De Leeuw, 1990, and references therein). Particularly if concentrations of iron are too low to form pyrite, sulphur is increasingly incorporated into organic matter (Sinninghe Damsté et al., 1989; Sinninghe Damsté and De Leeuw, 1990). Compared to the concentration of iron in shales, black shales and limestones (50,000, 65,300 and 9,500 ppm, respectively; Li, 2000), the iron concentration (mean 51.4 ppm; SD = 39.2) is extremely low in the Shibantan carbonate (Tab. 3.2). Accordingly, direct evidence for pyrite is rare and is limited to dark, pyrite-rich, macro-crystalline limestone beds at the base of the Shibantan Member (cf. Och, 2011). Indirect indications of (secondary) pyrite oxidation are rusty colours of weathered bedding surfaces or elemental sulphur which both typically occur in association with fossils (Shen et al., 2009; Anderson et al., 2011; Chen et al., 2013). However, in most Shibantan carbonates iron was too limited to effectively buffer H_2S which was instead sequestered into organic matter. Thiophenes, for instance, are often abundant in environments with a high activity of sulphate reducing bacteria and were found to be particularly high in H_2S-influenced cyanobacterial mats (Philp et al., 1992). Such a scenario is likely for the Shibantan Member. Likewise, the dibenzothiophene/phenanthrene-ratio of ~5 for the Shibantan bitumen points to an anoxic early diagenetic environment that was very rich in free sulphide (Hughes et al., 1995).

3.4.4 Element-geochemical data

3.4.4.1 Validation of element-geochemical data

Even minor contamination by terrigenous detritus will mask any seawater REE + Y pattern because of significantly higher REE concentrations in detrital minerals (e.g. Webb and Kamber, 2000). A contamination by detritus can be reflected in certain patterns of Al, Fe, Th, Sc, REE, as well as by the Y/Ho-ratio (e.g. Webb and Kamber, 2000; Ling et al., 2013). Established thresholds for a marine seawater REE + Y signature are, amongst others, Th (< 0.5 ppm), Sc (< 2 ppm), ∑REE (< 12 ppm), as well as a Y/Ho-ratio of > 36 (Ling et al., 2013). In the analysed sample, concentrations of respective elements are close to detection limit and thus, as well as ∑REE contents, far below these thresholds (Tab. 3.2, 3.4). Furthermore, the calculated Y/Ho-ratio (mean 38.63, SD = 4.29; Tab. 3.4) is in good agreement with expected values for marine carbonates with little detrital influence. Thus, contamination with detrital material appears to be unlikely.

Another evidence for contamination by detrital material in rocks is a good correlation between Al, Th, or Sc with ∑REE and Ce/Ce*, respectively (Ling et al., 2013). Al appears to be primarily linked to detrital material (high linear relationship with Th; Fig. 3.8a), but has only low linear relationships with various redox-sensitive elements (∑REE, Co, Cr, V, Ni, Mo) and -proxies (Ce/Ce*) (Fig. 3.8b-i). Likewise, linear relationships of elements typically enriched in terrigenous detritus (see above) with the Y/Ho ratio are low (Fig. 3.8j-n). Thus, masking of the seawater signal due to significant contamination with detrital material can be excluded for our sample.

Phosphates as well as Fe and Mn oxides are known to incorporate REE disproportionately and unpredictably and therefore potentially affect the REE signatures of authigenic sedimentary rocks (German and Elderfield, 1990; Bau et al., 1996; Byrne et al., 1996; Reynard et al., 1999; Shields and Webb, 2004). The P-contents (Tab. 3.2) and a low linear relationship between ∑REE and P generally suggest limited significant influence of phosphates (Fig. 3.9a). Potential leaching of diagenetic phosphate can further be detected by negative correlations between Ce/Ce* with Eu/Eu* and Ce/Ce* with Dy_{SN}/Sm_{SN} (Shields and Stille, 2001), but respective linear relationships are low as well (Fig.

3.9b, c). Linear relationships between ∑REE and Nd_{SN}/Yb_{SN} with Fe and Mn (Fig. 3.9d-g) as well as between Fe with Ce/Ce* and Eu/Eu* are also low (Fig. 3.9h-i). Therefore, alteration of the authigenic REE + Y signature by phosphates or Fe- and Mn-oxides is negligible.

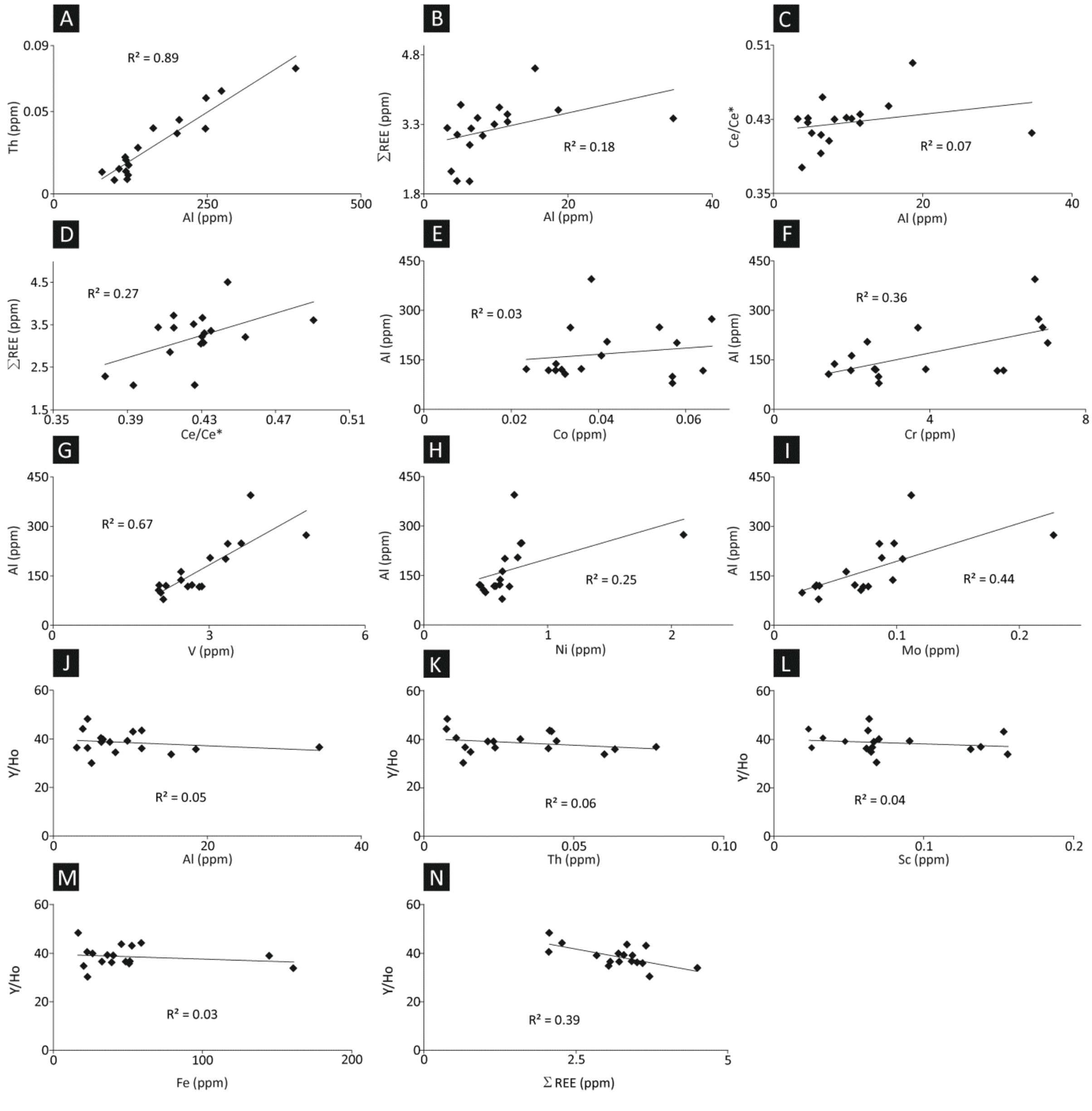

Fig. 3.8 Cross-plots for the validation of element-geochemical data (detritus).

REEs are not easily mobilised during diagenesis in carbonates (Webb et al., 2009) and REE + Y signatures of authigenic carbonate phases thus reflect seawater from which these carbonates precipitated (e.g. Webb and Kamber, 2000; Nothdurft et al., 2004). In contrast to REEs + Y, redox-sensitive elements potentially get remobilised and repartitioned during diagenesis (e.g. Tribovillard et al., 2006). However, in the absence of post-depositional replenishment of oxidising agents, (iron-) sulphides are stable and the elements co-precipitated with sulphides (e.g. V, Ni, Co) typically do not migrate during diagenesis (Tribovillard et al., 2006). Problematically, sulphide-minerals are not abundant in the sample analysed here. However, since a highly sulphidic environment is evident for the Shibantan Member during earliest diagenesis (see below) significant remobilisation due to post depositional oxidation can probably be neglected.

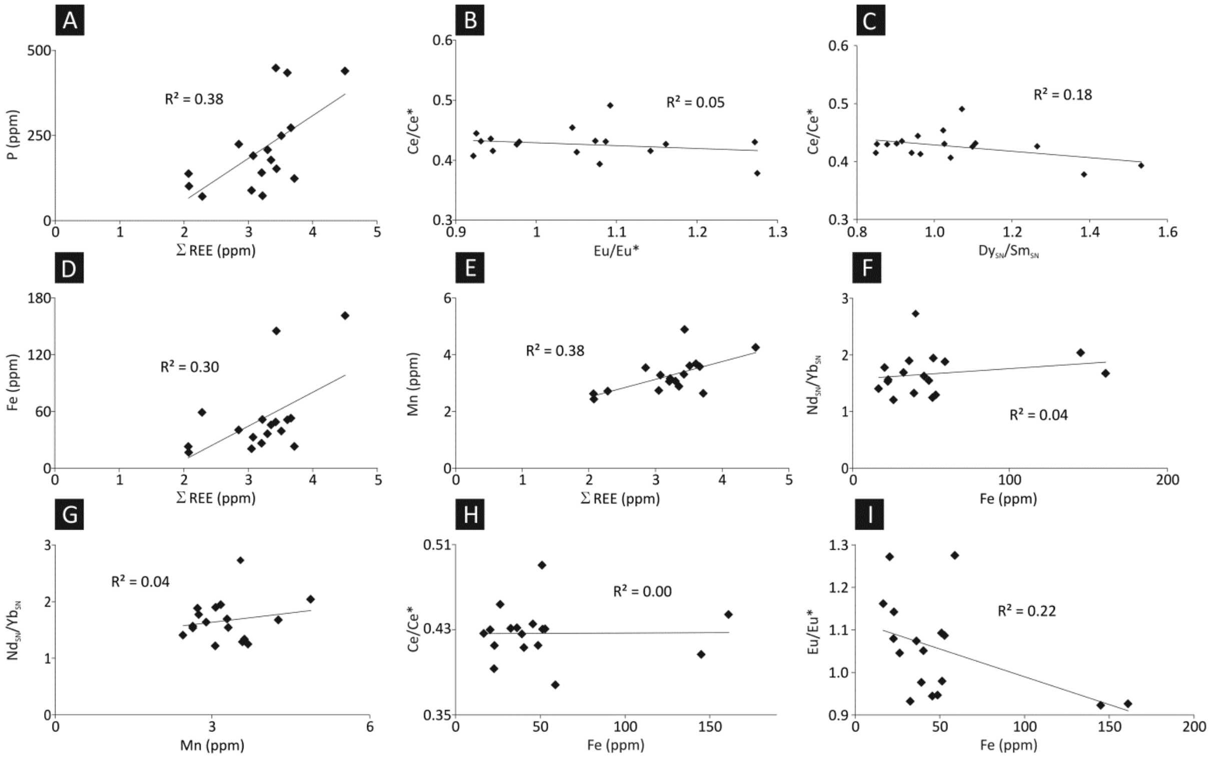

Fig. 3.9 Cross-plots for the validation of element-geochemical data (diagenesis).

Positive Eu anomalies in marine sediments are suggested to indicate an influence of hydrothermal fluids that may represent an important source of the dissolved REE load of seawater (Derry and Jacobsen, 1990). Eu/Eu* ratios in our samples are only slightly positive (mean 1.05, SD = 0.11; Tab. 3.4), which is in good agreement with results of Ling et al. (2013), who also describe Eu/Eu* values of ~1. A major hydrothermal imprint and thus, artificial masking of the seawater signal in Shibantan carbonates can therefore be excluded for the sample analysed here.

3.4.4.2 Redox environment

Trace elements including REE + Y are a well-established instrument for the investigation of the redox state of sea water, particularly with respect to the Neoproterozoic oxygenation event (e.g. Shields-Zhou and Och, 2011; Och and Shields-Zhou 2012, and references therein), and these techniques have also been applied to the Shibantan Member (Och, 2011; Ling et al., 2013). Well-oxygenated shallow ambient seawater is characterised by a uniform strong enrichment of heavy REEs (HREE) (expressed by Nd_{SN}/Yb_{SN}), consistent negative Ce anomalies (Ce/Ce*) and positive La anomalies (La/La*; ca. 1.3-1.5), distinctively high Y/Ho ratios (ca. 44-77), as well as slightly positive Gd anomalies (Gd/Gd*; ca. 1.15-0.30) (e.g. de Baar et al., 1991; Bau, 1996; Bau and Dulski, 1996; Webb and Kamber, 2000; Nothdurft et al., 2004; Allwood et al., 2010). Ce/Ce*-ratios of < 1.05 are interpreted as being real negative anomalies if Pr/Pr* > 1.15 (Bau and Dulski, 1996). The Shibantan carbonate is not enriched in HREEs (Nd_{SN}/Yb_{SN} mean 1.66, SD = 0.36; Tab. 3.4). Given the Pr/Pr*-ratios, Ce/Ce*-ratios represent real negative Ce_{SN}-anomalies (Fig. 3.10a), while La/La* values are due to a negative La_{SN}-anomaly (Tab. 3.4). The Y/Ho ratios (Tab. 3.4) are in good agreement with the respective ratio calculated based on data provided in Ling et al. (2013) (mean 41.96) and in modern seawater. On the other hand, the Gd_{SN} anomalies are higher than in modern seawater. Thus, only Ce/Ce*- and Y/Ho ratios are similar to modern oxygenated seawater (Fig. 3.10a). The presence of oxic conditions is supported by V/Cr ratios of < 2 (Fig. 3.10b) (Jones and Manning, 1994). However, V/Sc ratios (18.55 to 96.79) are by far higher than the range of crustal rocks in Earth history (4.7-9.1) which is considered to be associated with anoxic bottom waters (Kimura and Watanabe, 2001). This is supported by Ni/Co ratios of > 7 and V/(V+Ni) ratios < 0.85 (Fig. 3.10b-d), implying anoxic conditions (Hatch and Leventhal, 1992; Jones and Manning, 1994, respectively).

Taken together, our data reveal an apparent inconsistency between proxies supporting the presence of oxic waters (Ce/Ce*, Y/Ho, V/Cr) and those indicating sub- to anoxic waters (V/Sc, Ni/Co-, V/(V+Ni)). Such, at first glance, contradictory findings have also been reported from the Liuchapo Chert (basinal equivalent of the Dengying Formation), where Ce/Ce* points to the presence of oxygenated waters, while all other measured redox proxies (V/Cr, V/(V+Ni), V/Sc, Th/U) indicated deposition under extremely reducing and occasionally sulphidic/euxinic conditions (cf. Guo et al., 2007). This discrepancy is explained by a division into an upper oxygenated water body and less oxygenated deeper waters, where Ce is transported to the sediment by adsorption to Si. In the Shibantan carbonate, however, there is no relationship between Si and Ce ($r^2 = 0.073$) which argues against transportation of Ce with Si. Linear relationships between Ce and Mn concentrations are slightly higher ($r^2 = 0.412$), suggesting possible downward transport by adsorption to Mn-oxides and/or -hydroxides. Interestingly, such association of REE cycling with the redox cycling of Mn has been observed in anoxic basins with suboxic zones, namely the Black Sea (German et al., 1991).

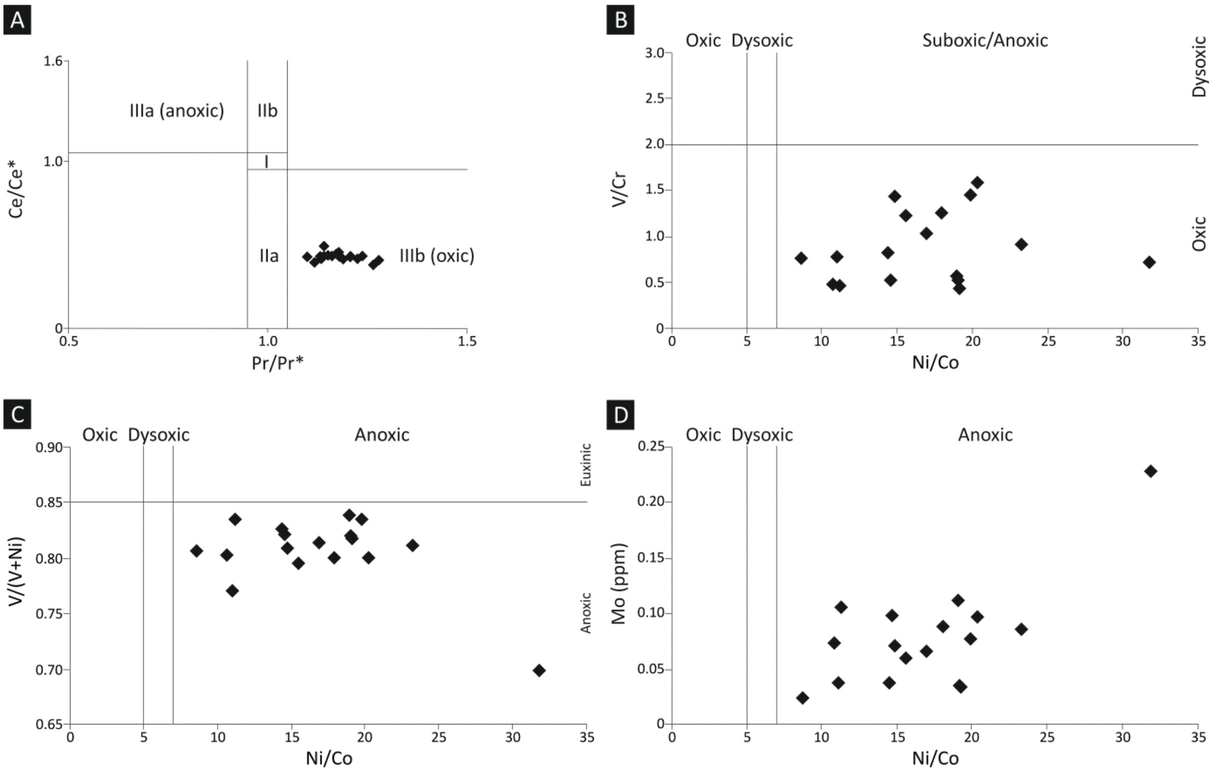

Fig. 3.10 Seawater redox-proxies.

3.4.5 Implications for the geobiology of the Shibantan Member

Strongly sulphidic conditions prevailed in the uppermost part of the sediment due to an extensive activity of sulphate reducing bacteria. The latter has been inferred previously by means of indirect approaches (e.g. presence of pyrite or secondary Fe-oxides, sulphur isotopes) in various settings with Ediacara-type organisms (e.g. Pflug, 1972; Waggoner, 1995; Fedonkin and Waggoner, 1997; Gehling, 1999; Steiner and Reitner, 2001; Dzik, 2003; Gehling et al., 2005; Bailey et al., 2006; Mapstone and McIlroy, 2006; Callow and Brasier, 2009). Our results reveal a similar scenario for the Shibantan Member, where vast amounts of H_2S were present during earliest diagenesis within the sediment, while molecular oxygen was at least temporarily present in the overlying seawater. A high activity of sulphate reducing bacteria, as evidenced by our data (see 3.5.3) requires the availability of sufficient sulphate in the setting. Increasing concentrations of sulphate due to continental run-off have already been discussed for the Doushantuo Formation (e.g. McFadden et al., 2008; Li et al., 2010). Thus, introduction of sulphate via enhanced continental weathering as result of the formation of the Trans-Gondwana mountain chain (Sawaki et al., 2010) could be a possible explanation in case of the Shibantan Member. An alternative explanation for a sufficient availability of sulphate could also be evaporation since hypersaline conditions prevailed at least locally during deposition of the Dengying Formation (e.g. Xi, 1987; Siegmund and Erdtmann, 1994; Steiner, 2001; Zhu et al., 2007). Enhanced evaporation and subsequent density differences in water masses would further have supported the proposed temporary stratification of the Shibantan basin depression (Fig. 3.11).

However, since stratification due to salinity is typically a regional phenomenon it is unclear if the Shibantan Member is comparable to other settings with Ediacara-type fossils in this regard. Nonetheless, varying redox states, as suggested for the Shibantan Member and other palaeoecosystems with Ediacara-type organisms (White Sea setting; Kelly, 2009), have implications for the evolution of complex life. It was suggested that the shift from redox-unstable conditions in the early Ediacaran Period to fully and persistently oxygenated environments in later Ediacaran Period was crucial in triggering end-Proterozoic evolutionary boosts (Johnston et al., 2012). Moreover, the proposed (at least temporal) stratification of the water column has implications for the interpretation of microbial mats in the Shibantan Member. Tight networks of intact filaments in the Shibantan Member are assigned to *Vendotaenia antiqua* (e.g. Sun, 1986; Steiner, 1994; Zhao et al., 1988; Weber et al., 2007; Zhu et al., 2007; Anderson et al., 2011) which are commonly interpreted as sulphur oxidising bacteria (e.g. Vidal, 1989; but see Cohen et al., 2009 for a different interpretation). However, modern sulphide oxidising bacteria are known to develop where opposed gradients of oxygen and sulphide are established (Jørgensen, 1982). A frequent shifting of the redox boundary towards the sediment/water interface, as indicated by our data, would have recurrently evoked suitable conditions for sulphide oxidising bacteria (Fig. 3.11). The ability of recent sulphide oxidising bacteria to bridge shorter periods with oxygen depleted bottom waters by using nitrate for the oxidation of sulphide (Schulz et al., 1999) could have been an advantageous strategy in this scenario. In the light of these findings it seems probable that sulphide oxidising bacteria were temporarily flourishing, making a respective interpretation of vendotaenid fossils in the Shibantan Member likely.

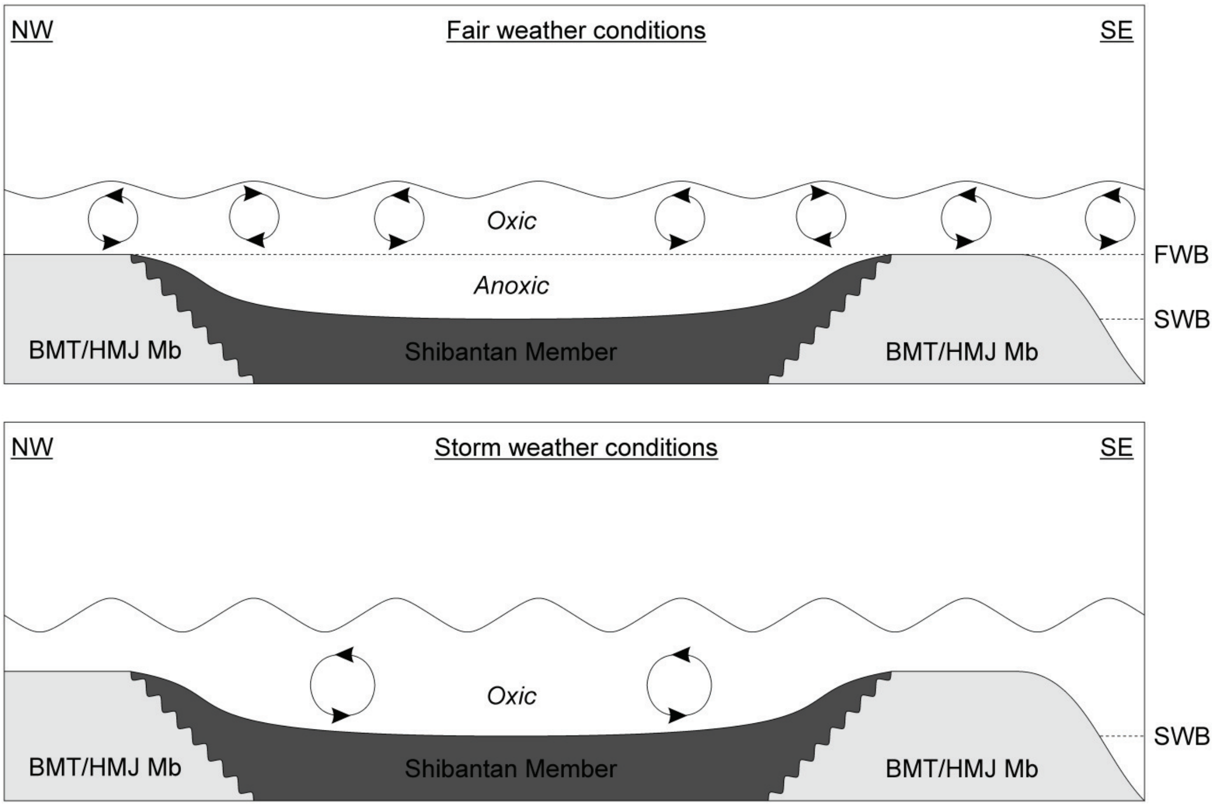

Fig. 3.11 Palaeoenvironmental model of the Shibantan Member. The water body is stratified under fair weather conditions while it is fully oxidised under storm weather conditions. BMT = Baimatuo Member; HMJ = Hamajing Member.

3.5 Conclusions

Summarising, the Shibantan Member represents a microbial mat environment with Ediacara-type organisms, which was frequently affected by erosion and re-deposition. A largely para-autochthonous origin of the carbonate sediment is evident. The depositional depth (< 50 m) was situated below fair weather base but above storm weather base. Trace elements demonstrate that the water body was temporarily stratified. Molecular O_2 was present in the water column (fair weather conditions) but frequent mixing during storm events led to the recurrent oxidation of the entire water column (Fig. 3.11). Dependent on the changeable biogeochemical conditions, particularly the availability of oxygen, Ediacara-Type organisms temporarily thrived in this setting.

Carbonate and organic matter were autochthonously formed by biogeochemical processes linked to microbial mats. Stable carbon isotopes of carbonate phases (+3.3 to +4.0‰, VPDB) and syngenetic *n*-alkanes in the extraction residue after applying HyPy (-31.7 to -36.3‰, VPDB) point to the presence of phototrophic primary producers (cyanobacteria and/or algae) within the mat facies of the Shibantan Member. Repeated cycles of mat-growth, reworking and re-deposition led to an effective burial of primary produced organic matter, and such withdrawal of ^{12}C enriched organic matter led to an enrichment of newly precipitated carbonate phases in residual ^{13}C.

Organic matter of the Shibantan Member (TOC = 0.6%) is highly mature ($T_{max} \geq 500$°C; HI = 125 mg HC/g TOC), causing overall low biomarker yields. However, abundant sulphurised compounds in the bitumen and HyPy-treated extraction residue hint at a high activity of sulphate reducing bacteria. In the light of these findings it seems highly probable that sulphide oxidising bacteria were temporarily flourishing, and a respective interpretation of vendotaenid fossils as sulphide oxidising bacteria thus appears plausible.

The combined results imply that the Shibantan palaeoecosystem was temporarily dynamic due to a complex interplay of biological and geological processes, which has to be considered in future discussions about the evolution of complex life in Ediacara palaeoecosystems. The environment, however, was not exceptional with regard to the elementary geobiological processes, and the sedimentary processes characterising the Shibantan Member are comparable to other Ediacara palaeoecosystems.

Acknowledgements

A. Pack, I. Reuber, D. Kohl (Department for Isotope Geology, University of Göttingen) and J. Dyckmans (Centre for Stable Isotope Research and Analysis, University of Göttingen) are thanked for stable isotope analyses. V. Karius and I. Ottenbacher (Department for Sedimentology & Environmental Geology, University of Göttingen) are acknowledged for XRD measurements. W. Riegel (Department of Geobiology, University of Göttingen) is acknowledged for the preparation of organic walled fossils. A. Reimer and B. Röring (Department of Geobiology, University of Göttingen) are thanked for CNS analyses. We are grateful to L. Laake, A. Hackmann, C. Conradt, and M. Reinhardt for technical and analytical support. We thank G. Love (University of California) and W. Meredith (University of Nottingham) for help with the installation of the HyPy system.

This work was financially supported by the Deutsche Forschungsgemeinschaft (grant BL971/1-3), the National Basic Research Program of China (2013CB835006), the National Natural Science Foundation of China, the Courant Research Center of the University Göttingen, and the German Academic Exchange Service.

References

Alibo, D.S., Nozaki, Y., 1999. Rare earth elements in seawater: particle association, shale-normalization, and Ce oxidation. Geochimica et Cosmochimica Acta 63, 363-372.

Allwood, A.C., Kamber, B.S., Walter, M.R., Burch, I.W., Kanik, I., 2010. Trace elements record depositional history of an Early Archean stromatolitic carbonate platform. Chemical Geology 270, 148-163.

Anderson, E.P., Schiffbauer, J.D., Xiao, S., 2011. Taphonomic study of Ediacaran organic-walled fossils confirms the importance of clay minerals and pyrite in Burgess Shale-type preservation. Geology 39, 643-646.

Arouri, K.R., Greenwood, P.F., Walter, M.R., 2000. Biological affinities of Neoproterozoic acritarchs from Australia: microscopic and chemical characterisation. Organic Geochemistry 31, 75-89.

Bailey, J.V., Corsetti, F.A., Bottjer, D.J., Marenco, K.N., 2006. Microbially-Mediated Environmental Influences on Metazoan Colonization of Matground Ecosystems: Evidence from the Lower Cambrian Harkless Formation. PALAIOS 21, 215-226.

Bau, M., 1996. Controls on the fractionation of isovalent trace elements in magmatic and aqueous systems: evidence from Y/Ho, Zr/Hf, and lanthanide tetrad effect. Contributions to Mineralogy and Petrology 123, 323-333.

Bau, M., Dulski, P., 1996. Distribution of yttrium and rare-earth elements in the Penge and Kuruman iron-formations, Transvaal Supergroup, South Africa. Precambrian Research 79, 37-55.

Bau, M., Koschinsky, A., Dulski, P., Hein, J.R., 1996. Comparison of the partitioning behaviours of yttrium, rare earth elements, and titanium between hydrogenetic marine ferromanganese crusts and seawater. Geochimica et Cosmochimica Acta 60, 1709-1725.

Bengtson, S., Zhao, Y., 1992. Predatorial Borings in Late Precambrian Mineralized Exoskeletons. Science 257, 367-369.

Blumenberg, M., Thiel, V., Riegel, W., Kah, L.C., Reitner, J., 2012. Biomarkers of black shales formed by microbial mats, Late Mesoproterozoic (1.1 Ga) Taoudeni Basin, Mauritania. Precambrian Research 196–197, 113-127.

Bosak, T., Newman, D.K., 2003. Microbial nucleation of calcium carbonate in the Precambrian. Geology 31, 577-580.

Bristow, T.F., Bonifacie, M., Derkowski, A., Eiler, J.M., Grotzinger, J.P., 2011. A hydrothermal origin for isotopically anomalous cap dolostone cements from south China. Nature 474, 68-71.

Brocks, J.J., Buick, R., Logan, G.A., Summons, R.E., 2003a. Composition and syngeneity of molecular fossils from the 2.78 to 2.45 billion-year-old Mount Bruce Supergroup, Pilbara Craton, Western Australia. Geochimica et Cosmochimica Acta 67, 4289-4319.

Brocks, J.J., Grosjean, E., Logan, G.A., 2008. Assessing biomarker syngeneity using branched alkanes with quaternary carbon (BAQCs) and other plastic contaminants. Geochimica et Cosmochimica Acta 72, 871-888.

Brocks, J.J., Love, G.D., Snape, C.E., Logan, G.A., Summons, R.E., Buick, R., 2003b. Release of bound aromatic hydrocarbons from late Archean and Mesoproterozoic kerogens via hydropyrolysis. Geochimica et Cosmochimica Acta 67, 1521-1530.

Brocks, J.J., Summons, R.E., 2003. Sedimentary Hydrocarbons, Biomarkers for Early Life. In: Heinrich, D.H., Karl, K.T. (Eds.), Treatise on Geochemistry. Pergamon, Oxford, pp. 63-115.

Byrne, R.H., Liu, X., Schijf, J., 1996. The influence of phosphate coprecipitation on rare earth distributions in natural waters. Geochimica et Cosmochimica Acta 60, 3341-3346.

Callow, R.H.T., Brasier, M.D., 2009. Remarkable preservation of microbial mats in Neoproterozoic siliciclastic settings: Implications for Ediacaran taphonomic models. Earth-Science Reviews 96, 207-219.

Canfield, D.E., Raiswell, R., 1991. Pyrite formation and fossil preservation. In: Allison, P.S.A., Briggs, D.E.G. (Eds.), Taphonomy: Releasing the Data Locked in the Fossil Record. Plenum Press, New York, pp. 338-388.

Castanier, S., Le Métayer-Levrel, G., Perthuisot, J.-P., 2000. Bacterial Roles in the Precipitation of Carbonate Minerals. In: Riding, R., Awramik, S.M. (Eds.), Microbial Sediments. Springer, Berlin.

Cohen, P.A., Bradley, A., Knoll, A.H., Grotzinger, J.P., Jensen, S., Abelson, J., Hand, K., Love, G., Metz, J., McLoughlin, N., Meister, P., Shepard, R., Tice, M., Wilson, J.P., 2009. Tubular Compression Fossils from the Ediacaran Nama Group, Namibia. Journal of Paleontology 83, 110-122.

Condon, D., Zhu, M., Bowring, S., Wang, W., Yang, A., Jin, Y., 2005. U-Pb Ages from the Neoproterozoic Doushantuo Formation, China. Science 308, 95-98.

Chen, M.-E., Chen, Y., Qiang, Y., 1981. Some tubular fossils from Sinian-Lower Cambrian boundary sequence, Yangtze Gorges. Tianjin Institute of Geology and Mineral Resources Bulletin 3, 117-124.

Chen, Z., Zhou, C., Meyer, M., Xiang, K., Schiffbauer, J.D., Yuan, X., Xiao, S., 2013. Trace fossil evidence for Ediacaran bilaterian animals with complex behaviors. Precambrian Research 224, 690-701.

Chen, Z., Zhou, C., Xiao, S., Wang, W., Guan, C., Hua, H., Yuan, X., 2014. New Ediacara fossils preserved in marine limestone and their ecological implications. Scientific Reports 4, 1-10

de Baar, H.J.W., Schijf, J., Byrne, R.H., 1991. Solution chemistry of the rare earth elements in seawater. European Journal of Solid State and Inorganic Chemistry 28, 357-373.

Derkowski, A., Bristow, T.F., Wampler, J.M., Środoń, J., Marynowski, L., Elliott, W.C., Chamberlain, C.P., 2013. Hydrothermal alteration of the Ediacaran Doushantuo Formation in the Yangtze Gorges area (South China). Geochimica et Cosmochimica Acta 107, 279-298.

Derry, L.A., Jacobsen, S.B., 1990. The chemical evolution of Precambrian seawater: Evidence from REEs in banded iron formations. Geochimica et Cosmochimica Acta 54, 2965-2977.

Ding, L., Zhang, L., Li, Y., Dong, J., 1992. The Study of the Late Sinian-Early Cambrian Biota from the Northern Margin of Yangtze Platform. Scientific and Technical Documents Publishing House, Beijing.

Ding, Q.X., Chen, Y.Y., 1981. Discovery of soft metazoan from the Sinian System along eastern Yangtze Gorge, Hubei. Journal of the Wuhan College of Geology 2, 53-57.

Dzik, J., 2002. Possible ctenophoran affinities of the precambrian ‘sea-pen’ *Rangea*. Journal of Morphology 252: 315-334.

Dzik, J., 2003. Anatomical Information Content in the Ediacaran Fossils and Their Possible Zoological Affinities. Integrative and Comparative Biology 43, 114-126.

Fedonkin, M.A., 1990. Systematic description of Vendian Metazoa. In: Sokolov, B.S., Ivanovskij, A.B. (Eds.), The Vendian System: Paleontology. Springer, Heidelberg, pp. 71-120.

Fedonkin, M.A., Vickers-Rich, P., 2007. The Siberian Tundra. In: Fedonkin, M.A., Gehling, J.G., Grey, K., Narbonne, G.M., Vickers-Rich, P. (Eds.), The Rise of Animals: Evolution and Diversification of the Kingdom Animalia. Johns Hopkins University Press, Baltimore, pp. 156-167.

Fedonkin, M.A., Waggoner, B.M., 1997. The Late Precambrian fossil Kimberella is a mollusc-like bilaterian organism. Nature 388, 868-871.

Gehling, J.G., 1999. Microbial mats in terminal Proterozoic siliciclastics: Ediacaran death masks. PALAIOS 14, 40-57.

Gehling, J.G., Droser, M.L., Jensen, S., Runnegar, B.N., 2005. Ediacaran organisms: relating form to function. In: Briggs, D.E.G. (Ed.), Evolving Form and Function: Fossils and Development Peabody Museum of Natural History, New Haven, pp. 43-66.

German, C.R., Elderfield, H., 1990. Application of the Ce anomaly as a paleoredox indicator: The ground rules. Paleoceanography 5, 823-833.

German, C.R., Holliday, B.P., Elderfield, H., 1991. Redox cycling of rare earth elements in the suboxic zone of the Black Sea. Geochimica et Cosmochimica Acta 55, 3553-3558.

Germs, G.J.B., 1972. New shelly fossils from the Nama Group, South West Africa. American Journal of Science 272, 752-761.

Grazhdankin, D.V., Balthasar, U., Nagovitsin, K.E., Kochnev, B.B., 2008. Carbonate-hosted Avalon-type fossils in arctic Siberia. Geology 36, 803-806.

Grotzinger, J.P., Watters, W.A., Knoll, A.H., 2000. Calcified metazoans in thrombolite-stromatolite reefs of the terminal Proterozoic Nama Group, Namibia. Paleobiology 26, 334-359.

Guo, Q., Shields, G.A., Liu, C., Strauss, H., Zhu, M., Pi, D., Goldberg, T., Yang, X., 2007. Trace element chemostratigraphy of two Ediacaran–Cambrian successions in South China: Implications for organosedimentary metal enrichment and silicification in the Early Cambrian. Palaeogeography, Palaeoclimatology, Palaeoecology 254, 194-216.

Hatch, J.R., Leventhal, J.S., 1992. Relationship between inferred redox potential of the depositional environment and geochemistry of the Upper Pennsylvanian (Missourian) Stark Shale Member of the Dennis Limestone, Wabaunsee County, Kansas, U.S.A. Chemical Geology 99, 65-82.

Hughes, W.B., Holba, A.G., Dzou, L.I.P., 1995. The ratios of dibenzothiophene to phenanthrene and pristane to phytane as indicators of depositional environment and lithology of petroleum source rocks. Geochimica et Cosmochimica Acta 59, 3581-3598.

Imbus, S.W., Macko, S.A., Douglas Elmore, R., Engel, M.H., 1992. Stable isotope (C, S, N) and molecular studies on the Precambrian Nonesuch Shale (Wisconsin-Michigan, U.S.A.): Evidence for differential preservation rates, depositional environment and hydrothermal influence. Chemical Geology: Isotope Geoscience section 101, 255-281.

Jacobsen, S.B., Kaufman, A.J., 1999. The Sr, C and O isotopic evolution of Neoproterozoic seawater. Chemical Geology 161, 37-57.

Jensen, S., Droser, M., Gehling, J., 2006. A Critical Look at the Ediacaran Trace Fossil Record. In: Xiao, S., Kaufman, A.J. (Eds.), Neoproterozoic Geobiology and Paleobiology. Springer Netherlands, pp. 115-157.

Jiang, G., Kennedy, M.J., Christie-Blick, N., Wu, H., Zhang, S., 2006. Stratigraphy, Sedimentary Structures, and Textures of the Late Neoproterozoic Doushantuo Cap Carbonate in South China. Journal of Sedimentary Research 76, 978-995.

Johnston, D.T., Poulton, S.W., Goldberg, T., Sergeev, V.N., Podkovyrov, V., Vorob'eva, N.G., Bekker, A., Knoll, A.H., 2012. Late Ediacaran redox stability and metazoan evolution. Earth and Planetary Science Letters 335-336, 25-35.

Jones, B., Manning, D.A.C., 1994. Comparison of geochemical indices used for the interpretation of palaeoredox conditions in ancient mudstones. Chemical Geology 111, 111-129.

Jørgensen, B.B., 1982. Mineralization of organic matter in the sea bed - the role of sulphate reduction. Nature 296, 643-645.

Kaufman, A.J., Knoll, A.H., 1995. Neoproterozoic variations in the C-isotopic composition of seawater: stratigraphic and biogeochemical implications. Precambrian Research 73, 27-49.

Kelly, A.E., 2009. Hydrocarbon Biomarkers for Biotic and Environmental Evolution through the Neoproterozoic-Cambrian Transition, Department of Earth, Atmospheric, and Planetary Sciences. Massachusetts Institute of Technology, Cambridge, p. 154.

Kimura, H., Watanabe, Y., 2001. Oceanic anoxia at the Precambrian-Cambrian boundary. Geology 29, 995-998.

Knoll, A., Walter, M., Narbonne, G.M., Christie-Blick, N., 2006. The Ediacaran Period: a new addition to the geologic time scale. Lethaia 39, 13-30.

Knoll, A.H., Grotzinger, J.P., Kaufman, A.J., Kolosov, P., 1995. Integrated approaches to terminal Proterozoic stratigraphy: an example from the Olenek Uplift, northeastern Siberia. Precambrian Research 73, 251-270.

Knoll, A.H., Hayes, J.M., Kaufman, A.J., Swett, K., Lambert, I.B., 1986. Secular variation in carbon isotope ratios from Upper Proterozoic successions of Svalbard and East Greenland. Nature 321, 832-838.

Knoll, A.H., Walter, M.R., Narbonne, G.M., Christie-Blick, N., 2004. A New Period for the Geologic Time Scale. Science 305, 621-622.

Li, C., Love, G.D., Lyons, T.W., Fike, D.A., Sessions, A.L., Chu, X., 2010. A Stratified Redox Model for the Ediacaran Ocean. Science 328, 80-83.

Li, Y.-H., 2000. A compendium of geochemistry. Princeton University Press, Princeton.

Ling, H.-F., Chen, X., Li, D., Wang, D., Shields-Zhou, G.A., Zhu, M., 2013. Cerium anomaly variations in Ediacaran–earliest Cambrian carbonates from the Yangtze Gorges area, South China: Implications for oxygenation of coeval shallow seawater. Precambrian Research 225, 110-127.

Love, G., Stalvies, C., Grosjean, E., Meredith, W., Snape, C.E., 2008. Analysis of molecular biomarkers covalently bound within Neoproterozoic sedimentary kerogen. In: Kelley, P.H., Bambach, R.K. (Eds.), From Evolution to Geobiology: Research Questions Driving Paleontology at the Start of a New Century. The Paleontological Society, pp. 67-83

Love, G.D., Bowden, S.A., Jahnke, L.L., Snape, C.E., Campbell, C.N., Day, J.G., Summons, R.E., 2005. A catalytic hydropyrolysis method for the rapid screening of microbial cultures for lipid biomarkers. Organic Geochemistry 36, 63-82.

Love, G.D., Grosjean, E., Stalvies, C., Fike, D.A., Grotzinger, J.P., Bradley, A.S., Kelly, A.E., Bhatia, M., Meredith, W., Snape, C.E., Bowring, S.A., Condon, D.J., Summons, R.E., 2009. Fossil steroids record the appearance of Demospongiae during the Cryogenian period. Nature 457, 718-721.

Love, G.D., Snape, C.E., Carr, A.D., Houghton, R.C., 1995. Release of covalently-bound alkane biomarkers in high yields from kerogen via catalytic hydropyrolysis. Organic Geochemistry 23, 981-986.

Mapstone, N.B., McIlroy, D., 2006. Ediacaran fossil preservation: Taphonomy and diagenesis of a discoid biota from the Amadeus Basin, central Australia. Precambrian Research 149, 126-148.

Marshall, C.P., Love, G.D., Snape, C.E., Hill, A.C., Allwood, A.C., Walter, M.R., Van Kranendonk, M.J., Bowden, S.A., Sylva, S.P., Summons, R.E., 2007. Structural characterization of kerogen in 3.4 Ga Archaean cherts from the Pilbara Craton, Western Australia. Precambrian Research 155, 1-23.

McFadden, K.A., Huang, J., Chu, X., Jiang, G., Kaufman, A.J., Zhou, C., Yuan, X., Xiao, S., 2008. Pulsed oxidation and biological evolution in the Ediacaran Doushantuo Formation. Proceedings of the National Academy of Sciences 105, 3197-3202.

McLennan, S.M., 1989. Rare earth elements in sedimentary rocks: Influence of provenance and sedimentary processes. In: Lipinand, B.R., McKay, G. (Eds.), Geochemistry and Mineralogy of Rare Earth Elements Mineralogical Society of America, pp. 169–200.

Meredith, W., Russell, C.A., Cooper, M., E. Snape, C., Love, G.D., Fabbri, D., Vane, C.H., 2004. Trapping hydropyrolysates on silica and their subsequent thermal desorption to facilitate rapid fingerprinting by GC–MS. Organic Geochemistry 35, 73-89.

Meyer, M., Xiao, S., Gill, B.C., Schiffbauer, J.D., Chen, Z., Zhou, C., Yuan, X., 2014. Interactions between Ediacaran animals and microbial mats: Insights from Lamonte trevallis, a new trace fossil from the Dengying Formation of South China. Palaeogeography, Palaeoclimatology, Palaeoecology 396, 62-74.

Narbonne, G.M., 2005. The Ediacarabiota: Neoproterozoic Origin of Animals and Their Ecosystems, Annual Review of Earth and Planetary Sciences. Annual Reviews, Palo Alto, pp. 421-442.

Nothdurft, L.D., Webb, G.E., Kamber, B.S., 2004. Rare earth element geochemistry of Late Devonian reefal carbonates, Canning Basin, Western Australia: confirmation of a seawater REE proxy in ancient limestones. Geochimica et Cosmochimica Acta 68, 263-283.

Och, L., 2011. Biogeochemical cycling through the Neoproterozoic-Cambrian transition in China: an integrated study of redox-sensitive elements, Department of Earth Sciences. University College London (UCL), London, p. 266.

Och, L.M., Shields-Zhou, G.A., 2012. The Neoproterozoic oxygenation event: Environmental perturbations and biogeochemical cycling. Earth-Science Reviews 110, 26-57.

Pflug, H.-D., 1972. Zur Fauna der Nama-Schichten in Südwest-Afrika; III, Erniettomorpha, Bau und Systematik. Palaeontographica A39, 134-168.

Pflüger, F., Gresse, P.G., 1996. Microbial sand chips - a non-actualistic sedimentary structure. Sedimentary Geology 102, 263-274.

Philp, R.P., Suzuki, N., Galvez-Sinibaldi, A., 1992. Early-stage incorporation of sulfur into protokerogens and possible kerogen precursors. In: Whelan, J., Farrington, J.W. (Eds.), Organic matter: Productivity, accumulation, and preservation in recent and ancient sediments pp. 264-282.

Radke, M., Welte, D.H., 1983. The methylphenanthrene index (MPI): a maturity parameter based on aromatic hydrocarbons. In: Bjoroy, M. (Ed.), Advances in Organic Geochemistry. Wiley, Chichester, pp. 504-512.

Reynard, B., Lécuyer, C., Grandjean, P., 1999. Crystal-chemical controls on rare-earth element concentrations in fossil biogenic apatites and implications for paleoenvironmental reconstructions. Chemical Geology 155, 233-241.

Sawaki, Y., Ohno, T., Tahata, M., Komiya, T., Hirata, T., Maruyama, S., Windley, B.F., Han, J., Shu, D., Li, Y., 2010. The Ediacaran radiogenic Sr isotope excursion in the Doushantuo Formation in the Three Gorges area, South China. Precambrian Research 176, 46-64.

Schidlowski, M., 1988. A 3,800-million-year isotopic record of life from carbon in sedimentary rocks. Nature 333, 313-318.

Schulz, H.N., Brinkhoff, T., Ferdelman, T.G., Mariné, M.H., Teske, A., Jørgensen, B.B., 1999. Dense Populations of a Giant Sulfur Bacterium in Namibian Shelf Sediments. Science 284, 493-495.

Shen, B., Xiao, S., Zhou, C., Yuan, X., 2009. *Yangtziramulus zhangi* New Genus and Species, a Carbonate-Hosted Macrofossil from the Ediacaran Dengying Formation in the Yangtze Gorges Area, South China. Journal of Paleontology 83, 575-587.

Shields, G., Stille, P., 2001. Diagenetic constraints on the use of cerium anomalies as palaeoseawater redox proxies: an isotopic and REE study of Cambrian phosphorites. Chemical Geology 175, 29-48.

Shields, G.A., Webb, G.E., 2004. Has the REE composition of seawater changed over geological time? Chemical Geology 204, 103-107.

Shields-Zhou, G., Och, L., 2011. The case for a Neoproterozoic Oxygenation Event: Geochemical evidence and biological consequences. GSA Today 21, 4-11.

Siegmund, H., Erdtmann, B.-D., 1994. Facies and diagenesis of some upper proterozoic dolomites of South China. Facies 31, 255-263.

Sinninghe Damsté, J.S., De Leeuw, J.W., 1990. Analysis, structure and geochemical significance of organically-bound sulphur in the geosphere: State of the art and future research. Organic Geochemistry 16, 1077-1101.

Sinninghe Damsté, J.S., Rijpstra, W.I.C., De Leeuw, J.W., Schenck, P.A., 1989. The occurrence and identification of series of organic sulphur compounds in oils and sediment extracts: II. Their presence in samples from hypersaline and non-hypersaline palaeoenvironments and possible application as source, palaeoenvironmental and maturity indicators. Geochimica et Cosmochimica Acta 53, 1323-1341.

Snape, C.E., Bolton, C., Dosch, R.G., Stephens, H.P., 1989. High liquid yields from bituminous coal via hydropyrolysis with dispersed catalysts. Energy & Fuels 3, 421-425.

Steiner, M., 1994. Die neoproterozoischen Megaalgen Südchinas. Berliner Geowissenschaftliche Abhandlungen E 15, 1-146.

Steiner, M., 2001. Die fazielle Entwicklung und Fossilverbreitung auf der Yangtze Plattform (Südchina) im Neoproterozoikum / frühesten Kambrium Freiberger Forschungshefte C 492, 1-26.

Steiner, M., Mehl, D., Reitner, J., Erdtmann, B.-D., 1993. Oldest entirely preserved sponges and other fossils from the Lowermost Cambrian and a new facies reconstruction of the Yangtze Platform. Berliner Geowissenschaftliche Abhandlungen E, 293-329.

Steiner, M., Reitner, J., 2001. Evidence of organic structures in Ediacara-type fossils and associated microbial mats. Geology 29, 1119-1122.

Summons, R.E., Taylor, D., Boreham, C.J., 1994. Geochemical tools for evaluating petroleum generation in Middle Proterozoic sediments of the McArthur Basin, Northern Territory, Australia. APPEA Journal 34, 692-706.

Sun, W., 1986. Late precambrian pennatulids (sea pens) from the eastern Yangtze Gorge, China: *Paracharnia* gen. nov. Precambrian Research 31, 361-375.

Sun, W., 1989. Subdivisions and correlations of the Upper Precambrian and Australia. Palaeontologica Cathayana 4, 1-22.

Tissot, B.P., Welte, D.H., 1984. Petroleum formation and occurrence, 2 ed. Springer, Berlin.

Tribovillard, N., Algeo, T.J., Lyons, T., Riboulleau, A., 2006. Trace metals as paleoredox and paleoproductivity proxies: An update. Chemical Geology 232, 12-32.

Vasconcelos, C., McKenzie, J.A., Bernasconi, S., Grujic, D., Tiens, A.J., 1995. Microbial mediation as a possible mechanism for natural dolomite formation at low temperatures. Nature 377, 220-222.

Vidal, G., 1989. Are late Proterozoic carbonaceous megafossils metaphytic algae or bacteria? Lethaia 22, 375-379.

Waggoner, B.M., 1995. Ediacaran Lichens: A Critique. Paleobiology 21, 393-397.

Walker, J.D., Geissman, J.W., Bowring, S.A., Babcock, L.E., 2013. The Geological Society of America Geologic Time Scale. Geological Society of America Bulletin 125, 259-272.

Wang, X.E., B.-D., Chen, X., Mao, X., 1998. Integrated sequence-, bio- and chemostratigraphy of the terminal Proterozoic to Lowermost Cambrian ‘black rock series’ from central South China. Episodes 21, 178-189.

Webb, G.E., Kamber, B.S., 2000. Rare earth elements in Holocene reefal microbialites: a new shallow seawater proxy. Geochimica et Cosmochimica Acta 64, 1557-1565.

Webb, G.E., Nothdurft, L.D., Kamber, B.S., Kloprogge, J.T., Zhao, J.-X., 2009. Rare earth element geochemistry of scleractinian coral skeleton during meteoric diagenesis: a sequence through neomorphism of aragonite to calcite. Sedimentology 56, 1433-1463.

Weber, B., Steiner, M., Zhu, M., 2007. Precambrian - Cambrian trace fossils from the Yangtze Platform (South China) and the early evolution of bilaterian lifestyles. Palaeogeography, Palaeoclimatology, Palaeoecology 254, 328-349.

Xi, X., 1987. Characteristics and environments of Sinian evaporite in Southern Sichuan, China. Earth Sciences 13, 23-29.

Xiao, S., Shen, B., Zhou, C., Xie, G., Yuan, X., 2005. A uniquely preserved Ediacaran fossil with direct evidence for a quilted bodyplan. Proceedings of the National Academy of Sciences of the United States of America 102, 10227-10232.

Zhao, Z., Xing, Y., Ding, Q., Liu, G., Zhao, Y., Zhang, S., Meng, X., Yin, C., Ning, B., Han, P., 1988. The Sinian System of Hubei. China University of Geosciences Press, Wuhan.

Zhu, M., Zhang, J., Steiner, M., Yang, A., Li, G., Erdtmann, B. D., 2003. Sinian-Cambrian stratigraphic framework for shallow- to deep-water environments of the Yangtze Platform: an integrated approach. Progress in Natural Science 13, 951-960.

Zhu, M., Zhang, J., Yang, A., 2007. Integrated Ediacaran (Sinian) chronostratigraphy of South China. Palaeogeography, Palaeoclimatology, Palaeoecology 254, 7-61.

- Chapter 4 -

Assessing possibilities and limitations for biomarker analyses on outcrop samples: A case study on carbonates of the Shibantan Member (Ediacaran Period, Dengying Formation, South China)

(*Acta Geologica Sinica, English edition; accepted*)

Jan-Peter Duda, Volker Thiel, Joachim Reitner, Martin Blumenberg:

Abstract

The Shibantan Member (Dengying Formation, South China) represents one of only two carbonate settings with Ediacara organisms and offers the rare opportunity to study the biogeochemistry of these ecosystems. To evaluate possibilities and limitations for future biomarker studies on fossil-bearing outcrop samples of the Shibantan Member, we analysed the spatial distribution of hydrocarbons in extractable organic matter (i.e. bitumen) on a millimetre scale. Our study demonstrates that the sample and most likely also other rocks from the same setting are contaminated with petroleum-derived compounds that bear the potential for erroneous interpretations in palaeo-reconstructions. The contamination was revealed by distribution patterns and amounts of extractable *n*-alkanes and acyclic isoprenoids. The contamination is linked to the external weathering surfaces but also to cracks within the rock, and the extent most likely depends on concentration gradients between these contamination sources. Here we show that contamination can successfully be distinguished from syngenetic signals obtained from non-extractable organic matter (i.e. kerogen) using catalytic hydropyrolysis (HyPy). However, we observed that decalcification is necessary to achieve sufficient yields of kerogen-bound hydrocarbons and to avoid artificial alteration of the biomarker signals due to matrix effects.

Keywords

Ediacaran, biomarkers, contamination, syngeneity, slice-experiments, catalytic hydropyrolysis (HyPy)

4.1 Introduction

Contamination and thus introduction of non-syngenetic information into a rock is a serious problem for biomarker studies based on extractable hydrocarbons. In addition to the natural migration of petroleum-derived fluids into the geological formation of interest, there are numerous further possibilities for organic contamination of rock samples during exposure in the outcrop, sampling (e.g. drilling), storage, preparation, or analyses. Sources of contaminants range from immature organic compounds (e.g. organic material derived from ubiquitous higher land-plants or epi-/endolithic microorganisms) to mature organic material (e.g. petroleum-derived fluids). Regardless of the source, such naturally or artificially introduced compounds potentially obscure syngenetic hydrocarbons within a sample and are thus problematic with respect to palaeoenvironmental interpretations (e.g. Eigenbrode, 2004; Sherman et al., 2007; Brocks et al., 2008; Brocks, 2011). The contamination problem is generally addressed by strictly adhering to well established laboratory protocols for cutting, cleaning, crushing and extraction (Sherman et al., 2007). Cutting off the outer layer of a rock sample and subsequent separate analyses of the internal and external parts (i.e. interior vs. exterior experiments; cf. Brocks et al., 2008) is commonly used to identify and to eliminate possible surficial contaminants (Sherman et al., 2007; Brocks et al., 2008). However, contamination is not necessarily restricted to the external weathering surfaces of rock samples but can also be linked to internal surfaces (e.g. cracks). Both contamination paths can be evaluated by measuring concentration gradients of hydrocarbons on a millimetre-scale (i.e. slice-extraction experiments; Brocks et al., 2008; Brocks, 2011). Micro-ablation-technique was suggested as potential tool to remove contaminated surfaces and to conduct interior vs. exterior experiments on a sub-millimetre scale, enabling to analyse small sample fragments remaining after exposure of internal crack-surfaces (Jarrett et al., 2013). Other useful strategies include an evaluation of the bitumen maturity with regard to the thermal history of the host rock, as well as comparisons of stable carbon isotope ratios and molecular characteristics of extractable (i.e. bitumen) versus macromolecular organic matter (i.e. kerogen) (cf. Brocks et al., 2003a, b; Eigenbrode, 2004; Sherman et al., 2007; Rasmussen et al., 2008). The immobile kerogen fraction is commonly considered to be less prone to contamination and molecular structures that are covalently bound to the kerogen matrix are likely syngenetic (cf. Brocks et al., 2003b). Sequential chemical degradation (e.g. Michaelis and Albrecht, 1979; Boucher et al., 1991; Richnow et al., 1992) as well as analytical pyrolysis (e.g. Py-GC/MS; e.g. Larter and Horsfield, 1993) allow isolation and characterisation of subunits of the kerogen (Whelan and Thompson-Rize, 1993), but in both cases the pyrolysate yields are relatively low (Love et al., 1995). In contrast, catalytic hydropyrolysis (HyPy) was shown to release high yields of covalently-bound hydrocarbons from the kerogen and to maintain their biologically-inherited stereochemistries largely intact by using high pressure and temperature in an H_2 atmosphere (Love et al., 1995). Consequently, HyPy was successfully applied for numerous palaeo-reconstruction studies (e.g. Brocks et al., 2003b; Love et al., 2008; Love et al., 2009; Blumenberg and Wiese, 2012; Duda et al., in revision / chapter 3 in this thesis).

Precambrian rocks are particularly prone to contamination because of their commonly (i) long geological history, (ii) high thermal maturities and thus, (iii) low abundances of syngenetic biomarkers. This is probably also true for the Shibantan Member (Dengying Formation, ca. 551-541 Ma; Condon et al., 2005; Walker et al., 2013) in South China, one of only two known pure carbonate settings in the world with Ediacara-type fossils (e.g. Sun, 1986; Xiao et al., 2005; Shen et al., 2009; Chen et al., 2014). These fossils of architecturally complex soft-bodied organisms include the first stem-group metazoans (e.g. *Dickinsonia* and *Kimberella*) and are thus an important milestone in the evolution of animals (e.g. Narbonne, 2005; Xiao and Laflamme, 2009; Narbonne et al., 2012; and references therein). Preliminary biomarker analyses on the bitumen fractions extracted from the Shibantan Member indicated that the organic matter is highly mature and contamination might be an essential problem (Kelly, 2009; Duda et al., in revision / chapter 3 in this thesis). In a previous study we were though able to analyse evidently syngenetic biomarkers released from the kerogen by HyPy and to demonstrate the syngeneity of aromatic hydrocarbons in the bitumen (Duda et al., in revision / chapter 3 in this thesis). Abundant thiophenes in the Shibantan carbonate have been attributed to a highly sulphidic palaeoenvironment during earliest diagenesis (Duda et al., in revision / chapter 3 in this thesis). The preservation of syngenetic biomarkers is important since biomarkers are only known from one further setting with Ediacara-type organisms (i.e. the White Sea setting in Russia; Kelly, 2009). Further biomarker-studies on the Shibantan Member could therefore be promising, but the general contamination pathways and sources of the allochthonous bitumen compounds are still unclear. This study aims at critically assessing the possibilities and limitations of biomarker studies on thermally mature outcrop samples from the Shibantan Member, with implications for the analysis of similar rocks in other ancient settings. Pathways for hydrocarbon contamination were elucidated via slice-extraction experiments (*sensu* Brocks et al., 2008; Brocks, 2011) and the potential of the direct use of extraction residues for HyPy was critically assessed.

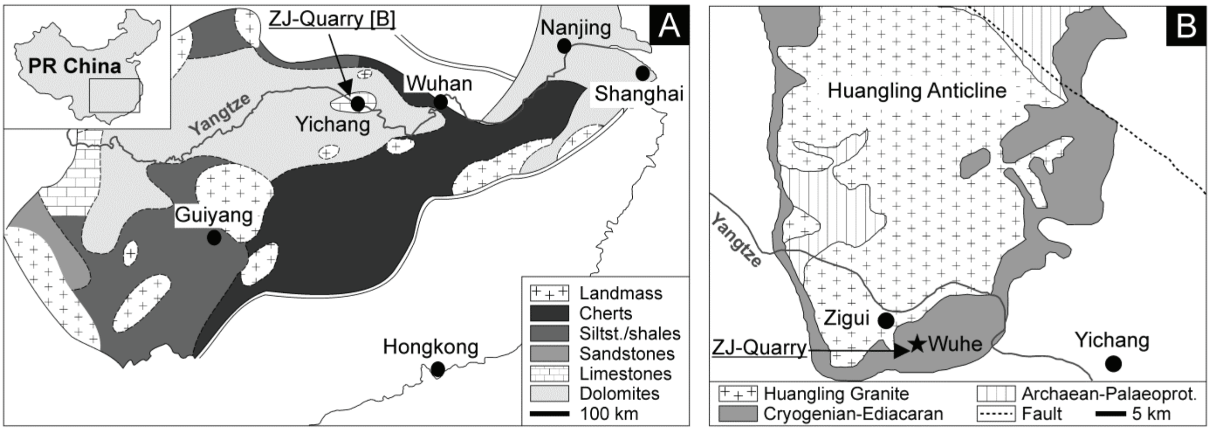

Fig. 4.1 General overview (A) and exact location (B) of the Zhoujia'ao (ZS-) Quarry in South China. A: modified after Zhu et al. (2007); B: modified after Chen et al. (2013).

4.2 Material and methods

Analyses were conducted on one fresh and representative outcrop sample from the Shibantan Member collected in 2011 in the still exploited Zhoujia'ao Quarry in the Yangtze Gorges close to Yichang (Fig. 4.1, 4.2). In the quarry the Shibantan limestone is mined and directly calcined for lime production. The analysed sample was characterised by an Ediacara-type organism exposed on the outer surface (Fig. 4.2). The bitumen and decalcified extraction residue of the innermost part of the sample (i.e. slice 6; Fig. 4.3) have previously been analysed and respective data are already published (Duda et al., in revision / chapter 3 in this thesis).

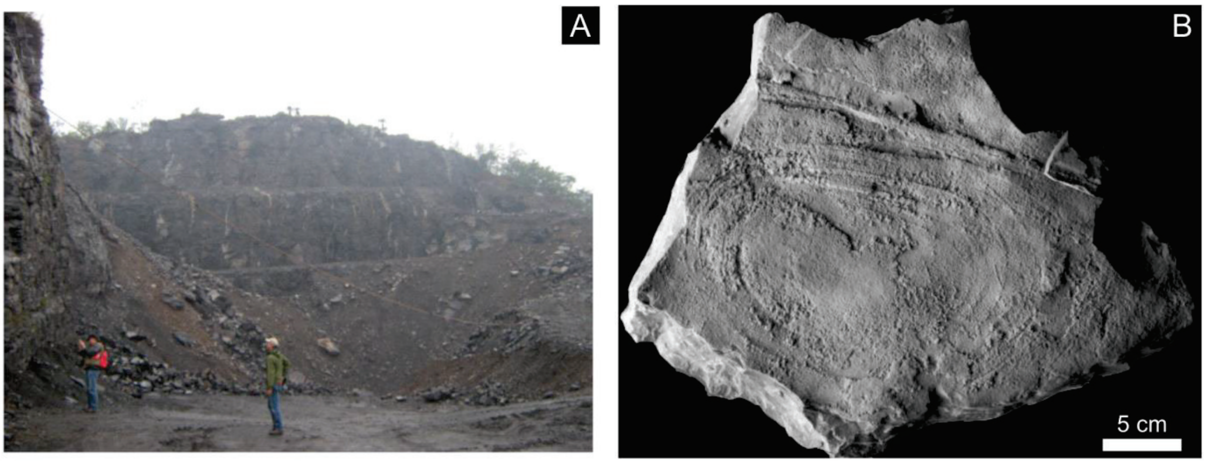

Fig. 4.2 Sampling location with the outcropping Shibantan carbonates in the Zhoujia'ao Quarry (A) and top view of the analysed sample block with Ediacara-type fossil (B).

For biomarker analyses, all glassware and silica gel were heated to 500°C for 3h. The sample block was roughly formatted and all but one external surfaces were removed using a pre-cleaned (with acetone) rock saw. For analyses of the bitumen, adjoining slices of 6.5 mm (slice 1; i.e. the external weathered surface) and 3 mm (slices 2 to 5) thickness were cut from the sample block perpendicular to the bedding planes (cf. Brocks et al., 2008; Brocks, 2011) using a pre-cleaned high precision saw (Buehler; Isomet 1000) (Fig. 4.3). Slice 6 stems from the innermost part of the big sample block and was thus not immediately adjacent to slice 5 (Fig. 4.3). After cutting, all slices were carefully crushed and powdered using a pebble mill (Retsch MM 301). The sample powder (slice 1: 25.0 g; slices 2 to 5: 11.5 g) was extracted with 40 ml (slice 1) and 20 ml (slices 2 to 5) each of methanol, dichloromethane/*n*-hexane (1/1; v/v) and then *n*-hexane using ultrasonication (15 min). The sample powder of slice 6 (99 g) was extracted with 100 ml each of dichloromethane, dichloromethane /*n*-hexane (1/1; v/v) and *n*-hexane using ultrasonication (15 min.) (Duda et al., in revision / chapter 3 in this thesis). Extracts were combined, desulphurised with activated copper and gently dried in a pre-

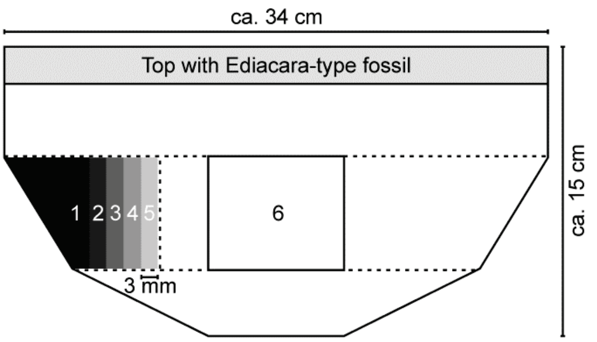

Fig. 4.3 Sketch of the analysed sample block from the Shibantan Member (side view of Fig. 4.1b). HyPy analysis was only conducted on slice 6.

cleaned rotary evaporator followed by N_2. The samples were not completely dried in order to avoid evaporative loss of short-chain *n*-alkanes (cf. Ahmed and George, 2004).

For HyPy, an aliquot of the extraction residue of slice 6 (core of the sample block; Fig. 4.3) was again Soxhlet extracted using dichloromethane/methanol (9/1, v/v; 24 h), and subjected to HyPy without further treatment. The overall load of the HyPy reactor was about 3.05 g (2.30 g bulk sample + 0.30 MoS_2 catalyst + 0.45 g sand). A second aliquot of the extraction residue was analysed with HyPy after decalcification with HCl (~3 mol/l), and subsequent extraction of the residue with dichloromethane, dichloromethane/*n*-hexane and *n*-hexane (Duda et al., in revision / chapter 3 in this thesis). Because the sample consisted of virtually pure limestone it was not additionally treated with hydrofluoric acid. The overall load of the HyPy reactor was about 1.05 g (0.49 g decalcified sample + 0.06 g MoS_2 catalyst + 0.50 g sand).

Samples were pyrolysed using a Strata HyPy system (Strata Ltd., Nottingham, UK) according to Snape et al. (1989) and Love et al. (1995). The temperature program included heating from ambient temperature to 250°C at 50°C min^{-1} and from 250°C to 500°C at 8°C min^{-1}. A hydrogen pressure of 150 bar was applied at a flow of 5 L min^{-1}. The hydrocarbons released were trapped downstream in a dry ice cooled silica gel trap (see Meredith et al., 2004). The hydropyrolysates were eluted from the silica gel with *n*-hexane, and elemental sulphur was removed with activated copper.

Bitumen extracts and HyPy products were subsequently fractionated into a saturated (F1), an aromatic (F2) and a polar fraction (cf. Blumenberg et al., 2012). F1 and F2 were analysed by combined gas chromatography–mass spectrometry (GC–MS) using a Varian CP-3800 GC coupled to a Varian 1200L triple quadrupole MS. The GC was equipped with a deactivated retention gap (internal diameter (i.d.) 0.53 mm) connected to a fused silica capillary column (Phenomenex Zebron ZB-5MS, 30 m, 0.32 mm i.d., 0.25 µm film thickness). He was used as carrier gas. The GC oven was programmed from 80°C (held for 3 min) to 310°C (4°C min^{-1}; held for 25 min.). Fractions were injected on column using a PTV injector. The injector was initially held at 80°C for 0.2 min and then heated by 150°C min^{-1} to 320°C (held for 15 min). The ion source in the MS was operated at 200°C in electron ionisation mode at 70 eV ionisation energy, and analyses were conducted in full scan and selected ion monitoring (SIM) modes. Hydrocarbons were identified by comparing mass spectra and retention times with published data and/or reference compounds. For SIM analyses of the polycyclic aromatic hydrocarbons (PAHs) selected mass fragments were used (m/z 178 for phenanthrene; m/z 192 for methylphenanthrenes; m/z 184 for dibenzothiophenes; m/z 198 for methyldibenzothiophenes; m/z 252 for perylene).

4.3 Results

4.3.1 Extractable hydrocarbons (bitumen)

Considerable differences in the distributions and abundances of extractable hydrocarbons were observed between the analysed samples. The *n*-alkanes in slice 1 ranged in carbon chain length from C_{16} to C_{36} and showed a bimodal distribution with maxima at *n*-C_{18} and, less pronounced, at *n*-C_{29} (Fig. 4.4). The high abundance of short-chain *n*-alkanes (i.e. < *n*-C_{23}) was not found in slices 2 to 5, where homologues ranged from *n*-C_{18} to *n*-C_{35} and displayed a smooth distribution with a maximum around *n*-C_{29} (Fig. 4.4). The slice 6 was fairly similar to slices 2 to 5, with *n*-alkanes ranging from *n*-C_{16} to *n*-C_{39} (maxima at *n*-C_{27} and, less pronounced, at *n*-C_{36}) and low amounts of short-chain *n*-alkanes (i.e. < *n*-C_{23}) (Duda et al., in revision / chapter 3 in this thesis) (Fig. 4.4, 4.5). Considerable differences in the abundances of hydrocarbons were observed between the samples, with aliphatic compounds in slices 1 and 5 being higher concentrated than in the other slices (corrected for sample weight; Fig. 4.4a).

Acyclic isoprenoids (i.e. pristane and phytane) were only detected in slice 1, where pristane/*n*-C_{17} and phytane/*n*-C_{18} ratios were 0.57 and 0.95, respectively.

Fig. 4.4 *n*-Alkane yields (corrected for sample weight) and distribution patterns in bitumen of the analysed slices 1-6. Comparison of *n*-alkane distribution patterns in a bar chart (A) and a line chart (most significant peak of each slice normalised to 1; only the C_{22}-C_{36} range shown) (B). Data of bitumen from slice 6 from Duda et al. (in revision) / chapter 3 in this thesis.

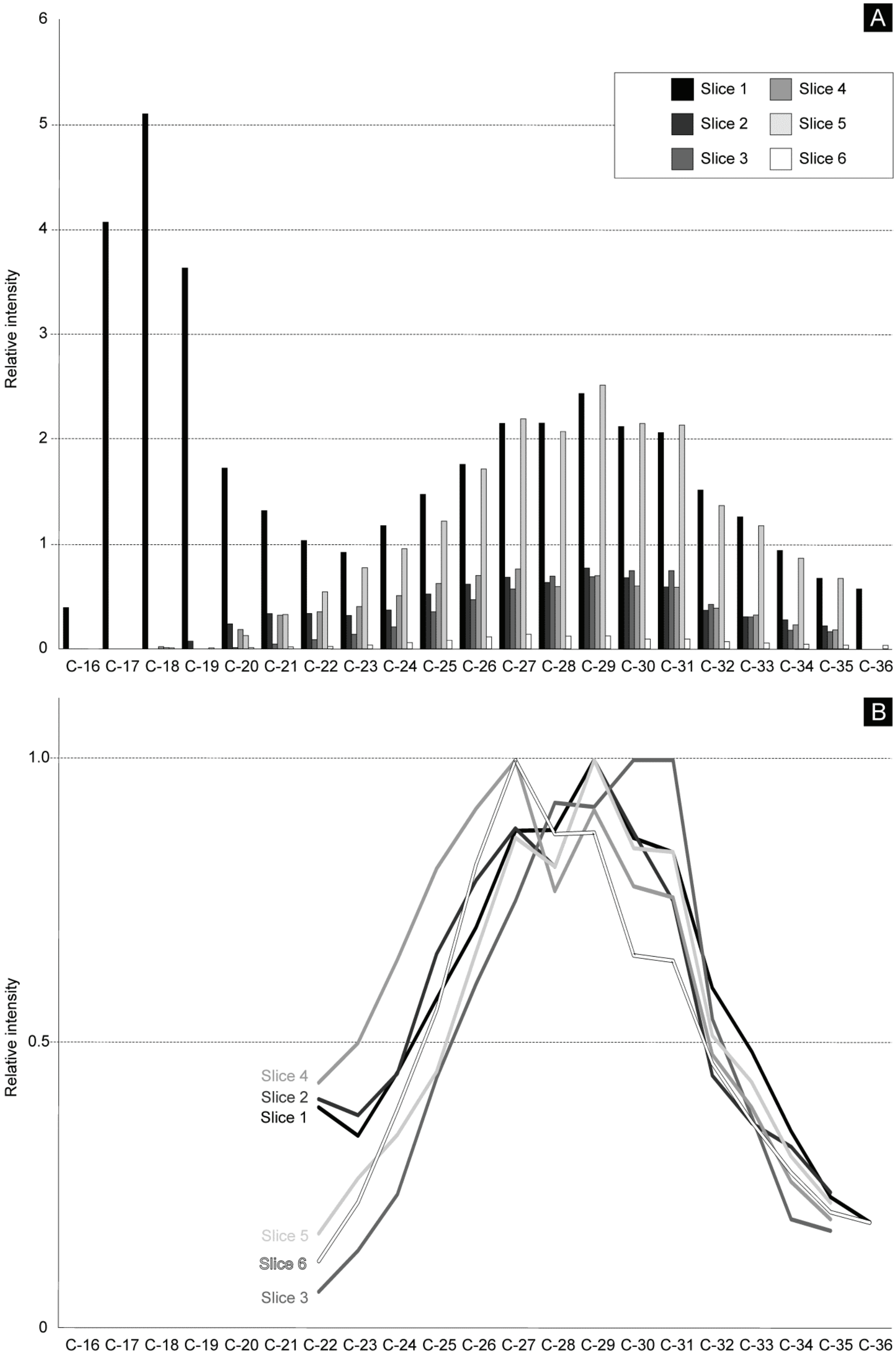
A
Slice 1
Slice 2
Slice 3
Slice 4
Slice 5
Slice 6
Relative intensity
0
1
2
3
4
5
6
C-16 C-17 C-18 C-19 C-20 C-21 C-22 C-23 C-24 C-25 C-26 C-27 C-28 C-29 C-30 C-31 C-32 C-33 C-34 C-35 C-36
B
Relative intensity
0
0.5
1.0
Slice 4
Slice 2
Slice 1
Slice 5
Slice 6
Slice 3
C-16 C-17 C-18 C-19 C-20 C-21 C-22 C-23 C-24 C-25 C-26 C-27 C-28 C-29 C-30 C-31 C-32 C-33 C-34 C-35 C-36

4.3.2 Non-extractable hydrocarbons (HyPy-treated extraction residue)

HyPy on the bulk extraction residue resulted in *n*-alkanes with carbon chain lengths from *n*-C_{18} to *n*-C_{39} and a bimodal distribution with maxima at *n*-C_{22} and, less pronounced, at *n*-C_{30} (Fig. 4.5). *n*-Alkanes cleaved from the decalcified extraction residue had carbon chain lengths from *n*-C_{16} to *n*-C_{40} and a bimodal distribution (maxima at *n*-C_{18} and, more pronounced, at *n*-C_{22}) as reported previously (Duda et al., in revision / chapter 3 in this thesis) (Fig. 4.5). Amounts of the released *n*-alkanes were about twenty times higher after decalcification (corrected for sample weight and TOC content; Fig. 4.5).

The HyPy products of the bulk extraction residue were found to be rich in PAHs such as (methyl-) phenanthrenes and, less pronounced, sulphur bearing PAHs such as various (dibenzo-) thiophenes. The same was observed for the decalcified extraction residue (Duda et al., in revision / chapter 3 in this thesis) (Fig. 4.6). If compared to the decalcified extraction residue, however, the ratio between PAHs and thiophenes was higher in the bulk extraction residue (Fig. 4.6).

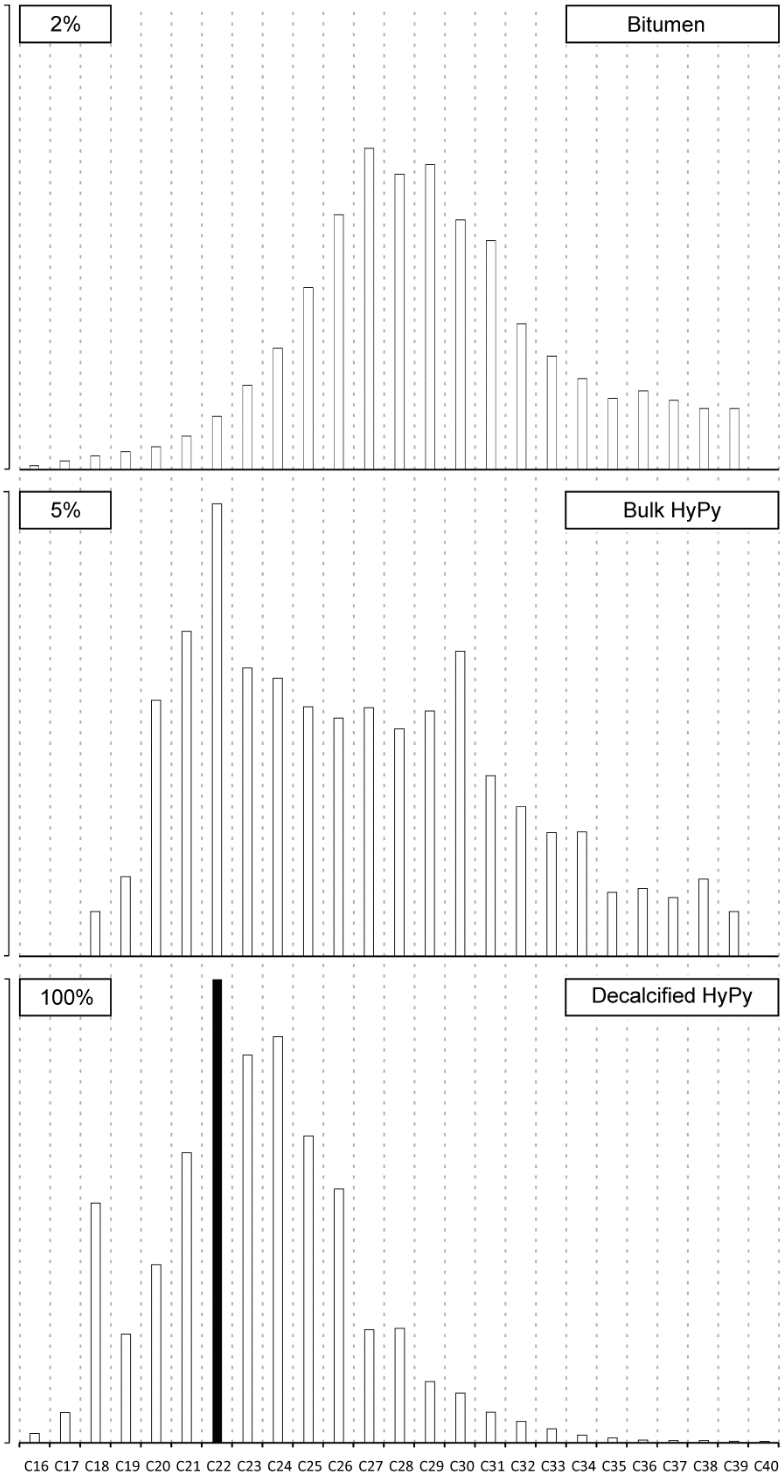

Fig. 4.5 Comparison of yields of *n*-alkanes in bitumen and extraction residue (bulk and decalcified) of slice 6 (corrected for sample weight and TOC content) relative to main compound (i.e. the C_{22} *n*-alkane in kerogen; indicated by black bar). Data of decalcified extraction residue and bitumen from Duda et al. (in revision) / chapter 3 in this thesis.

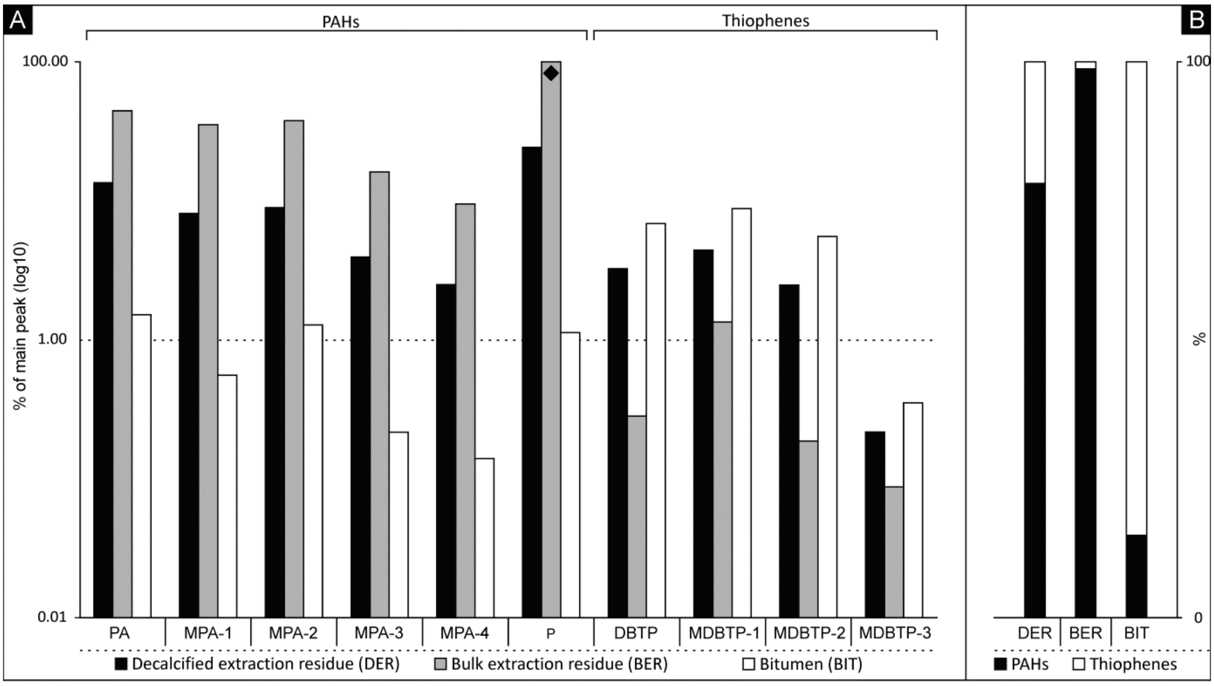

Fig. 4.6 Relative yields of aromatic compounds from slice 6 (corrected for sample weight and TOC content). A: Various PAHs and thiophenes in bitumen and extraction residue (bulk and decalcified) relative to P in bulk extraction residue (indicated by black diamond). B: Relative ratios of ∑PAHs (PA, MPA) and ∑thiophenes (DBTP, MDBTP). PA: Phenanthrene; MPA: Methylphenanthrenes; P: Perylene; DBTP: Dibenzothiophene; MDBTP: Methyldibenzothiophenes. Data of decalcified extraction residue and bitumen from Duda et al. (in revision) / chapter 3 in this thesis.

4.4 Discussion

4.4.1 Contamination sources and impact on the organic inventory

The different distribution patterns and higher amounts of extractable *n*-alkanes, as well as the presence of acyclic isoprenoids clearly reveal contamination of the external weathered surface (slice 1), as it has been described for another outcrop sample from the Shibantan Member (Kelly, 2009). Similarly, *n*-alkanes in the innermost part of the block (i.e. slice 6) have been attributed to contamination with fossil (i.e. already matured) compounds because of a different chain-length distribution and dissimilar δ^{13}C-signatures compared to the kerogen-bound compounds (Duda et al., in revision / chapter 3 in this thesis). While no voids or cracks were macroscopically visible in the innermost part of the sample (i.e. slice 6; Fig. 4.3), a few very thin cracks were detected by thin section analysis (Fig. 4.7). However, other cracks were only visible because slight wet rims persisted after defrosting, indicating that they have not been cemented. Contamination via such tiny cracks plausibly explains the similar absolute concentrations of aliphatic hydrocarbons in slices 1 (i.e. the external weathered surface) and 5 (representing an internal crack), as well as in slices 2 to 4 which were positioned between these two contaminated rock volumes. The innermost part of the block (slice 6, Fig. 4.3), however, shows the same *n*-alkane distribution as slices 2 to 4 but even lower concentrations of these compounds (Fig. 4.4). This underlines that the grade of contamination of outcrop samples from the Shibantan Member is not

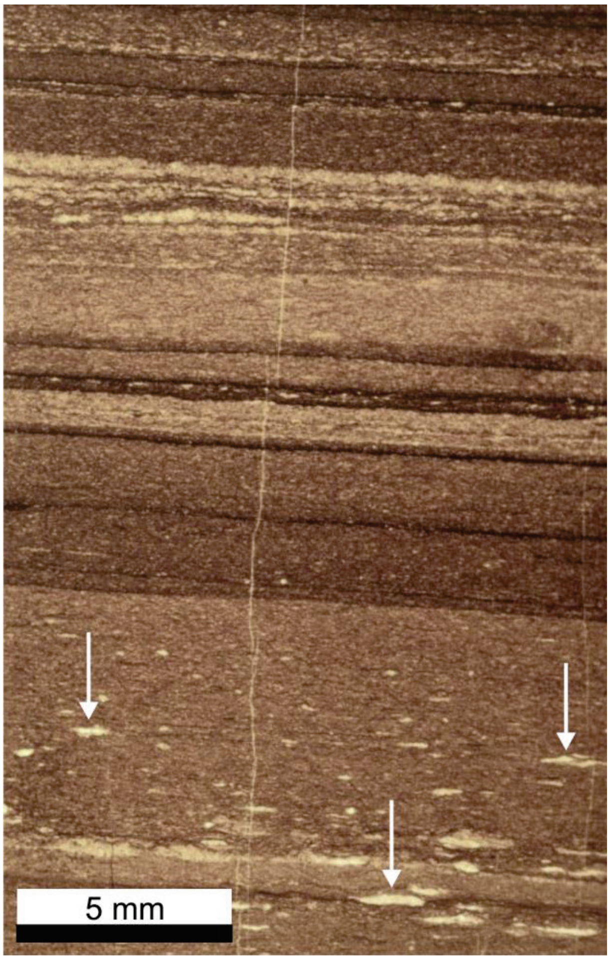

Fig. 4.7 Thin section of the innermost part of the sample (i.e. slice 6; Fig. 4.3). Note that no voids are visible (compounds marked by arrows are grains) and that observable cracks are negligible.

only controlled by the weathering surface but also by cracks. Therefore, slice experiments (Brocks, 2011; Brocks et al., 2008) as well as careful thin section analysis are important to understand the sources and distribution patterns of biomarkers and to assess the likeliness of contamination.

The occurrences of short-chain *n*-alkanes and acyclic isoprenoids (pristane and phytane) on the external weathered surface (i.e. slice 1; Fig. 4.3) are in good agreement with an external, petroleum-derived contamination, but these compounds are absent in the slice 5 in the vicinity of the inner crack (Fig. 4.4). An analytical bias due to excessive evaporation of short-chain *n*-alkanes during sample preparation (drying with N_2) (Ahmed and George, 2004) can be excluded since all slices were treated in parallel under the same conditions and should therefore be influenced equally by the work-up procedure. A possible explanation is therefore that the external weathered surface was affected by a second contamination source. Taken together, however, the distribution patterns of *n*-alkanes and acyclic isoprenoids clearly show that aliphatic hydrocarbons in the Shibantan bitumen are indeed not syngenetic.

4.4.2 Applicability of bulk extraction residues for HyPy

HyPy has already been successfully used on the decalcified extraction residue from the Shibantan carbonate (Duda et al., in revision / chapter 3 in this thesis). Decalcification prior to HyPy, however, is time consuming and involves further risks for contamination. Therefore the use of excessively pre-extracted bulk rock powder, i.e. without decalcification, was tested. The resulting *n*-alkane concentrations and distributions, however, greatly differed from those released from the decalcified sample, whose hydrocarbon yields were about 20 times higher after correction for the sample weight and TOC content, and short chain *n*-alkanes were much more prominent than long-chain *n*-alkanes (Fig. 4.5). As the long-chain *n*-alkanes in the Shibantan bitumen were suspected to represent a contamination (see 4.4.1), we argue that the respective *n*-alkanes found in the pyrolysate may represent non-entirely extracted bitumen contaminants that had been sequestered in the carbonate lattice, and thus escaped extraction (Fig. 4.5). Consequently, decalcification of carbonates is required for a complete extraction of the bitumen and the removal of contaminations contained therein.

A further potential problem that has to be addressed when omitting decalcification are matrix effects. The overall load in the HyPy reactor was three-fold higher for the bulk extraction residue as compared to the decalcified extraction residue (~3g and ~1g, respectively). After correction for the respective sample weight and TOC content much lower yields of syngenetic short chain *n*-alkanes are evident for the bulk extraction residue (Fig. 4.5). A possible explanation is that the different sample loads had an impact on the bond cleaving- and product removal processes within the HyPy reactor. Evidence for such matrix effects can also be deduced from the relative distributions of PAHs and thiophenes in the HyPy products of the decalcified and bulk sample. The observed conspicuous drop in thiophene concentrations relative to PAHs in the HyPy products of the bulk extraction residue (Fig. 4.6) may be explained by an ineffective removal from the hot zone and thus a longer dwell time of released compounds in the reactor because of the high sample load. Though thiophenes are usually regarded as relatively stable (e.g. Koopmans et al., 1995, and references therein), the sample containing the carbonate matrix obviously experienced a partial thermal decomposition during the HyPy-process, i.e. cleaving of C-S bonds of thiophenes and production of PAHs from dibenzothiophenes. The vulnerability of (dibenzo-) thiophenes to decomposition during HyPy has been previously reported, and consequently ratios of methyl homologues of dibenzothiophene should not be used for kerogen-bound biomarkers (Lockhart et al., 2007). Given that a moderate sample load is the precondition for a rapid removal of the released moieties from the hot zone of the reactor, the decalcification of carbonates prior to HyPy is necessary to concentrate the organic matter and to avoid artificial alteration of the signal, particularly for biomarker-lean carbonate rocks with a high maturity.

4.5 Conclusions

Bitumens in outcrop samples of the Shibantan Member are affected by contamination with mature organic material, most likely introduced through anthropogenic activity. In addition to severe contamination of the external weathered surface, it has been demonstrated that contamination is also linked to cracks. The degree of contamination in different parts of the sample depends most likely on concentration gradients between these contamination pathways. The distribution patterns and concentrations of short-chain *n*-alkanes and acyclic isoprenoids demonstrate that the external contaminations are largely petroleum-derived, thus precluding reliable palaeo-reconstructions based on biomarker analyses of the Shibantan bitumen. Our study supports the utility of slice experiments for assessing the existence and extent of contamination and underlines the usefulness of thin section studies conducted in parallel with biomarker analyses.

Biomarkers released from the extraction residue through HyPy are most likely syngenetic. However, decalcification of the samples as well as extraction prior and after decalcification are necessary to obtain these compounds in high yields from the kerogen. Decalcification also avoids artificial alteration of the released compounds due to high sample load in the HyPy reactor, which may otherwise severely influence the distributions of released biomarkers, such as the relative amounts of thiophenes versus PAHs.

Acknowledgements

We are indebted to M. Zhu (Nanjing Institute of Geology and Palaeontology, Chinese Academy of Sciences) for supporting the field work. L. Laake, A. Hackmann, C. Conradt, and M. Reinhardt (all Geoscience Centre, University of Göttingen) are thanked for technical and analytical support. W. Meredith and S. Xiao are acknowledged for comments that greatly improved the manuscript. This work was financially supported by the Deutsche Forschungsgemeinschaft (grant BL971/1-3), the 553 National Basic Research Program of China (2013CB835006), the National Natural Science 554 Foundation of China, the Courant Research Centre of the University Göttingen, and the German Academic Exchange Service.

References

Ahmed, M., George, S.C., 2004. Changes in the molecular composition of crude oils during their preparation for GC and GC–MS analyses. Organic Geochemistry 35, 137-155.

Blumenberg, M., Wiese, F., 2012. Imbalanced nutrients as triggers for black shale formation in a shallow shelf setting during the OAE 2 (Wunstorf, Germany). Biogeosciences 9, 4139-4153.

Blumenberg, M., Thiel, V., Riegel, W., Kah, L.C., Reitner, J., 2012. Biomarkers of black shales formed by microbial mats, Late Mesoproterozoic (1.1 Ga) Taoudeni Basin, Mauritania. Precambrian Research 196-197, 113-127.

Boucher, R.J., Standen, G., Eglinton, G., 1991. Molecular characterization of kerogens by mild selective chemical degradation - ruthenium tetroxide oxidation. Fuel 70, 695-702.

Brocks, J.J., Love, G.D., Snape, C.E., Logan, G.A., Summons, R.E., Buick, R., 2003b. Release of bound aromatic hydrocarbons from late Archean and Mesoproterozoic kerogens via hydropyrolysis. Geochimica et Cosmochimica Acta 67, 1521-1530.

Brocks, J.J., 2011. Millimeter-scale concentration gradients of hydrocarbons in Archean shales: Live-oil escape or fingerprint of contamination? Geochimica et Cosmochimica Acta 75, 3196-3213.

Brocks, J.J., Buick, R., Logan, G.A., Summons, R.E., 2003a. Composition and syngeneity of molecular fossils from the 2.78 to 2.45 billion-year-old Mount Bruce Supergroup, Pilbara Craton, Western Australia. Geochimica et Cosmochimica Acta 67, 4289-4319.

Brocks, J.J., Grosjean, E., Logan, G.A., 2008. Assessing biomarker syngeneity using branched alkanes with quaternary carbon (BAQCs) and other plastic contaminants. Geochimica et Cosmochimica Acta 72, 871-888.

Chen, Z., Zhou, C., Meyer, M., Xiang, K., Schiffbauer, J.D., Yuan, X., Xiao, S., 2013. Trace fossil evidence for Ediacaran bilaterian animals with complex behaviors. Precambrian Research 224, 690-701.

Chen, Z., Zhou, C., Xiao, S., Wang, W., Guan, C., Hua, H., Yuan, X., 2014. New Ediacara fossils preserved in marine limestone and their ecological implications. Scientific Reports 4, 4180.

Condon, D., Zhu, M., Bowring, S., Wang, W., Yang, A., Jin, Y., 2005. U-Pb Ages from the Neoproterozoic Doushantuo Formation, China. Science 308, 95-98.

Duda, J.-P., Blumenberg, M., Thiel, V., Simon, K., Zhu, M., Reitner, J., in revision. Geobiology of an Ediacara palaeoecosystem: The Shibantan Member (Dengying Formation, South China). Precambrian Research

Eigenbrode, J., 2004. Late Archean Microbial Ecology: An Integration of Molecular, Isotopic and Lithologic Studies. PhD-thesis Thesis, Pennsylvania State University

Jarrett, A.J.M., Schinteie, R., Hope, J.M., Brocks, J.J., 2013. Micro-ablation, a new technique to remove drilling fluids and other contaminants from fragmented and fissile rock material. Organic Geochemistry 61, 57-65.

Kelly, A.E., 2009. Hydrocarbon Biomarkers for Biotic and Environmental Evolution through the Neoproterozoic-Cambrian Transition. PhD-thesis Thesis, Massachusetts Institute of Technology, Cambridge

Koopmans, M.P., Sinninghe Damsté, J.S., Lewan, M.D., De Leeuw, J.W., 1995. Thermal stability of thiophene biomarkers as studied by hydrous pyrolysis. Organic Geochemistry 23, 583-596.

Larter, S.R., Horsfield, B., 1993. Determination of structural components of kerogens using analytical pyrolysis methods. In: Engel, M., Macko, S. (Eds.), Organic Geochemistry. Plenum Press, New York, pp. 271-287.

Lockhart, R.S., Meredith, W., Snape, C.E., 2007. Kerogen-Bound Biomarker Parameters at Elevated Maturities. In: Fairmond et al. (Eds.), The 23rd International Meeting on Organic Geochemistry. Integrated Geochemical Interpretation Ltd., Torquay, Devon, United Kingdom, pp. 897-898.

Love, G., Stalvies, C., Grosjean, E., Meredith, W., Snape, C.E., 2008. Analysis of molecular biomarkers covalently bound within Neoproterozoic sedimentary kerogen. In: Kelley, P.H., Bambach, R.K. (Eds.), From Evolution to Geobiology: Research Questions Driving Paleontology at the Start of a New Century. Paleontological Society Papers. The Paleontological Society Short Course, 67-83

Love, G.D., Grosjean, E., Stalvies, C., Fike, D.A., Grotzinger, J.P., Bradley, A.S., Kelly, A.E., Bhatia, M., Meredith, W., Snape, C.E., Bowring, S.A., Condon, D.J., Summons, R.E., 2009. Fossil steroids record the appearance of Demospongiae during the Cryogenian period. Nature 457, 718-721.

Love, G.D., Snape, C.E., Carr, A.D., Houghton, R.C., 1995. Release of covalently-bound alkane biomarkers in high yields from kerogen via catalytic hydropyrolysis. Organic Geochemistry 23, 981-986.

Meredith, W., Russell, C.A., Cooper, M., E. Snape, C., Love, G.D., Fabbri, D., Vane, C.H., 2004. Trapping hydropyrolysates on silica and their subsequent thermal desorption to facilitate rapid fingerprinting by GC–MS. Organic Geochemistry 35, 73-89.

Michaelis, W., Albrecht, P., 1979. Molecular fossils of archaebacteria in kerogen. Naturwissenschaften 66, 420-422.

Narbonne, G.M., 2005. The Ediacara Biota: Neoproterozoic Origin of Animals and Their Ecosystems. Annual Review of Earth and Planetary Sciences, 421-442.

Narbonne, G.M., Xiao, S., Shields, G.A., Gehling, J.G., 2012. Chapter 18 - The Ediacaran Period. In: Gradstein, F., Ogg, J., Schmitz M., Ogg, G. (Eds.), The Geological Time Scale 2012, Elsevier, Amsterdam, pp. 413-435

Rasmussen, B., Fletcher, I.R., Brocks, J.J., Kilburn, M.R., 2008. Reassessing the first appearance of eukaryotes and cyanobacteria. Nature 455, 1101-1104.

Richnow, H.H., Jenisch, A., Michaelis, W., 1992. Structural investigations of sulphur-rich macromolecular oil fractions and a kerogen by sequential chemical degradation. Organic Geochemistry 19, 351-370.

Shen, B., Xiao, S., Zhou, C., Yuan, X., 2009. *Yangtziramulus zhangi* New Genus and Species, a Carbonate-Hosted Macrofossil from the Ediacaran Dengying Formation in the Yangtze Gorges Area, South China. Journal of Paleontology 83, 575-587.

Sherman, L.S., Waldbauer, J.R., Summons, R.E., 2007. Improved methods for isolating and validating indigenous biomarkers in Precambrian rocks. Organic Geochemistry 38, 1987-2000.

Snape, C.E., Bolton, C., Dosch, R.G., Stephens, H.P., 1989. High liquid yields from bituminous coal via hydropyrolysis with dispersed catalysts. Energy & Fuels 3, 421-425.

Sun, W., 1986. Late precambrian pennatulids (sea pens) from the eastern Yangtze Gorge, China: *Paracharnia* gen. nov. Precambrian Research 31, 361-375.

Walker, J.D., Geissman, J.W., Bowring, S.A., Babcock, L.E., 2013. The Geological Society of America Geologic Time Scale. Geological Society of America Bulletin 125, 259-272.

Whelan, J., Thompson-Rizer, C., 1993. Chemical Methods for Assessing Kerogen and Protokerogen Types and Maturity. In: Engel M., Macko, S. (Eds.), Organic Geochemistry. Topics in Geobiology. Springer US, pp. 289-353.

Xiao, S., Shen, B., Zhou, C., Xie, G., Yuan, X., 2005. A uniquely preserved Ediacaran fossil with direct evidence for a quilted bodyplan. Proceedings of the National Academy of Sciences of the United States of America 102, 10227-10232.

Xiao, S., Laflamme, M., 2009. On the eve of animal radiation: phylogeny, ecology and evolution of the Ediacara biota. Trends in ecology & evolution (Personal edition) 24, 31-40.

Zhu, M., Zhang, J., Yang, A., 2007. Integrated Ediacaran (Sinian) chronostratigraphy of South China. Palaeogeography, Palaeoclimatology, Palaeoecology 254, 7-61.

- Chapter 5 -

Summary and conclusions

The Shibantan Member is one of only two known carbonate settings characterised by a 'typical' Ediacaran fossil association including Ediacara-type fossils. Aim of this project was a comprehensive geobiological characterisation of the Shibantan Member, addressing both sedimentological and biogeochemical issues in order to gain a better understanding of these palaeoecosystems in which early metazoans thrived. Since organic biomarker analyses are problematical if applied on thermally mature outcrop samples, contamination paths were critically assessed and the potential of the direct use of extraction residues for catalytic hydropyrolysis (HyPy) of the non-extractable portion of organic matter (kerogen) was evaluated.

Sedimentological analysis revealed that the depositional system of the Shibantan Member can be best explained with a carbonate ramp model linked to an intra-platform basin situated on the Dengying carbonate platform (Fig. 5.1). The Dengying carbonate platform was generally characterised by evaporitic dolomites deposited in sub- to supratidal inner-ramp environments as represented by the Hamajing Member. The black bituminous and laminated limestones of the lower Shibantan Member, which overlay the Hamajing Member with a sharp contact, were in contrast deposited in a subtidal lower- to middle-ramp environment. This strong facies contrast point to a rapid deepening event that was most likely due to a tectonically-induced increase in local subsidence (Fig. 5.1). Sedimentation was probably condensed during lower Shibantan times as evidenced by common occurrences of early diagenetic chert bands and -concretions. However, the basin became then subsequently filled as indicated by a gradual transition to the dark wavy dolomites of the upper Shibantan Member, which was deposited in a subtidal middle-ramp environment and, ultimately, the Baimatuo Member, which essentially represents the same facies as the Hamajing Member (i.e. sub- to supratidal inner-ramp environments). A distinct slumping horizon as well as mass-flow deposits evidence that the sedimentation in the Shibantan basin was highly dynamic, partly due to wave affection and, most likely, tectonic processes.

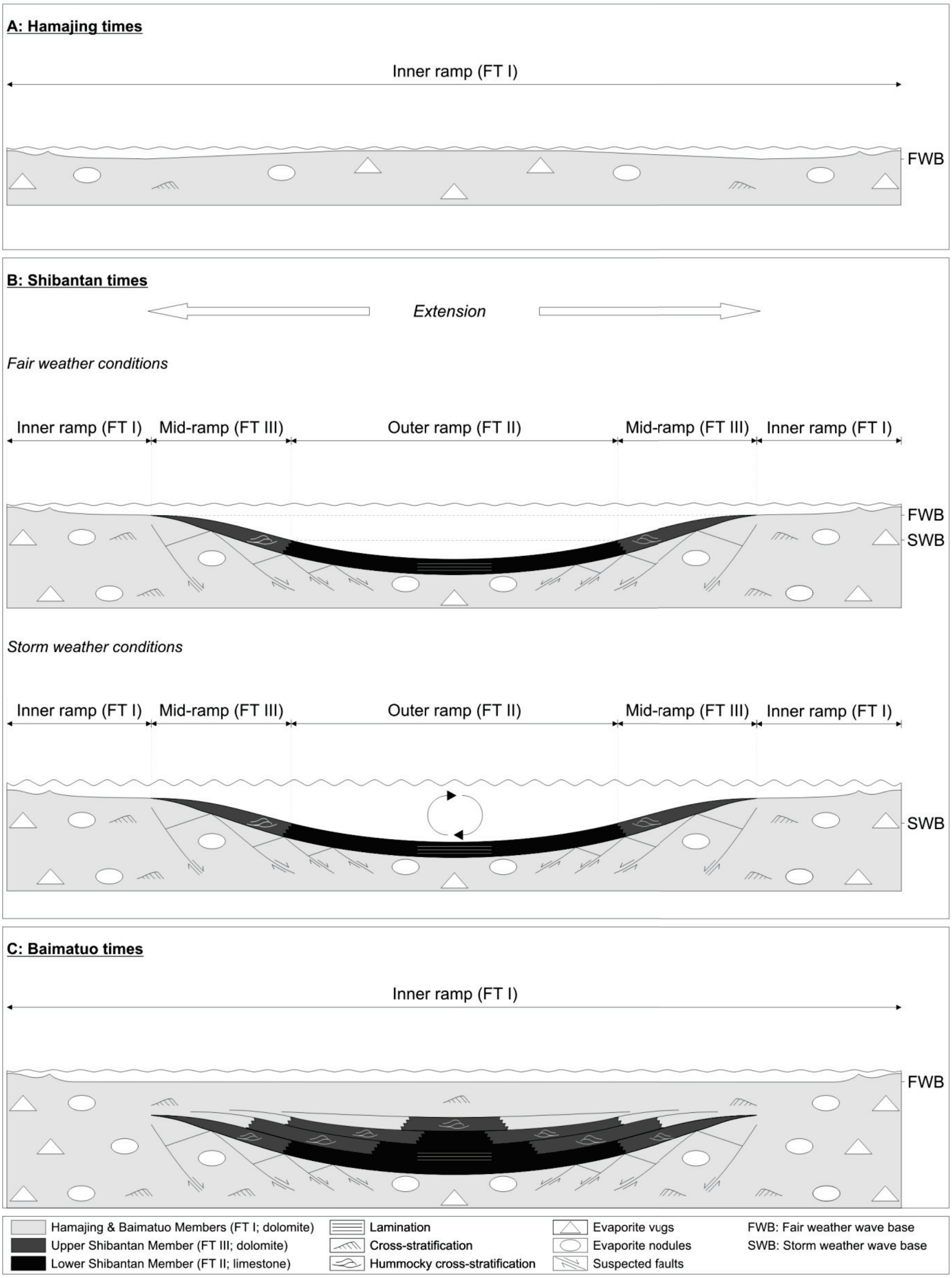

Fig. 5.1 Comprehensive model for the geodynamic evolution and palaeoenvironmental interpretation of the Shibantan Member. The investigated Xinshipai-Section represents the central part of the basin. (A) The Dengying platform was tectonically stable and solely characterised by an inner-ramp facies during Hamajing times in the Yichang area. (B) A sudden increase of local subsidence (probably due to the reactivation of old faults by regional extensional processes) led to the formation of the Shibantan basin. The water body was stratified under fair weather conditions while it was fully oxidised under storm weather conditions. The microbial mat associated biota including Ediacara-type organisms occur in the deepest depositional environment represented by the lower Shibantan Member (e.g. in the Zhoujia'ao-Quarry). (C) The Shibantan basin was then successively filled by carbonate ramp systems so that widespread inner-ramp settings were re-established during Baimatuo times. Please note that the depicted faults are only suspected and the tectonic processes responsible for the formation of the Shibantan Member are still unclear.

The microbial mat associated biota (i.e. Ediacara-type fossils, horizontal traces, and *Vendotaenia*-like fossils) flourished in the environments represented by the lower Shibantan Member. Given the close spatial relationship between the autochthonous fossil associations and allochthonous event deposits in this setting, the event deposits were probably not only important for the preservation of fossils but also for the supply of nutrients. This close linkage between abiotic and biotic processes was further constrained by the comprehensive biogeochemical analysis of a sample from the lower Shibantan Member. Trace elements demonstrate that the water body was temporarily stratified so that free molecular O_2 was restricted to the upper water column during fair weather conditions (Fig. 5.1). However, frequent mixing during storm events, as revealed by sedimentological analysis, probably led to the recurrent oxidation of the entire water column. Consequently, biogeochemical conditions were probably not stable during lower Shibantan times.

Organic biomarker analyses were conducted to gain further insights into the biosphere of the Shibantan Member but are problematical since the organic matter is highly mature ($T_{max} \geq 500°C$) and bitumens in outcrop samples of the Shibantan Member are affected by external, most likely anthropogenic contamination. However, abundant sulphurised compounds in the bitumen and HyPy-treated extraction residue of the Shibantan carbonates hint at a high activity of sulphate reducing bacteria. Considering the evidences for mixing of the water column by storm events, sulphide oxidising bacteria were possibly temporarily favoured whenever oxygen was available at the sediment-water interface. Assuming that not all *Vendotaenia*-like fossils in the Shibantan Member represent shreds of microbial mats disrupted by storms and/or event deposition, an interpretation as sulphide oxidising bacteria appears reasonable. Stable carbon isotopes of carbonate phases (+3.3 to +4.0‰, VPDB) and syngenetic *n*-alkanes in the extraction residue after applying HyPy (-31.7 to -36.3‰, VPDB) point to the presence of phototrophic primary producers (cyanobacteria and/or algae) within the mat facies of the Shibantan Member and would also be in line with a changeable setting. Repeated cycles of mat-growth, reworking and re-deposition led to an effective burial of primary produced organic matter, and such withdrawal of ^{12}C enriched organic matter caused an enrichment of newly precipitated carbonate phases in residual ^{13}C. Thus, palaeoenvironmental conditions dynamically changed through a complex interplay of biogenic and abiogenic processes.

Dependent on the changeable biogeochemical conditions, particularly the availability of oxygen, the microbial mat associated biota including Ediacara-type organisms temporarily thrived in this setting. This implies that stable environmental conditions (with respect to oxygen) were not necessarily a crucial prerequisite for the early evolution and diversification of early metazoan as commonly assumed. In case of the Shibantan Member one could even speculate that environmental instability has provoked innovative lifestyles and -strategies, allowing organisms to cope with the changeable conditions. However, this hypothesis has to be tested in future studies on other settings with Ediacara-type fossils (e.g. the Khatyspyt Formation in Siberia) and first calcifying metazoans.

- Chapter 6 -

Reconsiderations and corrigenda

Refers to Chapter 3: 'Geobiology of an Ediacara palaeoecosystem: The Shibantan Member (Dengying Formation, South China)' (*Precambrian Research; in revision*)

In chapter 3 of this thesis, mm-sized sparite-filled irregularly shaped voids in layers of the lower Shibantan Member were initially interpreted as 'microbial chips' (i.e. intraclasts derived from the reworking of autochthonous microbial mats). Following sedimentological analysis of a whole section, covering the upper Hamajing Member, the Shibantan Member, as well as the lower Baimatuo Member, revealed the presence of evaporite minerals in very shallow water sediments of the Dengying carbonate platform. Given these findings, the postulated 'microbial chips' now more likely represent reworked and re-deposited evaporite minerals and are re-interpreted accordingly.

Based on the interpretation as 'microbial chips' the material in sedimentary layers was assumed to be generally para-autochthonous (i.e. reworked and re-deposited within the same setting) in origin. The re-interpretation of the components therefore may cast doubt on the conclusion that the measured biogeochemical data necessarily reflect conditions in the environment represented by the lower Shibantan Member. However, the biogeochemical interpretation appears to be valid though since (i) no scattering of data is observed which could indicate a mixture of biogeochemical signatures and (ii) the stable carbon isotope signatures of the Shibantan carbonates are systematically different to that of the underlying Hamajing Member. Despite a still possible influence of allochthonous material, the so inferred presence of a syngenetic geochemical signature can maybe explained by (i) a yet para-autochthonous origin of the main part of the material, (ii) a possible domination of autochthonous signals due to the condensed sedimentation, and/or (iii) remineralisation and recrystallisation processes within the highly sulphidic environment of the lower Shibantan Member, leading to an integration of local geochemical signatures into the sediment.

Curriculum Vitae Jan-Peter Duda

Personal data

Date of birth: 03.09.1984
Place of birth: Bremen

Professional career

2010 – present	Graduate student (PhD), Georg-August-University Göttingen. Topic: '*Geobiology of bituminous carbonates from the Ediacaran Shibantan Member (Dengying Formation, South China)*' Supervisors: Prof. Dr. Joachim Reitner, Prof. Dr. Maoyan Zhu, Prof. Dr. Volker Thiel, Dr. Martin Blumenberg
2011	Stay (6 months) at the Nanjing Institute of Geology and Palaeontology (NIGPAS), Chinese Academy of Sciences (CAS). Supervisor: Prof. Dr. Maoyan Zhu
2007 – 2010	Graduate student (MSc), University Bremen. Master's thesis: '*The end of marine sedimentation in the southern Tethys-Himalaya (Tibet, PR China): Palaeoecology and facies development*' (written in German). Supervisor: Prof. Dr. Helmut Willems
2004 – 2007	Undergraduate student (BSc), University Bremen. Bachelor‘s thesis: '*Palaeocene iron oolite of the Spanboth-Formation (Ladakh, NW-India): Genesis and sedimentology*' (written in German). Supervisor: Prof. Dr. Helmut Willems

Awards & grants

2014	Travel grant IGCP 587 (Identity, Facies and Time- The Ediacaran (Vendian) Puzzle) *Best Oral Presentation Award* (3rd International Conference of Geobiology, Wuhan, PR China) Travel grant of the China University of Geosciences Wuhan (PR China) Travel grant of the Unibund Göttingen (Georg-August-University Göttingen)
2013	*Young Scientist Award* of the of the Paläontologische Gesellschaft (Germany) and the Palaeontological Society of China Travel grant of the Nagoya University (Japan) Travel grant of the International Association of Sedimentologists (IAS) Travel grant of Göttingen International (Georg-August-University Göttingen)
2011	PhD sholarship (6 months) of the German Academic Exchange Service (DAAD)

Publications

Peer-review journals

Duda, J.-P., Thiel, V. Reitner, J., Blumenberg, M. (accepted): Assessing possibilities and limitations for biomarker analyses on outcrop samples: A case study on carbonates of the Shibantan Member (Ediacaran Period, Dengying Formation, South China). Acta Geologica Sinica (English version)

Afşar, F., Duda, J.-P., Zeller, M., Verwer, K., Westphal, H., Eberli, G. P. (2014): First report of sponge rhaxes in the Picún Leufú Formation (Tithonian–Berriasian), Neuquén Basin, Argentina. In: Wiese, F., Reich, M., Arp, G. (Eds.): „Spongy, slimy, cosy & more...”. Commemorative volume in celebration of the 60th birthday of Professor Joachim Reitner. Göttingen Contributions to Geosciences 77, 49-56

Luo, C., Schäfer, N., Duda, J.-P., Li, L.-X. (2014): Preservation of organic matter in sponge fossils: a case study of ‘round sponge fossils’ from the Cambrian Chengjiang Biota with Raman spectroscopy. In: Wiese, F., Reich, M., Arp, G. (Eds.): „Spongy, slimy, cosy & more...”. Commemorative volume in celebration of the 60th birthday of Professor Joachim Reitner. Göttingen Contributions to Geosciences 77, 29-38

Sanchez-Beristain, F., Duda, J.-P., Lopez-Esquivel Kransksith, L., Garcia-Barrera, P. (2014): A brief synopsis on the history of sponge research in the Upper Triassic St. Cassian Formation (Dolomites, NE Italy). In: Wiese, F., Reich, M., Arp, G. (Eds.): „Spongy, slimy, cosy & more...”. Commemorative volume in celebration of the 60th birthday of Professor Joachim Reitner. Göttingen Contributions to Geosciences 77, 39-48

In revision

Duda, J.-P., Blumenberg, M., Thiel, V., Simon, K., Zhu, M., Reitner, J. (in revision): Geobiology of an Ediacara palaeoecosystem: The Shibantan Member (Dengying Formation, South China). Precambrian Research

Submitted

Duda, J.-P., Zhu, M., Reitner, J. (submitted): Depositional dynamics of a bituminous carbonate facies in a tectonically induced intra-platform basin: The Shibantan Member (Dengying Formation, Ediacaran Period). Carbonates and Evaporites

Extended abstracts

Reitner, J., Luo, C., Duda, J.-P. (2012): Early Sponge Remains from the Neoproterozoic-Cambrian Phosphate Deposits of the Fontanarejo Area (Central Spain). Proceedings of the 17th Field Conference of the Cambrian Stage Subdivision Working Group, International Subcommission on Cambrian Stratigraphy & Celebration of the 30th Anniversary of the Discovery of the Kaili Biota, Guizhou. Journal of Guizhou University (Natural Science) 29, 184-186 [Poster]

Relevant conference contributions (own presentations only)

Duda, J.-P., Blumenberg, M., Thiel, V., Simon, K., Zhu, M., Riegel, W., Reitner, J. (2014): Comprehensive geobiological characterization of a bituminous carbonate facies with Ediacara-type fossils (Shibantan Member, South China). The 3rd International Conference of Geobiology- combining ancient records with the present day observations. Wuhan, PR China [Talk]

Duda, J.-P., Blumenberg, M., Thiel, V., Simon, K., Zhu, M., Riegel, W., Reitner, J. (2013): Geobiology of a Carbonate System with Ediacara-type Organisms: The Shibantan Member (Dengying Formation, South China). In: Reitner, J., Qun, Y., Wang, Y. (Eds.): Palaeobiology and Geobiology of Fossil Lagerstätten through Earth History. A Joint Conference of the "Paläontologische Gesellschaft" and the "Palaeontological Society of China", Göttingen, Germany. Universitätsdrucke Göttingen, 39 [Talk]

Duda, J.-P., Blumenberg, M., Thiel, V., Simon, K., Zhu, M., Reitner, J. (2013): Geobiology of an Ediacaran Carbonate System: The Shibantan Member (South China). 30th International Meeting of Sedimentology, Manchester (UK) [Talk]

Duda, J.-P., Reitner, J., Thiel, V., Zhu, M., Blumenberg, M. (2013): Geochemical insights into an Ediacara palaeoecosystem: The Shibantan Member (South China). In: Gonzáles-Pérez, J.A., González-Vila, F.J., Jiménez-Morillo, T., Almendros, G. (Eds.): Organic Geochemistry: Trends for the 21th Century. Book of Abstracts of the Communications presented to the 26th International Meeting on Organic Geochemistry, Tenerife, Canary Islands (Spain) 1, 423-424 [Poster]

Other publications

Duda, J.-P. (2011): Bilateral Supervised PhD-Project in China- 6 Months Research Stay at the Nanjing Institute of Geology and Palaeontology, Chinese Academy of Sciences. *Newsletter of the Nanjing Office of the University of Göttingen (PR China)*, 16-17 [Article]